PRESTRESS LOSS AND CREEP CAMBER IN A HIGHWAY BRIDGE WITH REINFORCED CONCRETE SLAB ON PRETENSIONED PRESTRESSED CONCRETE BEAMS

by

Howard L. Furr, Research Engineer

Raouf Sinno, Former Assistant Research Engineer

Leonard L. Ingram, Research Associate

Research Report Number 69-3 (Final)

Creep in Prestressed Concrete

Research Project Number 2-5-63-69

Sponsored by

The Texas Highway Department
In Cooperation with the
U. S. Department of Transportation, Federal Highway Administration
Bureau of Public Roads

October 1968

TEXAS TRANSPORTATION INSTITUTE
Texas A&M University
College Station, Texas

ACKNOWLEDGEMENTS

The valuable assistance of Mr. H. D. Butler, Designing Engineer, Texas Highway Department in carrying out the work reported here is gratefully acknowledged.

TABLE OF CONTENTS

LIST OF FIGURES

LIST OF TABLES

ABSTRACT

A numerical procedure using a step-by-step method is used for computing both elastic and time dependent strains, deflections, and prestress losses in full size pretensioned prestressed concrete highway bridge beams. Both lightweight and normal weight structural concretes are used. The method uses creep and shrinkage functions, derived from control specimens, for making predictions.

The computed strains, deflections, and prestress losses agreed well, for the most part, with measured values during the time interval from date of casting of the slabs to end of tests. The beams were about 320 days old when the slab was cast, and tests terminated at 660-day beam age.

Measured elastic beam deflections under the weight of the plastic slab were a little over 50% of the deflections computed by theory. Prestress losses were about 15% in 40 ft. long lightweight concrete beams at 660 days. The 56 ft. LW beam loss at the same age was about 21% and the NW beam 14 1/2%.

The changes in camber and prestress losses after the slab was cast were minor.

CHAPTER 1

INTRODUCTION

A study of strains, camber, and prestress loss in pretensioned, prestressed beams began in 1964 is concluded with this report. The purpose of the study was to provide information that could be used by the highway bridge designer in prestressed concrete construction. It was concerned almost altogether with lightweight concrete because of certain advantages promised in that material and because little information on full size field structures made of that material was available.

A mathematical method for computing creep in prestressed beams was applied in predicting creep strains in laboratory beams early in the program. That application indicated that the approach would be feasible in predicting camber and prestress losses in full size prestressed highway bridge beams, and the program was extended for that purpose. Creep of concrete only, not steel, was treated.

After a study and field tests of instrumentation requirements, a full size bridge, then in the design stages, was designated as a test bridge for proving the prediction method.

An earlier report (1) gave details of the early work in the development of the prediction method. It also reported strains, camber, and prestress losses over a 300-day period for the beams of the test bridge.

In the study of the beams for the test bridge, questions concerning camber of beams with straight strands as compared with beams with draped strands arose. In order to develop some information

that would bear on those questions, four full size test beams were built. Two of those were straight strand beams with bond broken over end portions of some of the tendons. The other two beams had draped strands.

This report discusses the four test beams in Chapter 2, and the longer discussion of the continuation of the full size bridge study is given in Chapter 3.

CHAPTER 2

CAMBER AND PRESTRESS LOSSES IN BEAMS WITH DRAPED STRANDS AND WITH STRAIGHT STRANDS - LUFKIN BEAMS

2.1 Introduction

Camber in beams occurs only when strains at the top and bottom differ, and if such differences are minimized, camber will be minimized. Prestress loss, on the other hand, develops as the concrete strains at the centroid of the steel, whether or not the strains in the section vary from top to bottom.

Arrangement of prestressing steel in different patterns within a beam makes it possible to balance, approximately, the shear and moment capacities with the requirements of external loads. Post tensioned members have been more adaptable to such arrangements than pretensioned members.

The draped strand pattern used widely in highway bridge beams lowers the centroid of prestressing steel near mid-span. That arrangement provides a moment resistance which gradually increases from the end to the mid-span region where imposed moments are highest. The total pretensioning force is carried through the full length of the beam, but its eccentricity from the beam centroid decreases from near mid-span, the hold down points, to the ends of the beam. Since the full prestress is carried the full length of the beam, concrete strains, and consequently prestress loss, will have a corresponding development along the beam. The great difference between stresses at top and bottom of the beam near mid-span will

cause deflections consistent with those differences.

The same general moment resistant characteristics realized in the draped strand beam can be built into a beam with properly treated straight strands. In the latter, moment resisting capacity may be controlled by breaking bond between the strands and concrete in well defined, carefully controlled patterns. A beam with a gradual reduction of the number of effective strands between mid-span and its ends, accomplished by breaking bond over successive partial lengths of strands, will accomplish that control. The bond may be broken by placing an impervious rigid sleeve, such as plastic tubing, over the desired length. Such a beam would carry increasing amounts of prestressing force between the end and mid-span, and would possibly suffer less prestress loss than the draped strand beam.

A study was made of draped strand beams and blanketed strand beams for purposes of comparing deflections and prestress losses. The beams were made in two pairs, one pair was of normal weight concrete; the other, lightweight. Each pair consisted of one beam with draped strands and one with straight blanketed strands. The beams were fabricated at Lufkin, Texas, and are referred to here as Lufkin beams.

Details of the study follow.

2.2 Objectives

1. To determine the effect on camber and prestress loss when bond of prestressing strands is broken over a portion of length of full size highway bridge beams.

2. To compare the behavior of full size normal weight and lightweight highway bridge beams with partial blanketing of prestressing

strands.

2.3 Test Specimens -- Lufkin Beams

Four full size 50 ft. prestressed concrete beams, Texas Highway Department Type B served as the test specimens. Two of those beams were made of normal weight concrete, and two were of lightweight concrete. One normal weight and one lightweight beam were prestressed with draped strands. The prestressing strands in the other two were straight. Part of those straight strands were encased in impervious plastic tubes over a portion of each end for purposes of breaking bond of those blanketed strands. Full bond was assumed to be effective 2 ft. from the end of the tubes. Fig. 2-1 gives details of those beams.

Strain gage points and elevation points were installed in these beams in the same way as those described in an earlier report (1).

All beams were cured under wet mat until cylinder breaks indicated that release strength had been reached. After removal from the prestressing line they were cured an additional three days under impervious matting. The beams were wetted frequently by rain during their first three weeks of open yard storage.

2.4 Materials

Prestressing steel was specified as 250 K, stress relieved, 9/16 inch diameter, 7-wire strand meeting ASTM Specification A-416 with 27,000 lb. minimum ultimate strength. No tests were made on this material.

Normal weight concrete was made with Type III cement, natural sand, and crushed limestone proportioned by weight at 1:1.82:3.10, respectively. The water-cement ratio was 0.51.

TABLE 2.1 PRESTRESSED TEST BEAMS

Note: All beams 50 ft long; transported 130 miles by truck on April 22/68

Mark	Concrete Type	Strands	Date	
			Cast	Release
LWB	LW	Straight, blanketed	3/13/68	3/15/68
NWB	NW	Straight, blanketed	3/13/68	3/15/68
LW	LW	Draped	3/20/68	3/22/68
NW	NW	Draped	3/20/68	3/22/68

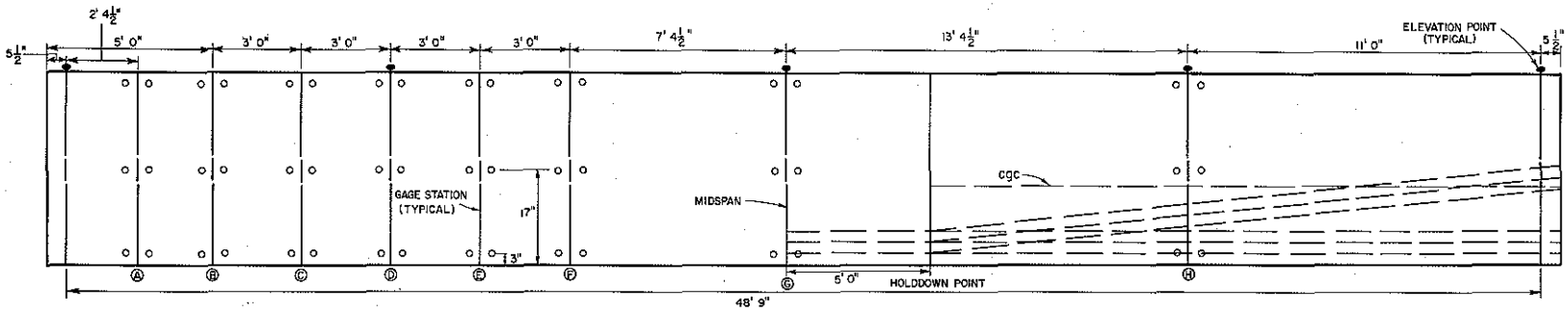

GAGE POINT LOCATIONS
DRAPED STRAND BEAMS
OMIT STATIONS B, D, F

DRAPED STRAND DETAILS
END OF BEAM e = 7.84 in
MIDSPAN e = 11.11 in

BLANKETED STRAND ARE STRAIGHT: DETAILS ARE SHOWN BELOW

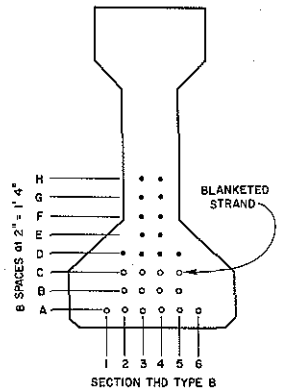

LENGTH OF BLANKETED PORTION OF STRAND MEASURED FROM END OF BEAM (FT)			e (in)
STRAND	ACTUAL	EFFECTIVE	
	0	0	3.6
C2, C3, C4, C5	3	5	4.93
B2, B3, B4, B5	6	8	6.13
A3, A4	9	11	6.75
A2, A5	12	14	7.26
A1, A6	15	17	7.70

BEAM DESIGNATION	TYPE	NUMBER OF STRANDS	f'_c (PSI)			E_c (KSI)			UNIT WEIGHT lb/ft³
			2 DAYS	7 DAYS	150 DAYS	2 DAYS	7 DAYS	150 DAYS	
DRAPED 1	NW	22	5020	6740	6690	4300	5150	5600	
DRAPED 2	LW	22	6620	7300	7290	3120	3250	3800	119
BLANKETED 1B	NW	26	4940	6280	6360	5360	5000	6000	
BLANKETED 2B	LW	26	5080	5970	7080	3480	2950	3500	120

FIGURE 2-1 PRESTRESSED BEAM DETAILS
LUFKIN BEAMS

Lightweight concrete was made with Type III cement, natural sand, and expanded shale (Featherlite Ranger) coarse aggregate. The weight ratios were 1:1.36:1.52, and the added water-cement ratio was 0.49. It contained 6% air (by pressure meter) and had a plastic weight of 119 lb./cf. The expanded shale was wet down overnight by sprinkler before mixing.

Slumps varied from 2 to 3 3/4 in.

2.5 Tests

Compression tests made on the standard 6 in. diameter cylinders yielded strength and stress-strain data for each concrete. Cylinders were preloaded to 30 kips three times before data collection began in these tests. Dial gages, mounted in each quadrant, measured strains over a six in. gage length. Strength and strains were averaged for three cylinders for each test. The secant moduli were determined at 1/2 f'_c.

Elevations and strains were taken from each beam just before release, just after release, daily for the first five days, weekly for one month, and at two to three week intervals thereafter.

Strains were averaged for the corresponding on opposite sides of the beam. Elevations were reduced to give camber at each elevation point.

Curves of strains and of elevations versus time were developed from the test data.

2.6 Test Results and Discussion

A. Strains

Beam strains for both sets of beams are listed in Table 2.2 and are displayed graphically in Fig. 2-2.

TABLE 2.2 STRAINS AT RELEASE

Beam	Position	STRAIN (MICRO-INS)					
		End		Quarter Span		Mid-span	
		Computed	Measured	Computed	Measured	Computed	Measured
NWB	Top	---	80	---	115	---	140
	Bottom	---	195	---	375	---	435
LWB	Top	---	90	---	110	---	120
	Bottom	---	240	---	470	---	555
NW	Top	-5	-25	6	-5	-6	-5
	Bottom	442	415	433	400	440	385
LW	Top	-12	-35	-12	-20	-36	-40
	Bottom	602	545	599	545	612	525

Ratio:		End	Quarter Span	Mid-span	
Computed bottom / Measured bottom	NW	1.065	1.083	1.143	Avg.=1.11
	LW	1.105	1.099	1.166	

The purpose of breaking bond was to reduce the difference in stress between the top of the beam and the bottom in order to reduce corresponding strain differences and thereby reduce camber of the beam. It is shown in Fig. 2-2 that the change in strains between top and bottom of the blanketed strand beams is much less than the change in draped strand beams. The reduction would not only cut down on elastic strains, but it would reduce time dependent camber as well.

Fig. 2-3 shows the strain gradient for the four beams under full dead load having undergone all anticipated elastic and time-dependent prestress losses at one year age. Prestress losses of 15% for normal weight concrete and 20% for lightweight concrete, determined in previous tests of similar beams (1), were used in computing strains.

Beams with draped strands undergo considerable changes in stress and strain between ends and mid-span, and further change is brought about with the addition of dead loads. See Figs. 2-2, 2-3, and 2-4. Camber, depending on the strain gradient from top to bottom of beam, would be expected to be greater in the draped beams than in their companion straight blanketed strand beams. Fig. 2-7 confirms that expectation. Under design live load plus impact, mid-span stresses in the bottom of the beam become essentially zero and the top stresses increase some 200 to 350 psi, well within limits of practice.

The fact that the addition of full dead load to prestressed beams reduces the stress gradient from top to bottom suggests that

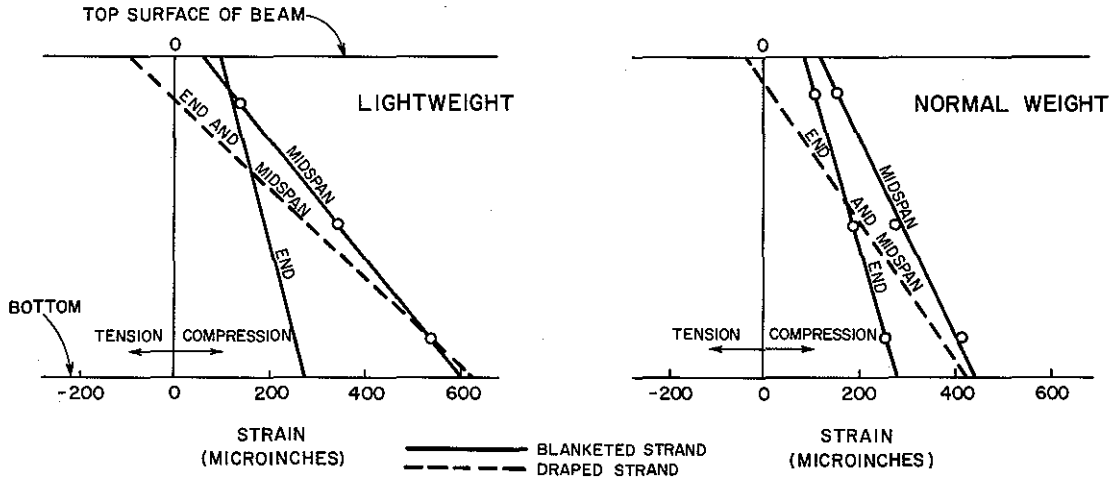

FIGURE 2-2 MEASURED STRAINS AT RELEASE OF PRESTRESS

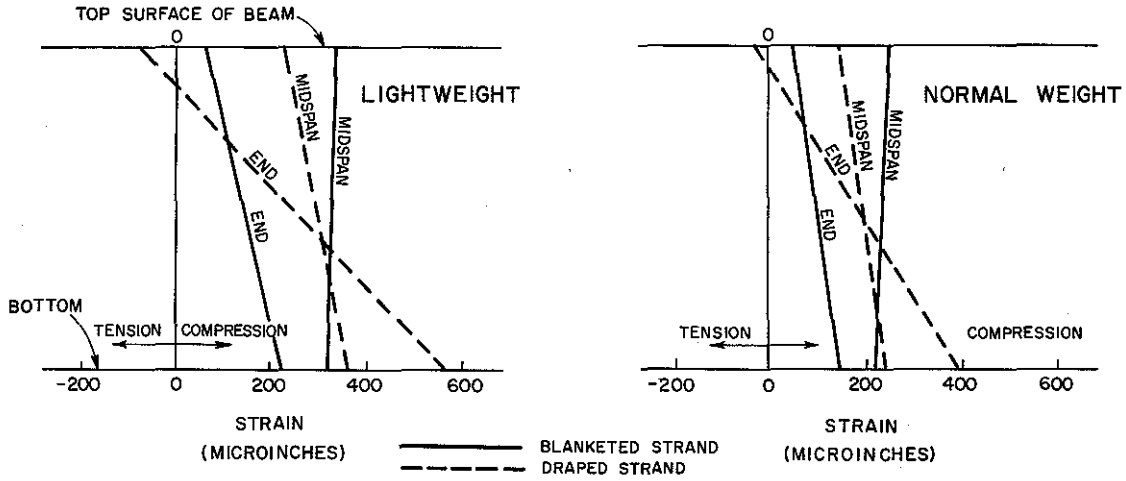

FIGURE 2-3 COMPUTED STRAINS UNDER FULL DEAD LOAD AFTER PRESTRESS LOSS ANTICIPATED AT ONE YEAR AGE

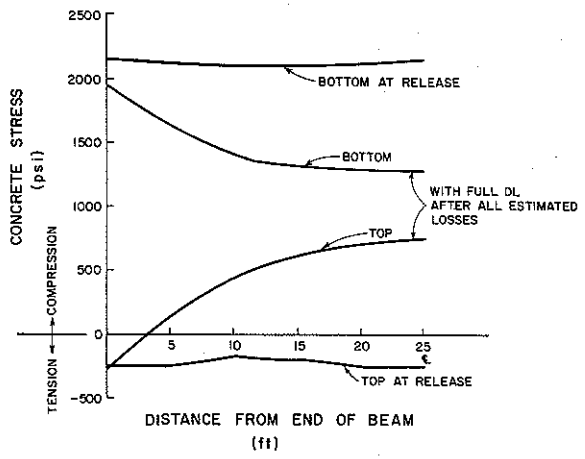

(a) BEAM NW

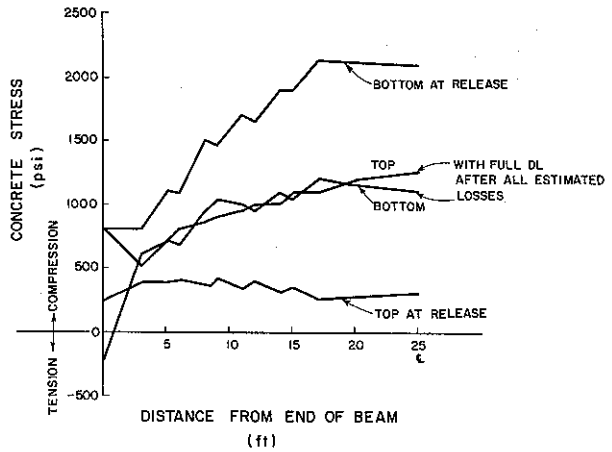

(b) BEAM NWB

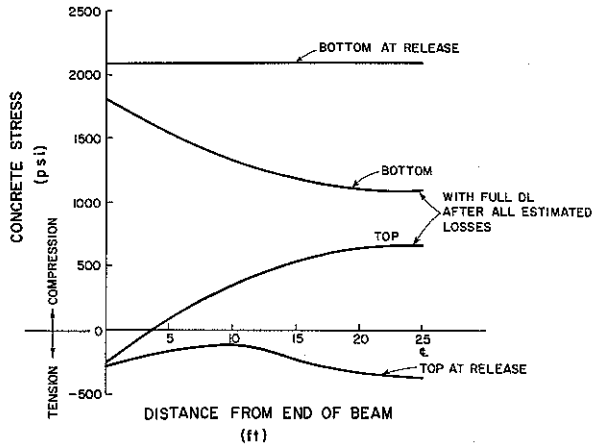

(c) BEAM LW

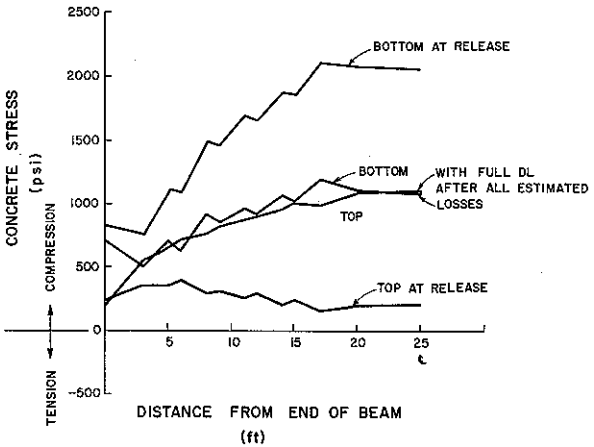

(d) BEAM LWB

FIGURE 2-4 STRESS VARIATIONS IN BEAMS

the beams should be loaded as soon after casting as the situation permits. The early loading would reduce camber growth due to sustained prestress and possibly permit a deck slab of more uniform thickness.

The influence of broken bond on strains in some of the prestressing strands can be seen in Fig. 2-5. The narrow range of strains in the draped strand beams is reflected in the curves of Fig. 2-4(a) and (c) where little change in stress at release is seen along the length of the beam. In the same way, the spread of strain curves for blanketed strand beams is reflected in the stress changes displayed in Fig. 2-4(b) and (d).

No attempt was made to smooth out the strain plots because the display is intended to show only the trend of strains along the beam length.

The blanketed strand beams, both normal weight and lightweight, deflected considerably less than the corresponding draped strand beams, Fig. 2-6 and Table 2.3. At mid-span the ratio of upward deflection of the blanketed strand normal weight beam to that of its companion draped strand beam was 0.57. The corresponding ratio for lightweight beams was 0.62. Corresponding values at quarter span were 0.50 and 0.58, respectively.

Fig. 2-6 indicates that creep camber in the blanketed strand beams had reached near stability at about six weeks to two months age, whereas the draped strand beams continued to creep noticeably at the end of the test period.

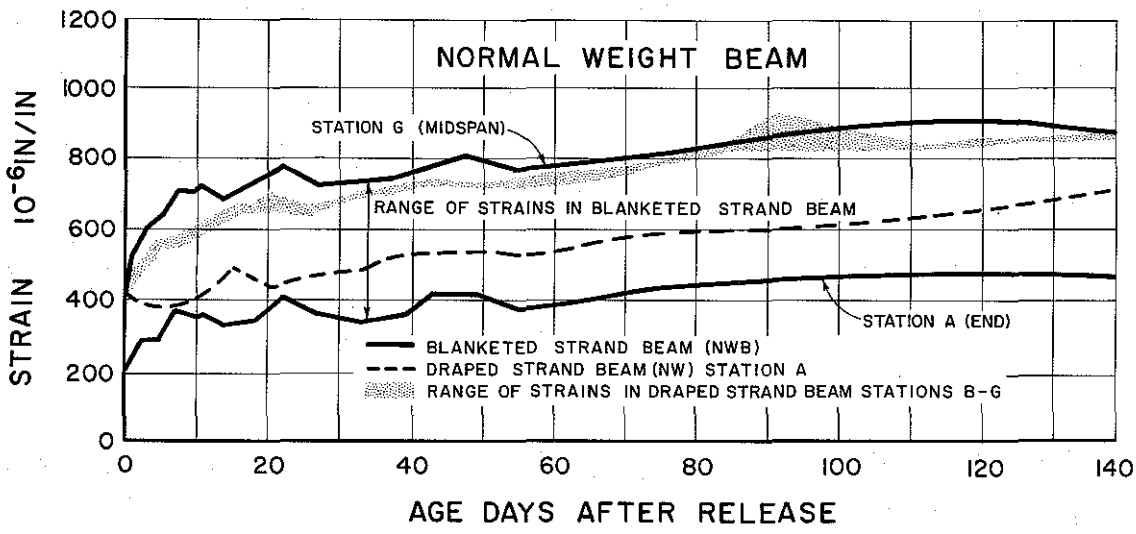

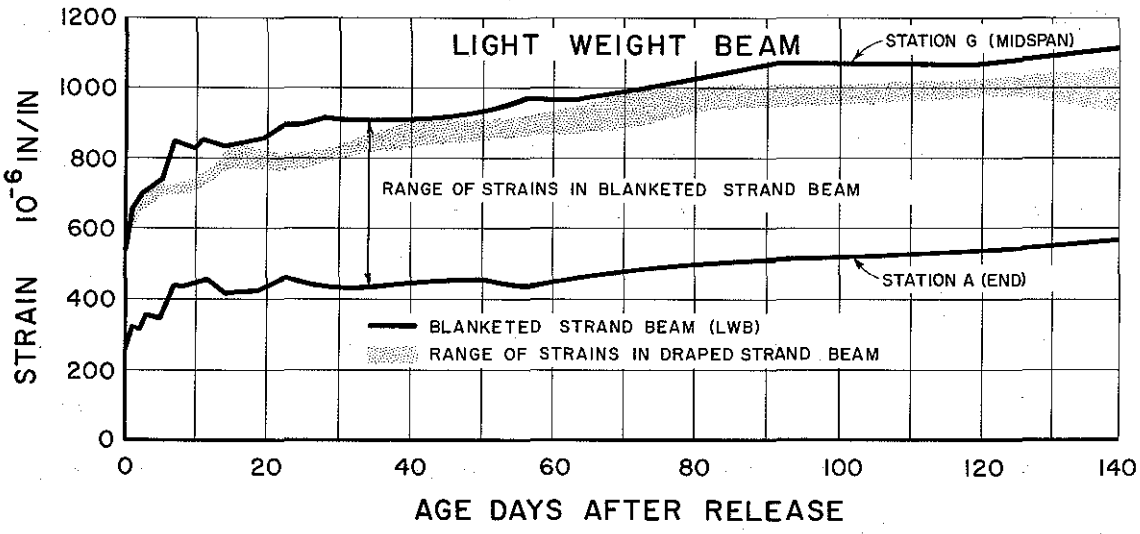

FIG. 2-5 STRAINS AT BOTTOM GAGE POINTS IN BEAM

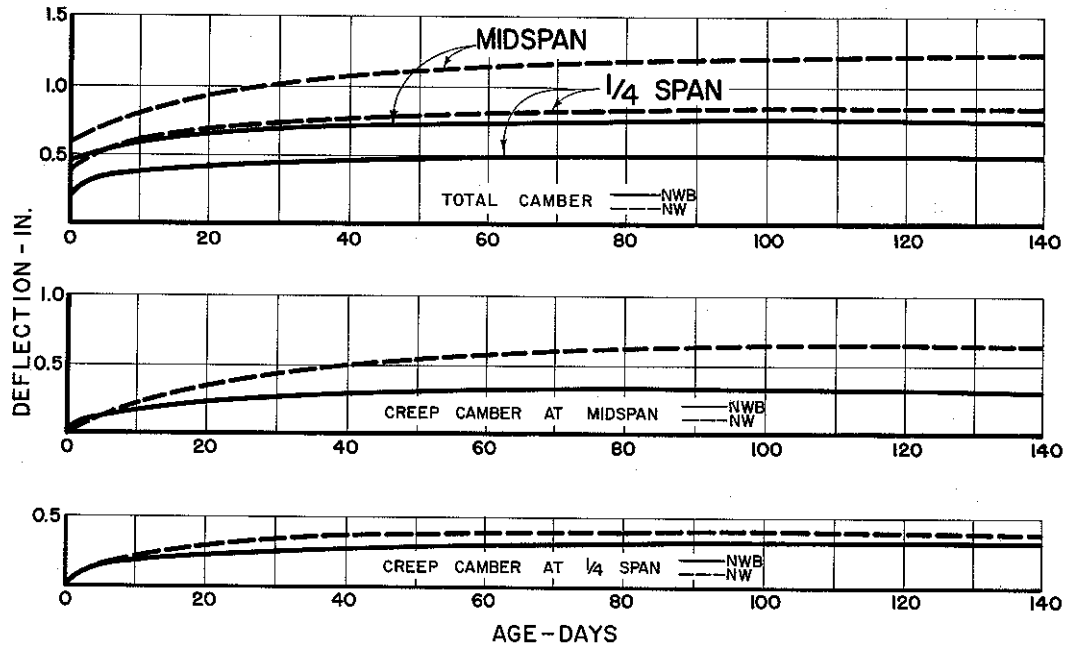

(a) CAMBER OF NORMAL WEIGHT CONCRETE BEAMS

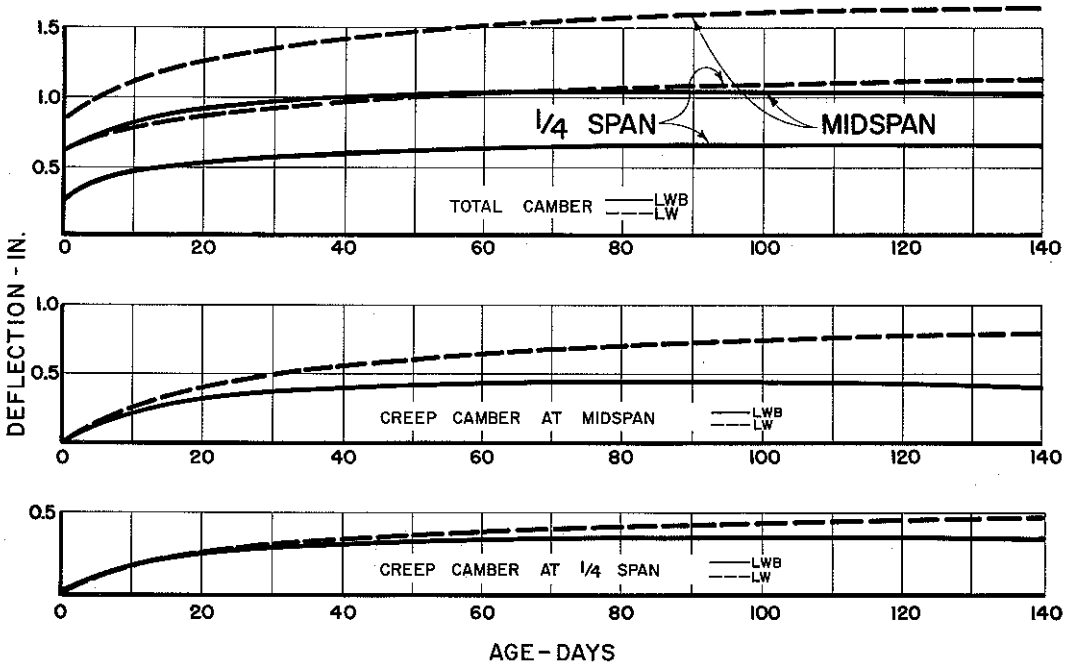

(b) CAMBER OF LIGHTWEIGHT CONCRETE BEAMS

FIG. 2-6 BEAM CAMBER

TABLE 2.3 BEAM CAMBER DUE TO PRESTRESS AND SELF WEIGHT

Beam	Mid-span Camber					Qtr-span Camber			Ratio of Cambers for Blanketed Strand Bm to That for Draped Strand Beam.						
	Release			140 Day		Re-	140 Day		Elastic		Creep		Total		
				Total	Creep	lease	Total	Creep							
	Com- puted	Meas- ured	Cmptd ÷ Msrd			Meas- ured			Mid- span	Qtr- span	Mid- span	Qtr- span	Mid- span	Qtr- span	Total ÷ Elastic
NW	0.67	0.62	1.07	1.22	.60	0.40	0.70	.31	.68	.50	.47	.84	.57	.50	1.97
NWB	0.47	0.42	1.12	.70	.28	0.20	0.45	.26							1.67
LW	0.97	0.85	1.14	1.68	.83	0.57	1.14	.57	.72	.40	.52	.75	.62	.58	1.97
LWB	.74	0.61	1.21	1.04	.43	0.23	.77	.43							1.71

Note: Computed camber at mid-span = $\frac{5\ \omega L^4}{384\ EI}$ + (Defl due to prestress).

Prestress deflections were computed by moment/areas.
Camber is expressed in inches.

Elastic camber accounted for 51% of the total camber for draped strand beams, and 59% for blanketed strand beams. Both beam types showed less measured elastic camber than computed. The drag of the bottom form on the ends of beams at release could possibly account for a small portion of the difference. The second elevation readings were taken on the day after release, and by that time creep had progressed noticeably. The influence of the size of beam (2), modulus of elasticity, and of the stress gradient in the beam possibly account for a further portion of the 10% to 20% between those computed and measured cambers.

Camber profiles shown in Fig. 2-7 give a good indication of the effect of blanketed strands on elastic and time dependent deflections. The ends, quarter span, and mid-span points are represented, and those points are connected by straight lines to aid in visualization of the profile. The draped strand beam profile is clearly the familiar parabolic type. The blanketed strand beam profile, however, is not so simple.

By referring to Fig. 2-4, it can be seen that the stress gradient at various sections of the blanketed strand beams, carrying only their own weights, varies from a relativley low value at ends to higher values at mid-span. Between the ends and quarter span sections, the gradient diverges, and one would expect the deflection profile to be concave upward along that region. Over the central region, the gradient gradually increases to a uniform value at 8 ft. from mid-span. Such a stress variation between top and bottom of

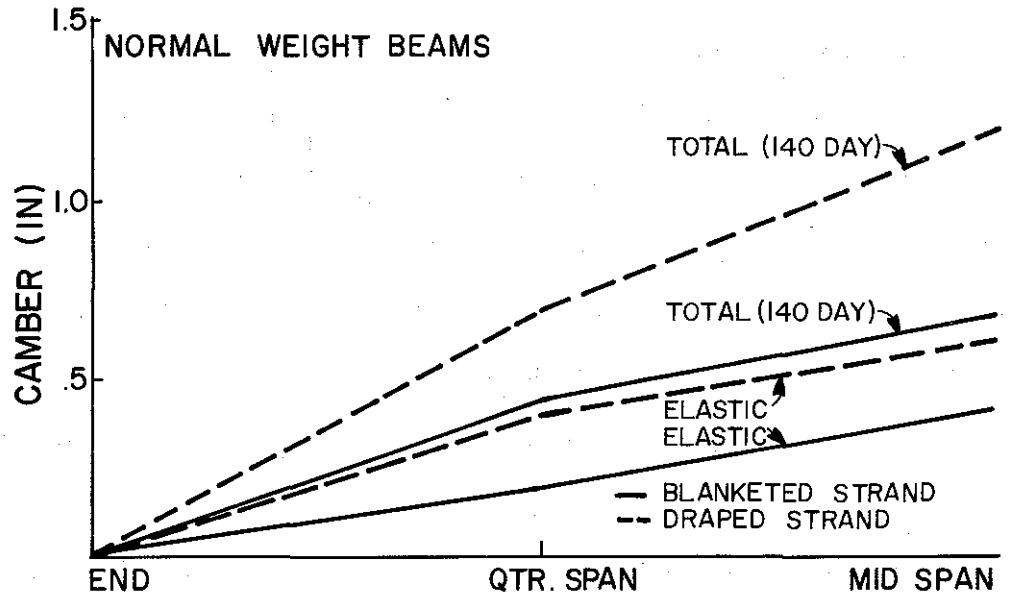

POSITION ALONG BEAM

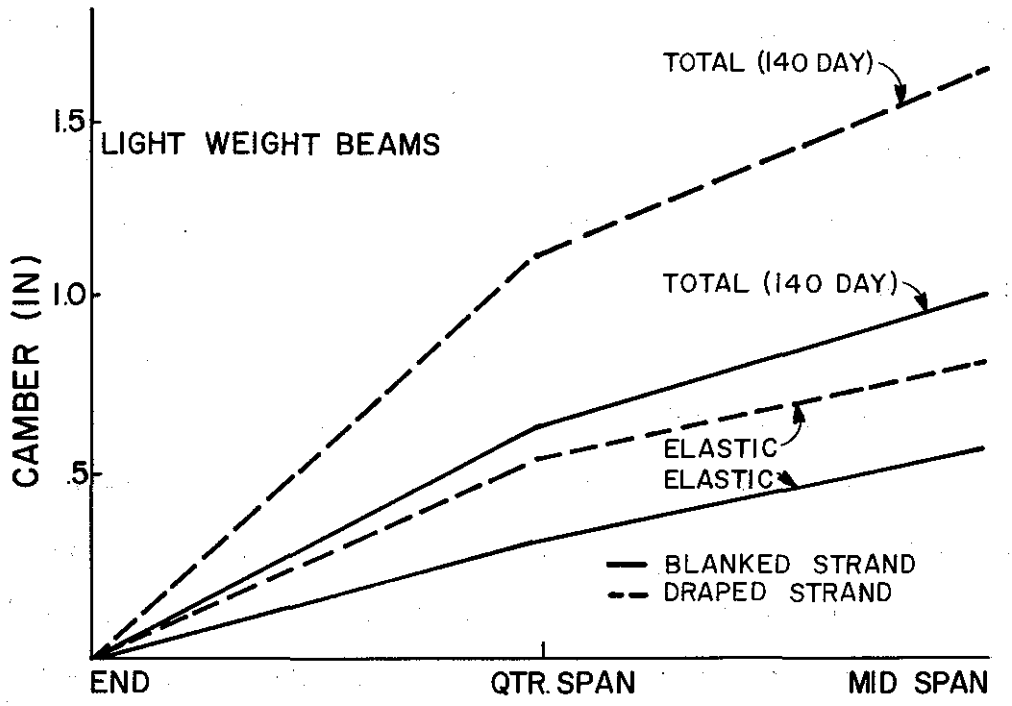

POSITION ALONG BEAM

FIGURE 2.7 CAMBER PROFILES

beam would produce a concave downward type of curve. By that reasoning the blanketed strand beam profile reverses curvature between the end and mid-span. Such a curve would fit the points shown in Fig. 2-7. It is very likely that the difference in strains at top and bottom of the beam in the central region of the span accounted for most of the blanketed strand beam camber.

C. Prestress Loss

The losses in pre-release steel stresses are tabulated in Table 2.4. They were computed by dividing the product of strain and modulus of elasticity by pre-release stresses. Strains at the level of the centroid of prestressing steel were used for the computations.

The variations of prestress losses with time at Stations A, C, and G corresponding approximately to the end, quarter span, and mid-span stations, are shown in Fig. 2-8.

The loss of prestress that is of primary interest to the designer of simply supported beams is that at mid-span. However, if prestress just sufficient to resist imposed loads is designed into the beam, the loss at every section becomes of equal importance. That is the condition approached, but not entirely realized, in the blanketed strand beams of this series. Ideally, stresses would be low at beam ends and would increase toward mid-span to meet the demands of anticipated loads. Prestress losses in such a situation would vary somewhat like the stresses.

The trend of losses shown in Table 2.4 follows the above reasoning. Draped strand beam losses are lower at ends than at mid-span, of course, but the difference is not so great, percentage wise, as for blanketed strand beams.

TABLE 2.4 PRESTRESS LOSSES IN STEEL

AGE	BEAM	PRESTRESS LOSS (%) (End) Sta A	Sta C	Sta E	(Midspan) Sta G
Release	NW	3.5*	5.6	6.8	6.5
	NWB	2.5	4.8	5.3	6.5
	LW	7.5	8.2	8.7	8.5
	LWB	3.0	6.2	7.4	8.5
140 day	NW	9.5	13	14	14
	NWB	6.5	10	12	13.5
	LW	14.0	15.5	16	16.5
	LWB	7.5	13	15	16.5

*Estimated.

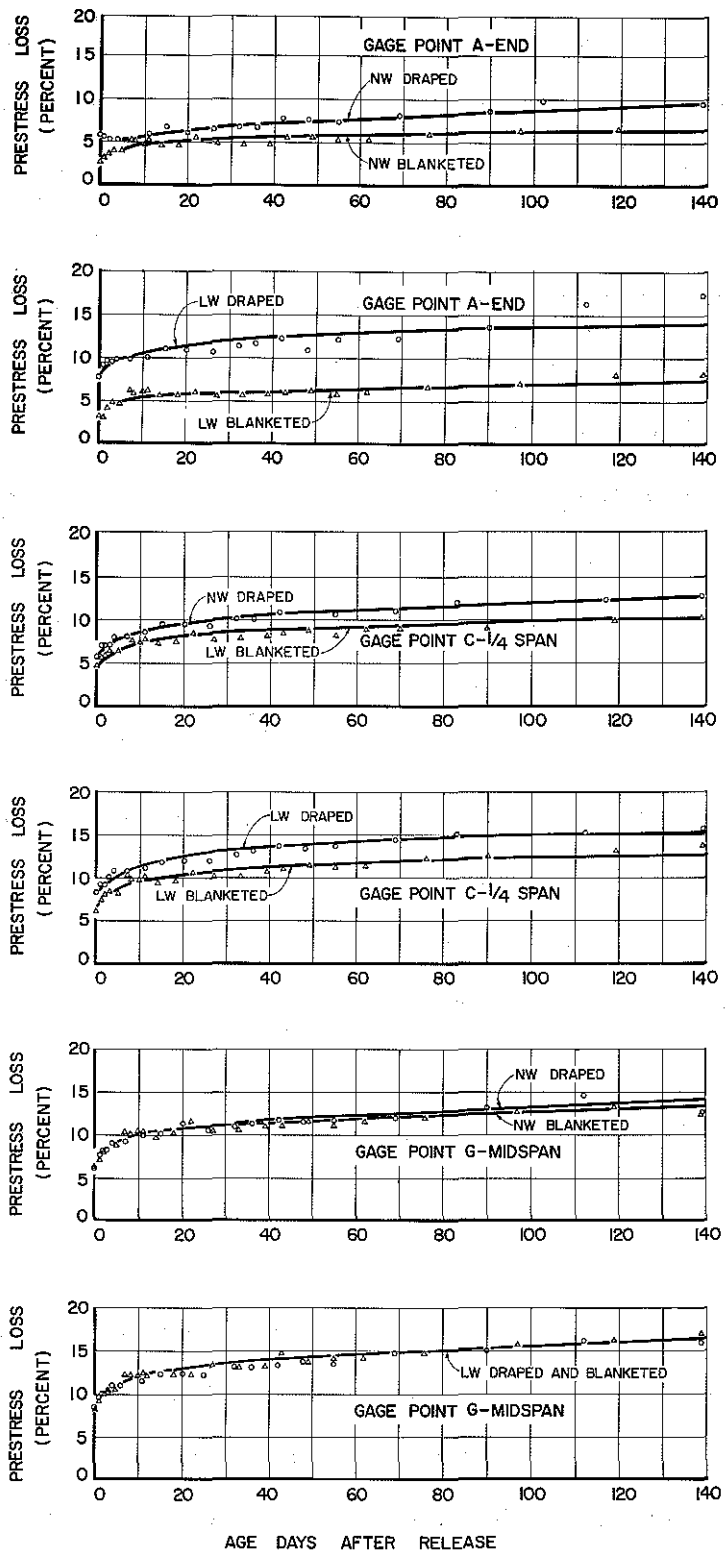

FIGURE 2-8 PRESTRESS LOSS

Mid-span losses at the end of the tests were about the same for the two beams of a given concrete. Normal weight concrete losses were about 14% and lightweight 16 1/2%. There is not as much difference in losses for these two concretes as was found in tests of Houston beams (1). At 140-day age the Houston beams had almost stabilized, and the 56 ft. normal weight and lightweight beams had lost 15% and 22% respectively of the initial prestress at 140-day age. Normal weight concrete losses were about the same for the two sets, but the Houston lightweight series lost considerably more prestress than the present series. Differences in curing methods and slight differences in mixes could account for at least some of the differences in behavior.

2.7 Conclusions

Results of the tests on four full size pretensioned prestressed highway bridge beams show that:

A. Blanketed strand beams can be designed to have less elastic and time dependent camber than draped strand beams.

B. Mid-span prestress losses for a given concrete were about the same for the designs studied.

2.8 Remarks:

Blanketed strand beams require a little more design time than do draped strand beams, but the additional effort is not excessive. There appears to be some advantage in the former type in that hold-downs are not required in the fabrication process thereby somewhat

simplifying construction. Camber is reduced by blanketing, and in larger spans with deeper beams a comparison of blanketed strand design with the normal draped strand type possibly should be made by the designer.

Disadvantages in blanketed strand beams are: (1) blanketing operations during fabrication must be carefully supervised, (2) there is a question of location of the section of full bond of blanketed strands near the end of broken bond, and (3) the effects on ultimate load capacity and repeated load capacity of blanketed strands are not known.

The designer can determine the layout of prestressing strands necessary for producing a desired camber in his beams by means of computer program in the Appendix. A plot of deflection versus eccentricity of strand can be produced from deflections found from different input eccentricities. Such a plot is almost linear. Desiring a given camber at time of construction, one might enter the chart with desired camber and read eccentricity of prestressing steel necessary for that camber. He must, however, realize that concrete stresses change with eccentricity, and he should always check for overstress.

CHAPTER 3

CREEP, CAMBER, AND PRESTRESS LOSSES - HOUSTON BRIDGE

3.1 Introduction

The bridge studied in this chapter was introduced in a previous report (1) in which details of a study of the prestressed beams fabricated for the Houston, Texas Urban Expressway test bridge were given. Details of the study which continued approximately one year subsequent to that report, are given in this chapter. The period of primary concern here begins at about 320-day age of the beams when the deck slabs were cast. The bridge, although not open to the public, was opened to construction traffic about one month after the deck was cast.

In order to prove a method proposed for predicting time dependent strains, camber, and prestress loss, measurements of strains and elevations were collected from the structure. At the beginning, the prestressed beams were instrumented in the casting yard and measurements were made for strains and elevations before the prestress was applied, after it was applied, and periodically thereafter until the end of the test. Those strains and elevations were compared with corresponding values computed from a step-by-step method discussed in detail in Ref. 1. Prestress losses computed from strain measurements were also compared with values predicted by the step-by-step method.

After the slab was cast the problem of predictions became considerably more complicated because of restrained differential shrinkage

and creep between the cast-in-place slab and the precast prestressed beams, and the different properties of beam and slab concretes.

Branson (3) summarized the work of Bartlett and Birkland, among others, in outlining the composite section method of analysis used here for accounting for differences in free strain of slab and beam. Hasnat (4) concluded, from laboratory beam tests, that stresses predicted by that method were in good agreement with his test results.

Briefly, the composite section method permits the slab and the beam to strain freely. Equal and opposite forces are then applied to the slab and beam, at their interface, sufficient to bring those elements back together. The forces so applied are then used to find the axial and bending components of stresses in slab and beam due to that action. Those stresses are then added to stresses computed earlier to produce total stresses for that instant of time.

Short time increments of five days were used for determining strain increments from test curves, and the beams were divided into 150 incremental lengths for purposes of computing cambers. A study by Sinno (6) showed that increments of this duration and length are entirely satisfactory for good precision.

The flow diagram for the computations is given in considerable detail in the appendix.

3.2 Description of the Test Bridge

Details of the bridge, the prestressed beams, and beam instrumentation are given in Ref. 1.

The dual bridges, separated by an open joint were designed for four 12 ft. traffic lanes over one 40 ft. span and three 56 ft. spans. The Texas Highway Department Type B prestressed concrete beams, spaced on 7' - 10 1/2" centers, supported the 7 1/4 in. deck slab during casting.

Information on beams and slabs is given in Table 3.1.

3.3 Objectives of the Study

The objectives of the study were:

A. Development of a method for predicting camber and prestress losses in the bridge.

B. Determine camber history of the deck.

C. Determine prestress loss in the beams.

3.4 Test Specimens

A. A number of 6 in. diameter x 12 in. long cylinders were cast on location from slab batches. Those specimens were used for strength and modulus tests of the concretes used in the slab.

B. Two shrinkage prisms and two creep prisms, 3 in. x 3 in. x 16 in., were cast with each instrumented slab in the bridge. Those prisms were instrumented with mechanical gage points set 10 in. apart on two opposite long sides of each of the prisms. They were prepared and treated in the same way as those described in Ref. 1, and dimensional details, too, were the same.

The creep prisms were mounted individually in frames and loaded to 1500 psi compression in a universal testing machine.

TABLE 3.1 BEAM AND SLAB DESIGNATIONS

Bridge	Span Number	Type of Instrumentation	Beam Designation	Span (ft)	Concrete Beam	Type Slab	Date Cast	
							Beam	Slab
Left	1	El.[1]	L1-1	40	LW	LW	8/24/66	6/28/67
		El.	L1-3	40	LW	LW	8/24/66	
		S[2] & El.	L1-5	40	LW	LW	8/24/66	
		El.	L1-6	40	LW	LW	8/24/66	
		El.	L1-8	40	LW	LW	8/24/66	
	2	None	None	56	LW	NW		
	3	El.	L3-1	56	NW	LW	9/10/66	8/7/67
		El.	L3-3	56	NW	LW	9/10/66	
		El. & S	L3-5	56	NW	LW	9/10/66	
		El.	L3-6	56	NW	LW	9/10/66	
		El.	L3-8	56	NW	LW	9/10/66	
	4	El.	L4-1	56	LW	LW	9/10/66	7/12/67
		El.	L4-3	56	LW	LW	9/10/66	
		El. & S	L4-5	56	LW	LW	9/10/66	
		El.	L4-6	56	LW	LW	9/10/66	
		El.	L4-8	56	LW	LW	9/10/66	
Right	1	El. & S	R1-5	40	LW	LW	8/27/66	7/27/67
	2	El.	R2-5	56	LW	LW	9/16/66	
	3	El.	R3-5	56	NW	LW	9/10/66	
	4	El. & S	R4-5	56	LW	NW	9/1/66	7/26/67

1. Elevation.
2. Strain.

That stress was maintained by heavy helical springs confined between the prism and the frame. Details of the arrangement are shown in Fig. 5-3 of Ref. 1.

The shrinkage prisms were never loaded, and they served to provide control measurements of strain (shrinkage) to be used in determining creep per psi in the creep prisms.

C. The prestressed beams and their companion 4 ft. long non-loaded shrinkage specimens, described in Ref. 1, continued under test throughout the period. The beams were hauled on pole trailers to the bridge site and were erected by mobile crane. They were approximately 10 months old when erected.

D. The deck slab, 7 1/4 in. thick, was made of lightweight concrete in all except spans L-2 and R4. Fig. 3-1 and 3-2 and Table 3.1 give details of the slab.

Two sets of mechanical gage points were installed on the top and bottom of the slab at each beam gage station. The bottom gages were set directly below those on the top surface. One set was located midway between beams 5 and 4, and the other was set 3 in. out from the top vertical face of beam 5 on the side toward beam 4. See Fig. 3-3.

A bottom-of-slab gage, then, was located 3 in. from the top gage on a beam, as close as possible for required clearance in gaging. The other one was set as far away from the beam gage as possible to still be at the same station.

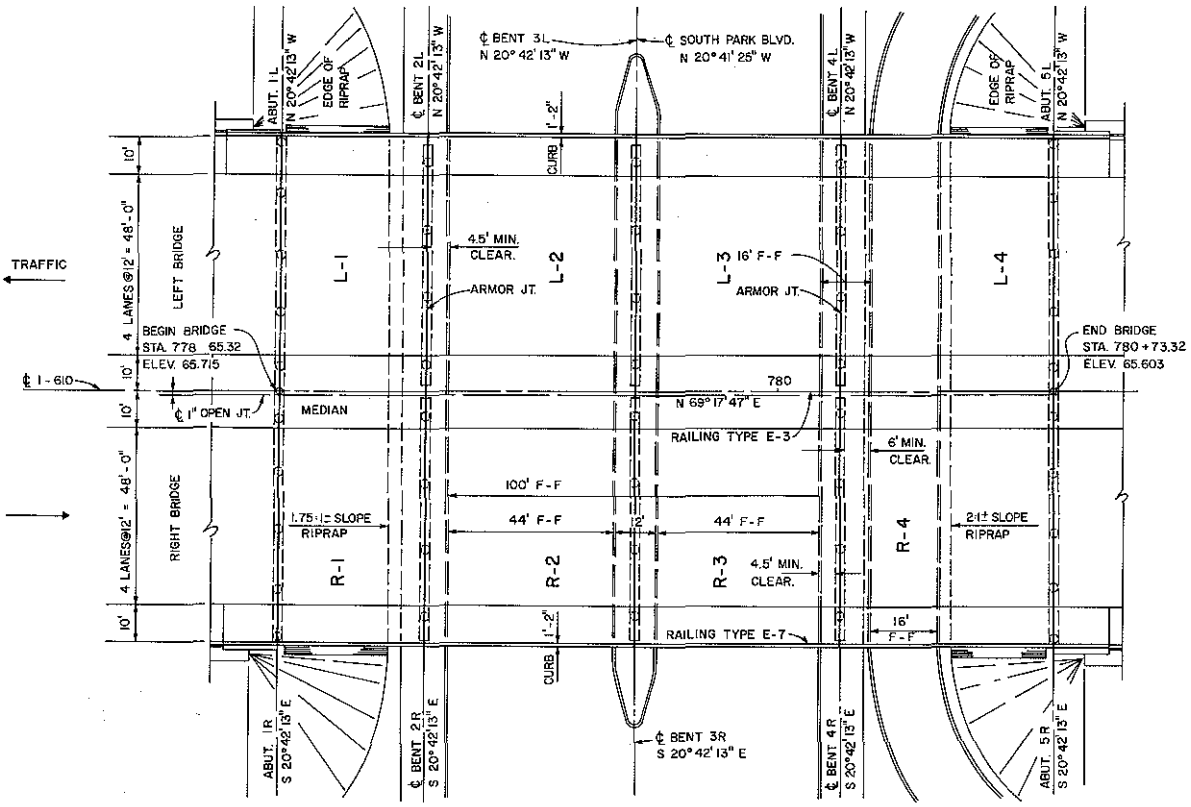

PLAN VIEW

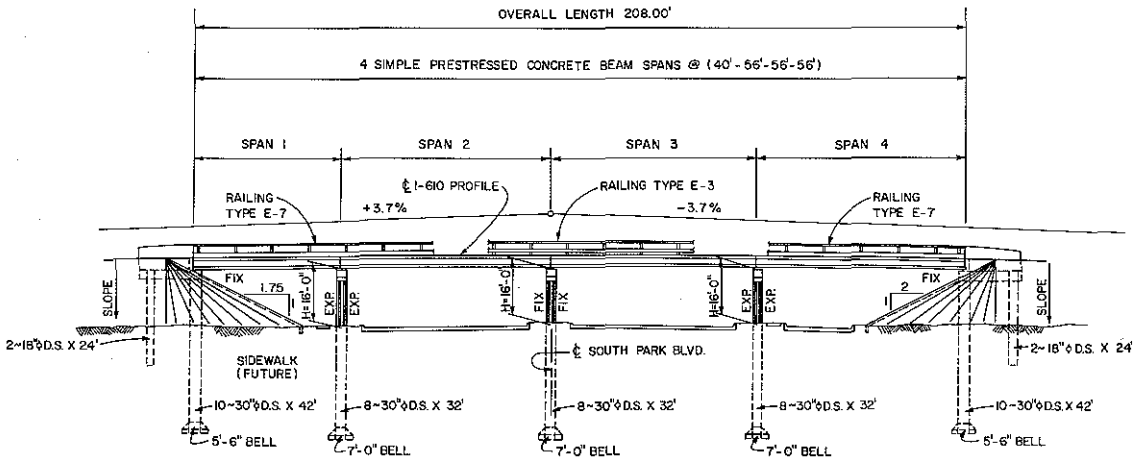

ELEVATION VIEW

FIGURE 3-1 GENERAL PLAN OF BRIDGE

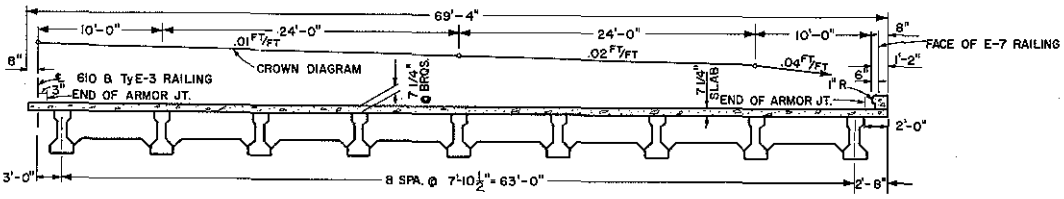

CROSS SECTION-WESTBOUND
SHOWING INTERIOR DIAFRAMS
LOOKING IN DIRECTION OF DECREASING STATIONS

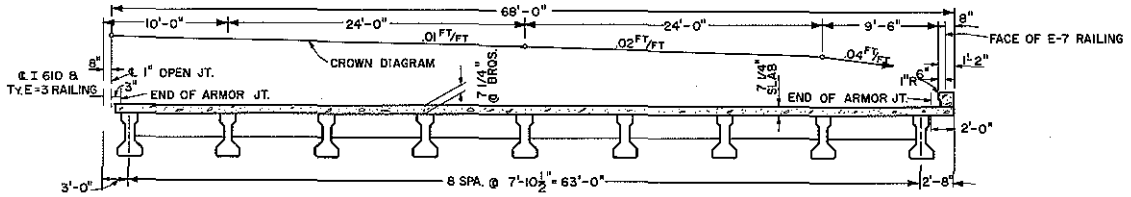

CROSS SECTION-EASTBOUND
SHOWING EXTERIOR DIAFRAMS
LOOKING IN DIRECTION OF INCREASING STATIONS

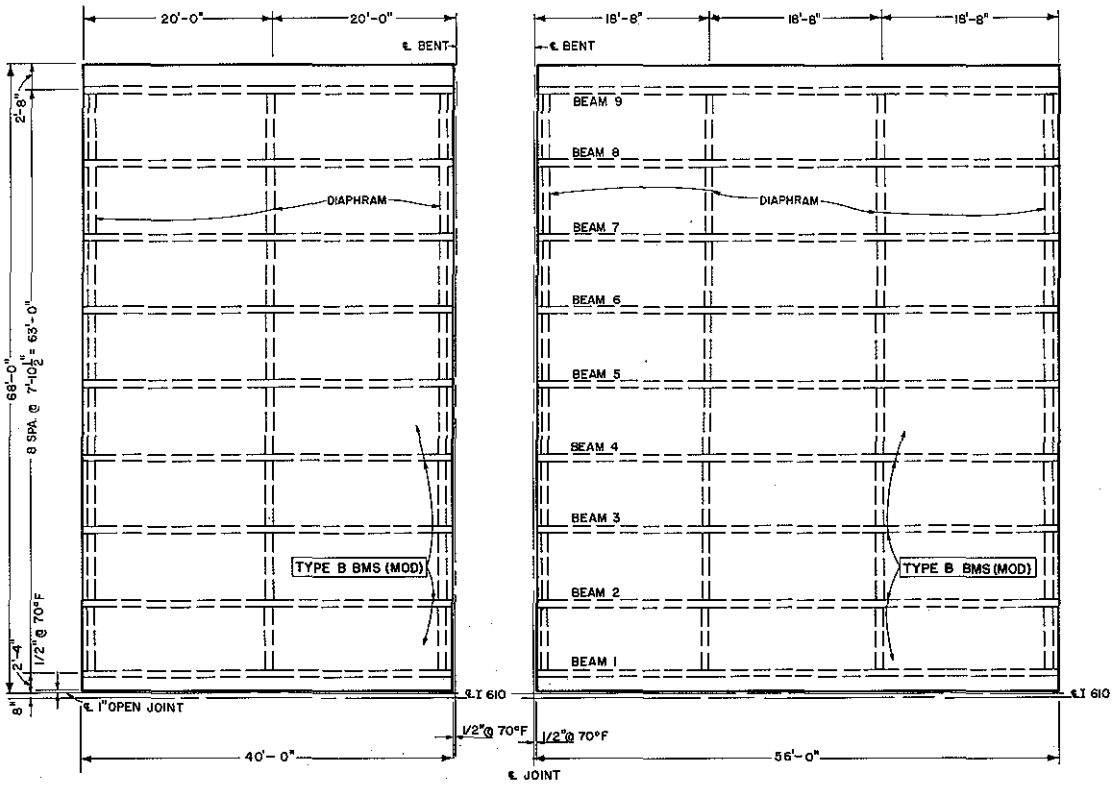

TYPICAL 40'-0" SPAN
PLAN

TYPICAL 56'-0" SPAN
PLAN

FIGURE 3-2 BRIDGE PLAN AND SECTION DETAILS

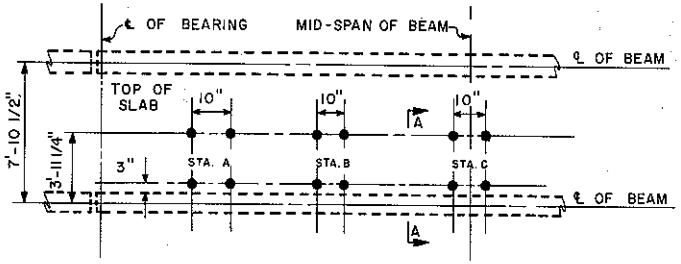

SLAB PLAN

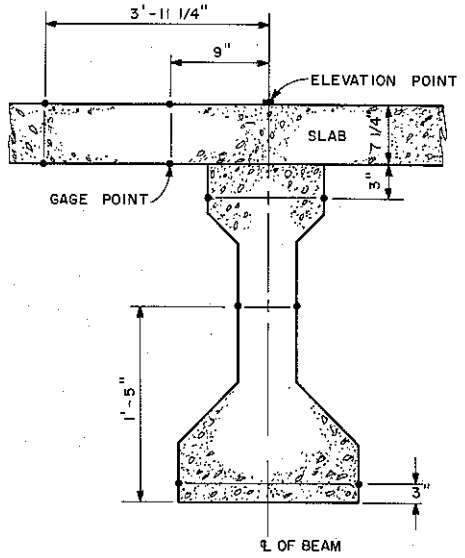

SECTION A-A

(a) GAGE SLAB POINTS

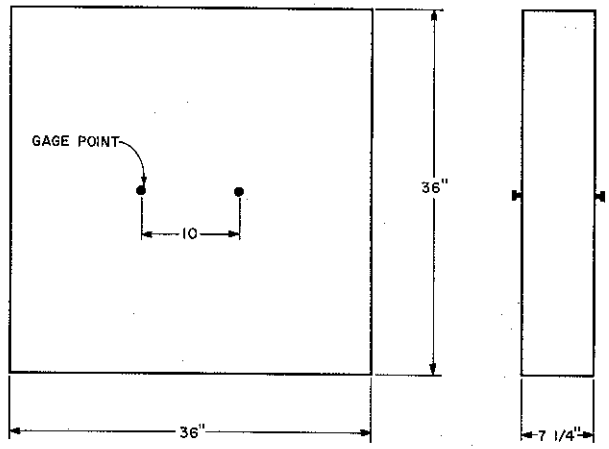

(b) SLAB SHRINKAGE SPECIMEN

FIG. 3-3 SLAB GAGES AND SHRINKAGE SPECIMEN

The slabs were cured under wet mat six days from the time of finishing. The wood bottom forms remained in place at least until the wet mat cure was complete.

E. One 3 ft. square shrinkage slab 7 1/4 in. thick was made for each instrumented deck slab. It was cast from the slab batch, and was instrumented by a set of mechanical gage points centered on one principal axis on each 3 ft. square surface. These specimens were never loaded, their purpose being to serve as shrinkage control specimens for the reinforced slab.

In order to begin collection of strain data as soon as possible, the slab shrinkage specimens were stood on one edge after hardening, and the wood forms were then removed. They were then blanketed with a heavy quilted cotton mat which was kept wet throughout the curing period of the companion slab.

3.5 Materials

The THD Class A, 5 sack, normal weight concrete had a water to cement ratio of 0.50, and a weight ratio of sand to gravel of 1.00 to 1.75. Slumps varied from 2 in. to 3 1/4 in.

The THD Class X, 5 1/2 sack, lightweight concrete used natural sand fines and the same expanded shale coarse aggregate as used in the beams. A slump averaging about 3 1/2 in. was obtained from the mix with a weight ratio of sand to C.A. of 1.22 to 1.00.

Air entraining and dispersing agents were used in both mixes. Air, by pressure meter, was nominally 5% for NW and 8% for LW.

Table 3.2 provides data on strength, secant modulus, and weight of the concrete. Different methods of curing were used by Texas Highway Department and Texas Transportation Institute, and cylinder strengths in that table reflect those different methods. Values of secant moduli were developed from tests on cylinders cured under the same conditions as the slab.

3.6 Tests

A. Concrete compressive strength tests were performed by the Texas Highway Department on cylinders handled according to its specifications.

Stress-strain tests were made on 6 in. diameter x 12 in. long cylinders cast in cardboard molds. Those cylinders were cured at the bridge site under a wet mat, the same as used in slab cure. After curing, they were stored in open air until tested. Strains were averaged from 6 in. gage length readings from 4 dial gages spaced at 90 degrees on the cylinders. The secant modulus at 1/2 f'_c was determined from averaging strains from three cylinders for each test.

Strength and stress-strain tests were made on the creep prisms incidental to their restrained load tests. Those strength tests were not planned in the formal program, and only limited data were collected.

B. Shrinkage and creep tests on specimens cast in 1967 from beam concrete continued throughout the period. Those specimens and tests are described in Chapter 5 of Ref. 1.

TABLE 3.2. SLAB CONCRETE PROPERTIES

			THD Test*			TTI Test **		
Slab	Type	Age	f'_c (psi)	Unit Wgt. (Dry) (pcf)	Speciman	f'_c (psi)	$E_{\frac{1}{2}f'_c}$ (ksi)	Specimen
LS-1	LW	1 da 10 hr	-	-		2222	2273	prism
		2 da 5 hr	-	-		2611	2653	prism
		7 day	-	-		3277	3080	prism
		7 day	4710		cyl	3893	3100	cyl
		8	-	-		-	3100	prism
		28	5677	112.0	cyl	4144	3234	cyl
LS-2	NW	7	4207					
LS-3	LW	5				2220	3160	prism
		7	4470		cyl	2890	3211	prism
		10				3260	3684	cyl
		28	5090	110.4	cyl	4200	3281	only 1 cyl
LS-4	LW	3	-			3111	2936	prism
		7			cyl	3556	3175	prism
		7	3837			3397	3192	cyl
		28	4823	111.1	cyl	5055	3010	prism
RS-1	LW	5				3944	3130	prism
		7				4000	3000	prism
		7				(3092)	2920	cyl
		28	4720	112.4	cyl			
		32				4233		cyl
		89				4529		cyl
RS-2	LW	7	4603		cyl			
		28	5433	110.4	cyl			
RS-3	LW	7	4197					
		28	5217	110.3				
RS-4	NW	5				2667	4677	prism
		7				3333	4630	prism
		7	3990			2950	5017	cyl
		33				3778	4500	prism
		90				3816	5021	cyl

* Std. test of and by THD personnel; cyls from water bath cure.

** Specimens field cured under same condition as slab; air dry at test;
1 - Prisms loaded to 3 kips three times before recording;
3 - Cyls loaded to 30 kips three times before recording.

Shrinkage and creep tests were carried out on the prisms cast with each instrumented slab, and shrinkage tests were made on the 3 ft. square slab specimens. Test procedures and methods were the same as reported for similar specimens in Chapter 5, Ref. 1.

C. Strain measurements on five prestressed beams were continued throughout the test. Those measurements are discussed in Ref. 1, and details on gage point locations and beams are given in Tables 5.1 and 2 of that report. Briefly, the beams were 40 ft. and 56 ft. THD Type B pretensioned prestressed beams gaged with mechanical gage points on both sides at one end, one quarter span point, and at mid-span near the top and bottom and mid-depth of the beams. Strain readings read from a demountable gage over a 10 in. gage length were taken before and after release, before and after slab casting and periodically throughout the test period.

D. Strain measurements were made on each of the two top-of-slab gages and the two bottom-of-slab gages. The first readings were made on the day after casting, and they continued periodically until the close of tests almost one year later. Daily readings were taken for 5 days, weekly readings for one month, then from two to four week intervals elapsed between readings.

E. Elevation readings were taken from elevation points on beams throughout the test period. Those points, cast in the beams when they were fabricated, were covered with slab concrete from a fraction of an inch to 1 1/2 in. when the slab was cast. The

tops were uncovered while slab concrete was still plastic so that uninterrupted continuity in elevation readings could be realized.

Readings were made before and after forms were placed; before and after steel was placed, and before and after slabs were cast. Those readings were made on the same time schedule as strain readings.

All readings of bridge elevation and strains were made early during the day beginning at or before sunrise. The direct rays from the sun had little time to act on the structure before readings were taken.

3.7 Test Results and Discussion

A. Strength and Secant Modulus of Slab Concrete

Some cylinder tests were made by THD, and others were made by TTI. Conditions of treatment of specimens were different in the two sets of tests, and it is only for that reason that both sets of values are given. The secant moduli were determined from TTI tests and it is deemed advisable to give TTI breaking strengths, too, to answer questions that might arise about correlation of values.

THD Test results: Tests made by THD included measurement of air content by pressure meter, unit weight, and breaking strength. The results of those tests are shown in Table 3.2. The cylinders were cast in steel molds and cured in water, and values shown for THD strength represent the average of 3 breaks on cylinders removed from the bath shortly before the test.

TTI Tests: Breaking strength and secant modulus for both cylinders and 3 in. x 3 in. x 16 in. prisms are given in Table 3.2 for tests made by TTI. Cylinders were cast in cardboard molds and field cured in the same way as the bridge slab and for the same period. Upon completion of the 6-day cure, specimens were stored in air in a small construction hut at the bridge site. Specimens tested before termination of the 6 day curing period were wrapped in wet mats then transported to the testing laboratory. They were removed from the wet mats about 2 hours prior to testing in a universal testing machine.

Strains from cylinders were taken over a 6 in. gage length from 4 dial gages equally spaced around the cylinder. The gage length on the 16 in. long prisms was 10 in., and strains were read from two opposite faces by a demountable gage from gage points set in the concrete. Except as noted in the table, the values shown for cylinders represent the average from three specimens. Values for prisms represent values from one specimen.

Although it is not a point to be studied at length here, it should be noted that the THD standard treatment of cylinders produced considerably greater strengths than was developed in the TTI cylinders cast in cardboard molds and field cured with the slab. Under TTI tests there is good agreement between

prism and cylinder secant moduli but strength values are not in good agreement, the cylinder strengths tending to be somewhat higher than the prism strengths. The greater length to thickness ratio for prisms; the greater influence of possible defects in the 9 sq. in. section of prism than the 28.3 sq. in. section of the cylinder; and the effect of shape might account for the differences. The secant moduli found in the tests are considerably higher than would be found from the current American Concrete Standard Building Code Requirements for Reinforced Concrete (ACI 318-63) (5) using test values for unit weight and breaking strength.

B. Shrinkage

Shrinkage in small prisms used as companion specimens to creep specimens is displayed in Fig. 3-4 for lightweight slab concrete; Fig. 3-6 for normal weight slab concrete; and in Fig. 3-10 for normal weight beam concrete. Shrinkages from those non-loaded specimens were deducted from strains read from spring loaded prisms to give creep in the stressed prisms. They are used in no other way in this work, but it is of some interest to compare values of the 4 different concretes, the beam concretes being about 660 days old at termination and slab concrete about 320.

Fig. 3-4, 6, 8, and 10 show that the LW prism shrinkage was more than that for the NW prisms in both beam and slab concretes. Terminal values at 660 days for beam concrete were 260

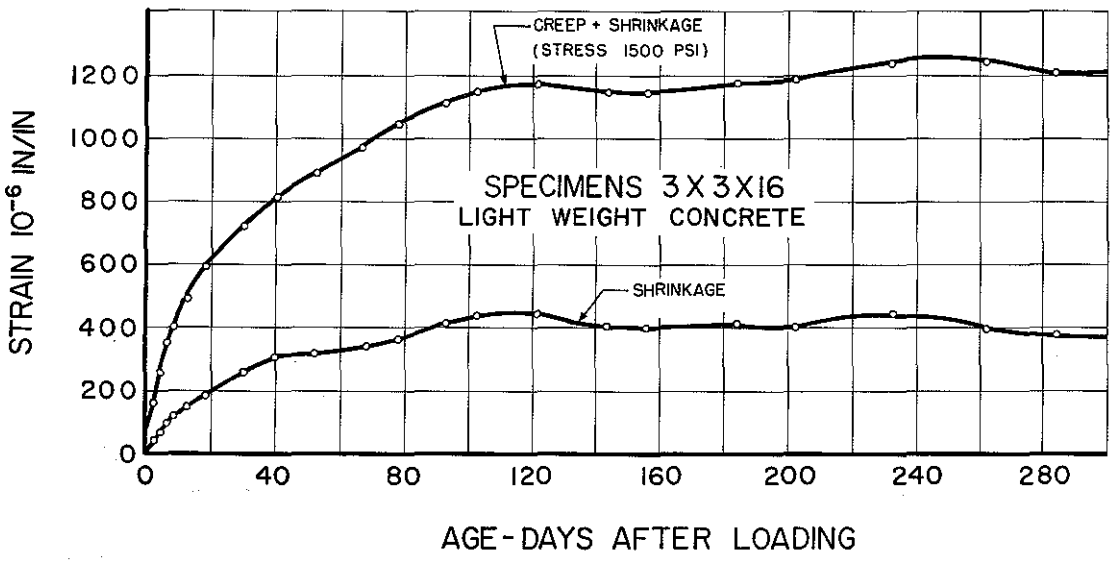

FIGURE 3-4 TOTAL CREEP AND SHRINKAGE OF SLAB CONCRETE (LIGHT WEIGHT)

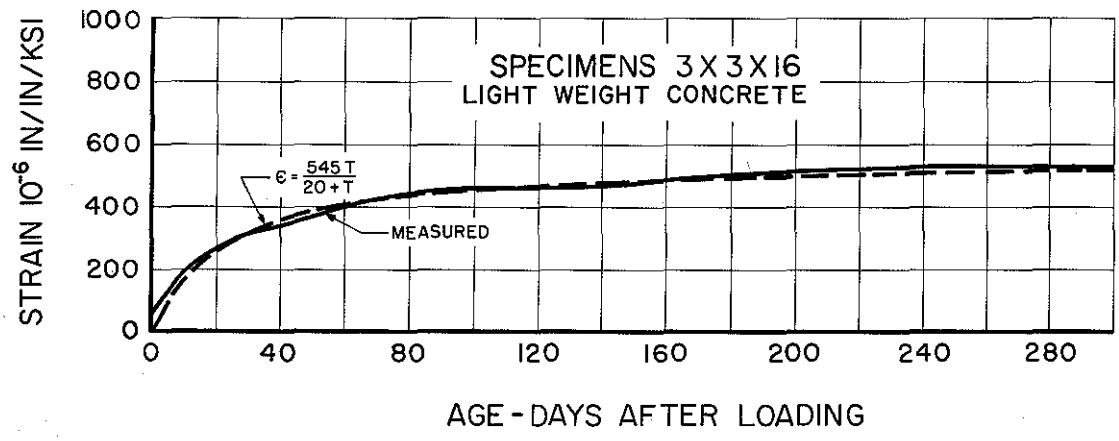

FIGURE 3-5 UNIT CREEP CURVE OF SLAB CONCRETE (LIGHT WEIGHT)

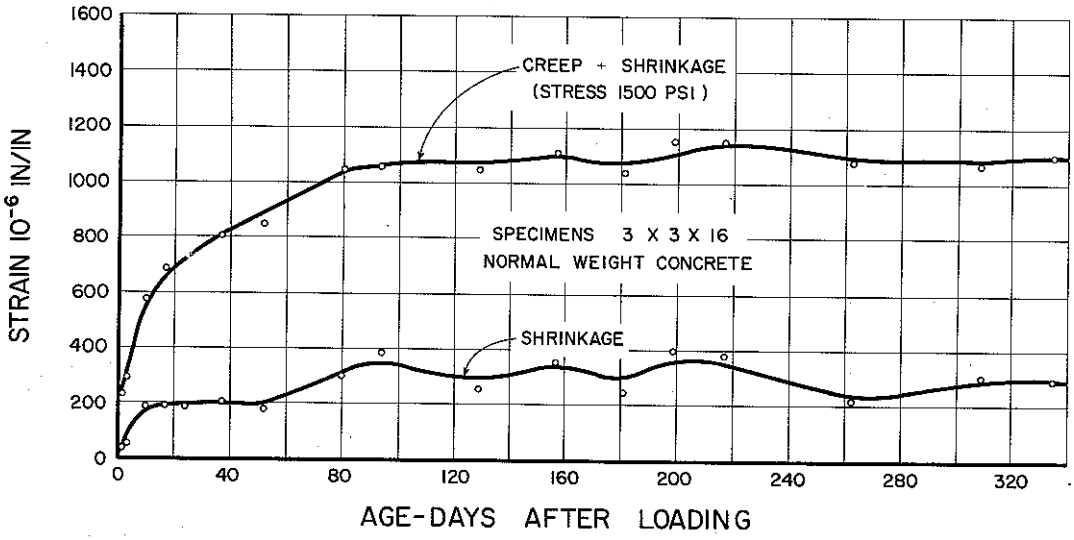

FIGURE 3-6 TOTAL CREEP AND SHRINKAGE OF SLAB CONCRETE (NORMAL WEIGHT)

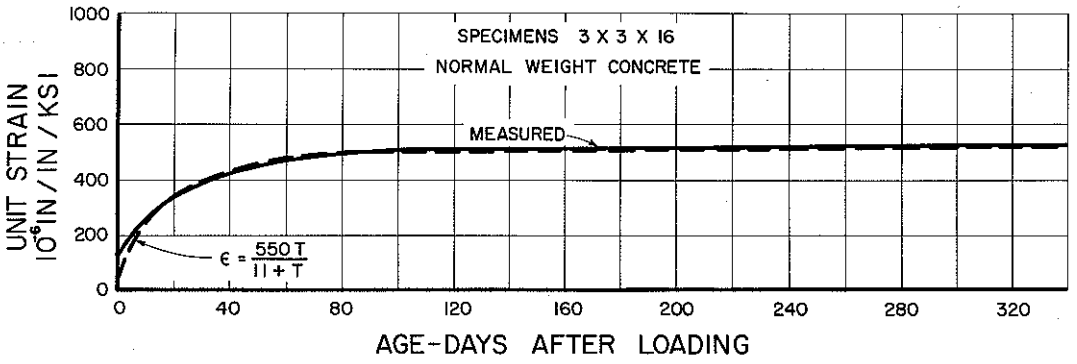

FIGURE 3-7 UNIT CREEP CURVE OF SLAB CONCRETE (NORMAL WEIGHT)

microinches for LW and 215 for NW, a ratio of 1.22. Corresponding values at 300 days for slab concrete were 370 and 285 microinches, giving a ratio of 1.30.

Both NW and LW slab prisms showed more shrinkage, 130% to 150%, than the beam prisms over the same age period. This was not over the same calendar period, however, the beams having been cast about 10 months before the slabs.

Shrinkages of the large specimens, 4 ft. long full section beams and 3 ft. square by 7 1/2 in. thick slabs, are of considerable interest because they were used in predicting strains in the bridge. Those specimens, being of the same section as the bridge elements and being relatively large, should have about the same shrinkage as the bridge members if all were free to shrink.

Shrinkage versus age plots for the non-loaded slab shrinkage specimens are shown in Fig. 3-12, NW concrete, and Fig. 3-13, LW concrete. The average of two gages, one on each 3 ft. square face, for one specimen is shown for NW concrete. The average of two opposite side gages on four specimens is shown for the LW concrete. The plots of shrinkage read from the latter specimens were so nearly identical that it would be difficult to discern differences on plots to the scale used here.

The non-loaded 4 ft. shrinkage beam shrinkages are shown in Fig. 3-14 for normal weight concrete and Fig. 3-15 for lightweight.

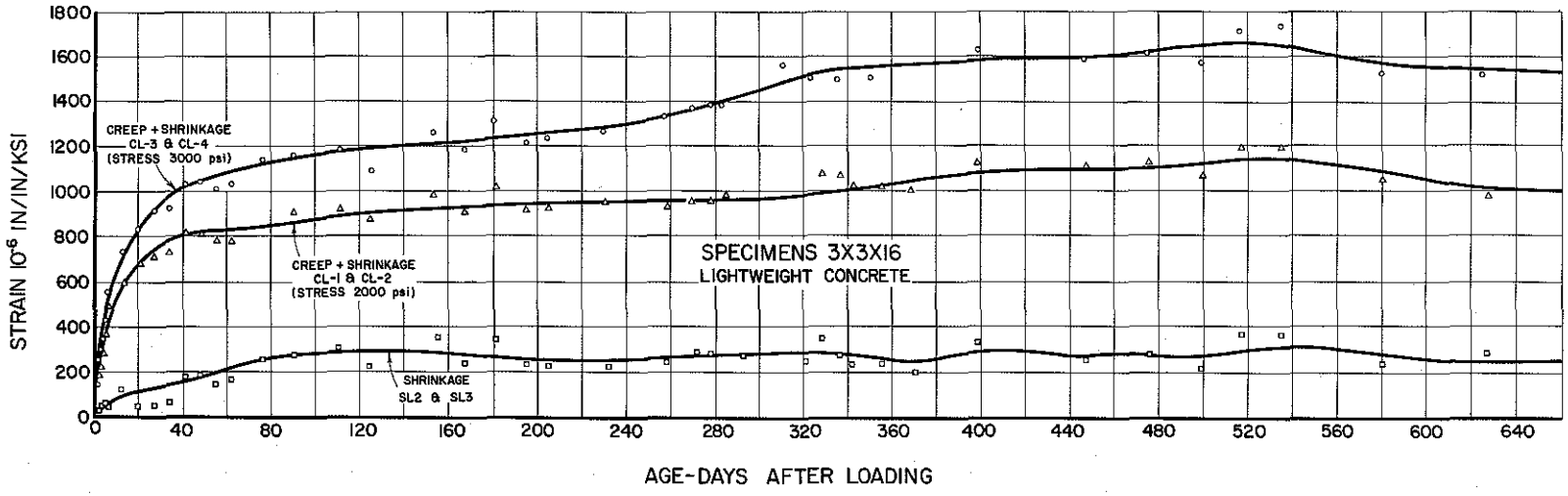

FIGURE 3-8 CREEP AND SHRINKAGE
IN 3X3X16 SPECIMENS
FOR BEAM CONCRETE (LIGHTWEIGHT)

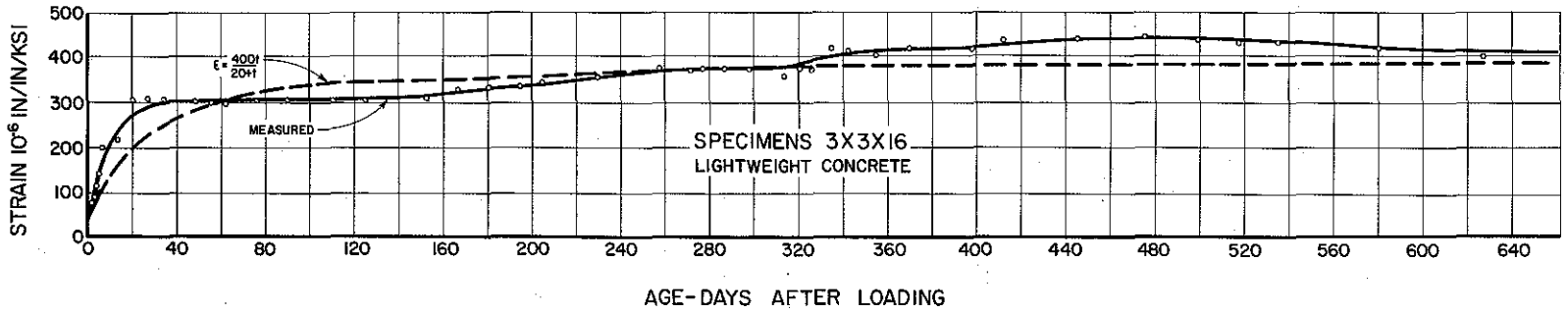

FIGURE 3-9 UNIT CREEP CURVE OF BEAM
CONCRETE (LIGHTWEIGHT)

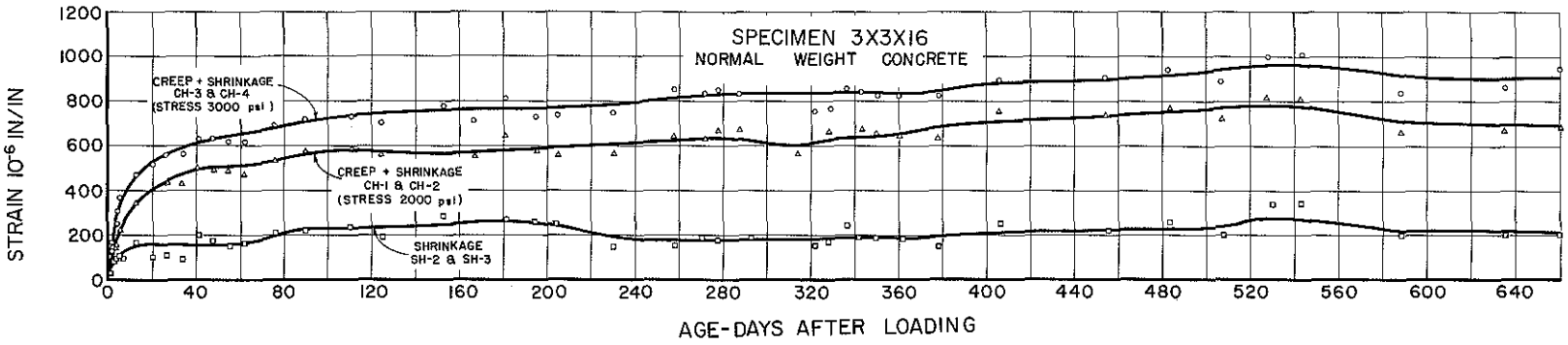

FIGURE 3-10 TOTAL CREEP AND SHRINKAGE OF BEAM CONCRETE (NORMAL WEIGHT)

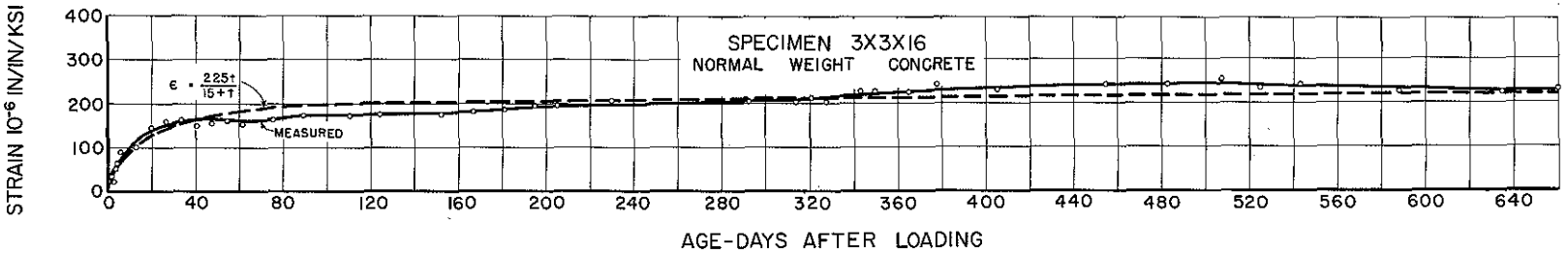

FIGURE 3-11 UNIT CREEP CURVE OF BEAM CONCRETE (NORMAL WEIGHT)

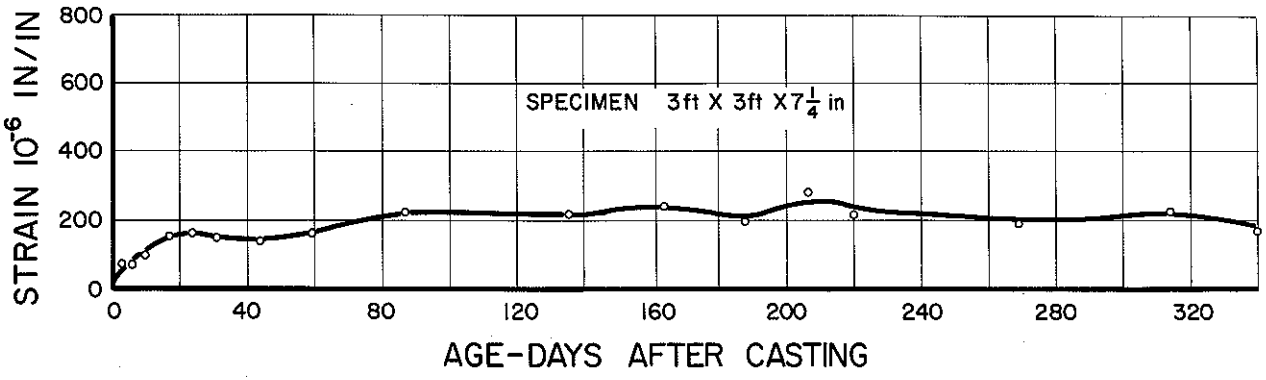

FIGURE 3-12 SHRINKAGE OF NORMAL WEIGHT SLAB

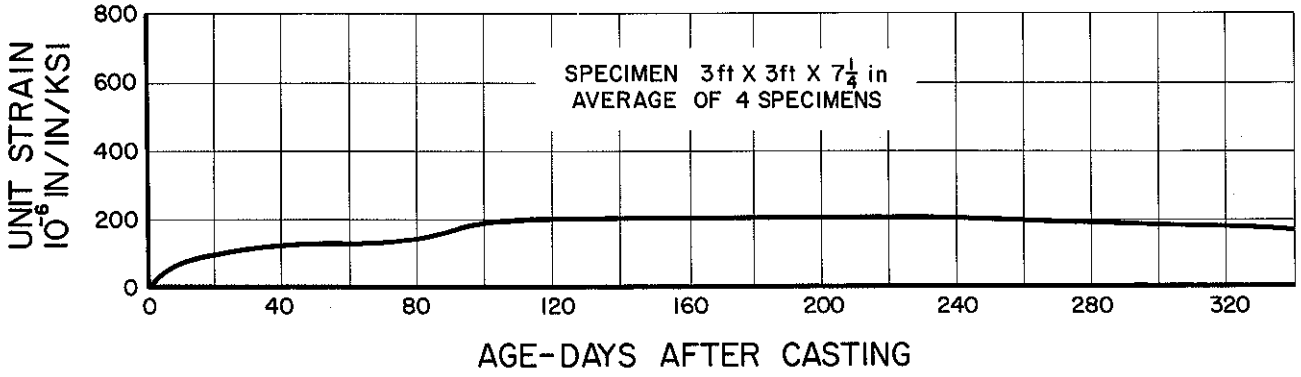

FIGURE 3-13 SHRINKAGE OF LIGHTWEIGHT SLABS

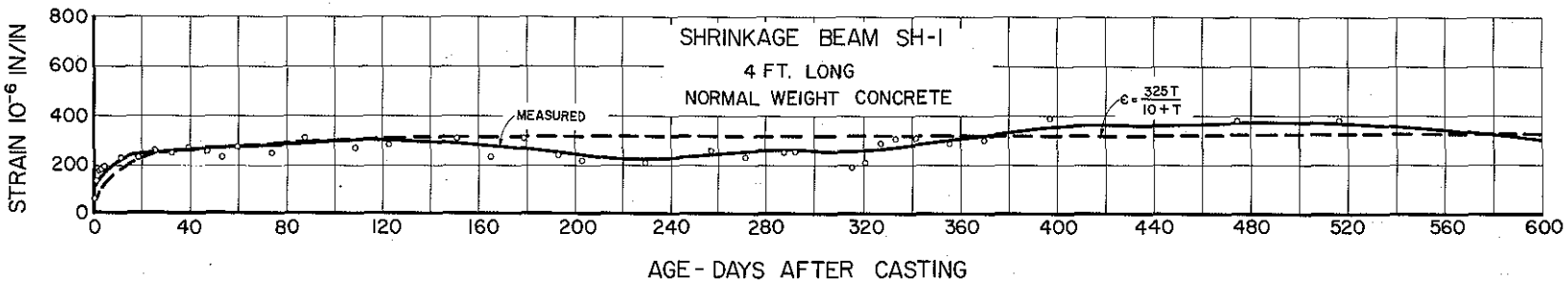

FIGURE 3-14 SHRINKAGE CURVE OF BEAM CONCRETE, (NORMAL WEIGHT)

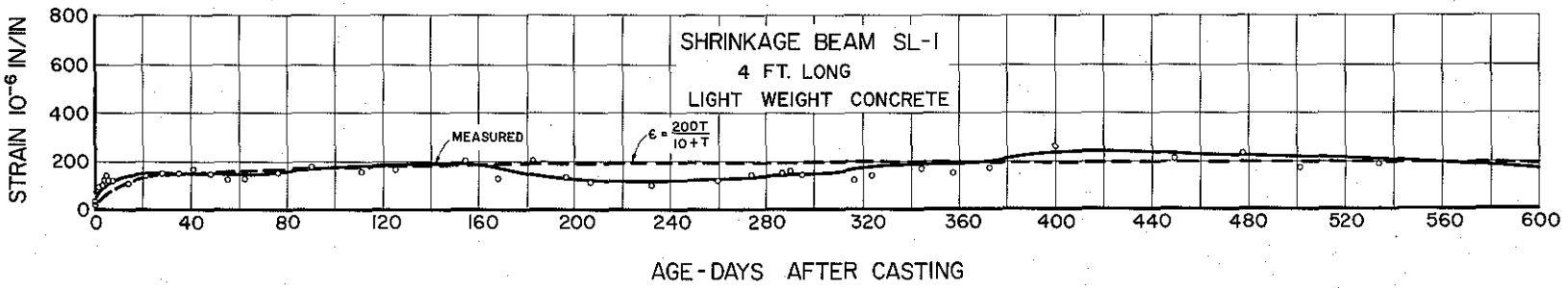

FIGURE 3-15 SHRINKAGE CURVE OF BEAM CONCRETE, (LIGHTWEIGHT)

Shrinkage at the LW slab specimen, Fig. 3-13, bears a close resemblance to the LW beam specimen, Fig. 3-15, in both magnitude and shape of curve. About 200 microinches of strain appears to be the value about which they fluctuate slightly.

Shrinkage of the NW beam specimen, on the other hand, Fig. 3-14, is somewhat higher than that for the slab specimen, Fig. 3-12. The former attains about 300 microinches of strain against some 200 for the latter. The difference appears to have occurred at very early age of the beam specimen when a rapid rate of shrinkage occurred. Comparisons of shrinkage from different size specimens of the same concrete show that NW beam prism shrinkage terminated at 210 microinches against 300 for the NW 4 ft. long full size section at the same terminal age. It would be expected that the former would have shrunk much more than the latter. No explanation can be given to explain the behavior.

The LW beam prisms terminal shrinkage was 240 microinches against about 200 for the LW 4 ft. long full size beam specimens. This is in the direction that one would expect, and size and shape factors would probably account for difference in magnitudes.

Deck slab NW concrete prism shrinkage, Fig. 3-6, was about 150% as much as that from the 3 ft. square specimen of NW slab concrete at termination, Fig. 3-12. The corresponding LW specimens, Figs. 3-4 and 3-13 showed about 200% as much shrinkage for the prism as for the slab.

The hyperbolic functional representations of shrinkage strains, see Ref. 1, Ch. 5, were changed for the beam specimens from those given in Figs. 5-13 and 5-14 of Ref. 1 to those shown in Figs. 3-14 and 3-15. The increased data collected over a larger period of time showed that the ordinates should be raised a little and that the shapes at early age would be changed only slightly. Those curves were used in predictions of beam strains, camber, and prestress losses which are to be discussed in sections that follow.

C. Creep in Small Specimens

Creep in specimens under sustained load is important here because it was used in predicting creep strains, camber, and prestress loss in full size prestressed beams, and in the composite beam-slab.

All sustained load prisms of slab concrete were loaded to 1500 psi and that stress was maintained by means of heavy helical springs as explained in Ref. 1. The total strain read from those specimens was reduced by the amount of shrinkage from the non-loaded prisms to give creep. Unit creep per ksi was obtained by dividing creep by the product of gage length and 1500 psi sustained stress.

Chapter 1 of Ref. 1 gives details of applying the unit creep in making predictions of creep in prestressed beams.

Unit creep in beam concrete was shown in Chapter 5, Ref. 1 for the first 300 days of the test. Those creeps are carried

to 660 days, termination of the test, in this report, Figs. 3-9 and 3-11. The extended portions covering 360 days to the end of testing show increases for both NW and LW specimens, but the increase is greater for LW.

Similar information for slab concrete is given in Fig. 3-5 for LW, and Fig. 3-7 for NW.

The unit creep of LW beam concrete is considerably greater than that of the NW beam throughout the history to termination at 660 days. Slab unit creep is, however, almost the same for both concretes.

D. Strains in Beams

Measurements of strain in five prestressed beams for a period of 660 days are represented in Figs. 3-16 to 3-21. Readings of strain were taken just before and just after prestress release, at beam erection, and at slab casting. The event of slab casting is clearly reflected in the plots at about 300-day age.

When the slab was cast the fibers elongated at the bottom gage and compressed at the top gage. Little change was noted in the gages at mid-depth, near the centroid of the beam. The mid-span gages showed the greatest strains at that event because of the higher bending moment at mid-span caused by the weight of the plastic slab. The strain curves for the first few days after casting of the slab have the characteristic shape of early creep curves.

Points on the curves are scattered somewhat, although care in measuring technique and time scheduling was followed. Some fluctuations due to seasonal changes may be noted in these plots as well as in the shrinkage curves of Figs. 3-4, 6, and 8. Weather information, temperature and relative humidity, Fig. 3-22, has been included to help explain those seasonal changes. Each point on the plot of temperature represents the average of 3 hour readings over a period of 10 days, and each R.H. point represnets the average over those same 10 days.

Strain predictions, made by the method outlined in detail in Ref. 1, and shown in the Appendix in the form of a computer flow diagram, are shown in Figs. 3-16 to 3-21 by dashed lines.

Predictions for L1-5 strains, Fig. 3-16, are good up to the time of casting of the slab. After that time there is considerable disagreement, especially at the end of the beam, station A. Terminal predictions, 660 day, are good for all of the other beams. Agreement of predictions with measured values at intermediate ages is generally fair to good.

These tests showed that strain measurements were very sensitive to changes, showing more scatter than the elevation measurements which did not appear to be so sensitive. Good agreement can be seen in camber in beam L1-5, for instance, over the entire test period whereas strains, as indicated above, are not always in agreement. Strain comparisons are

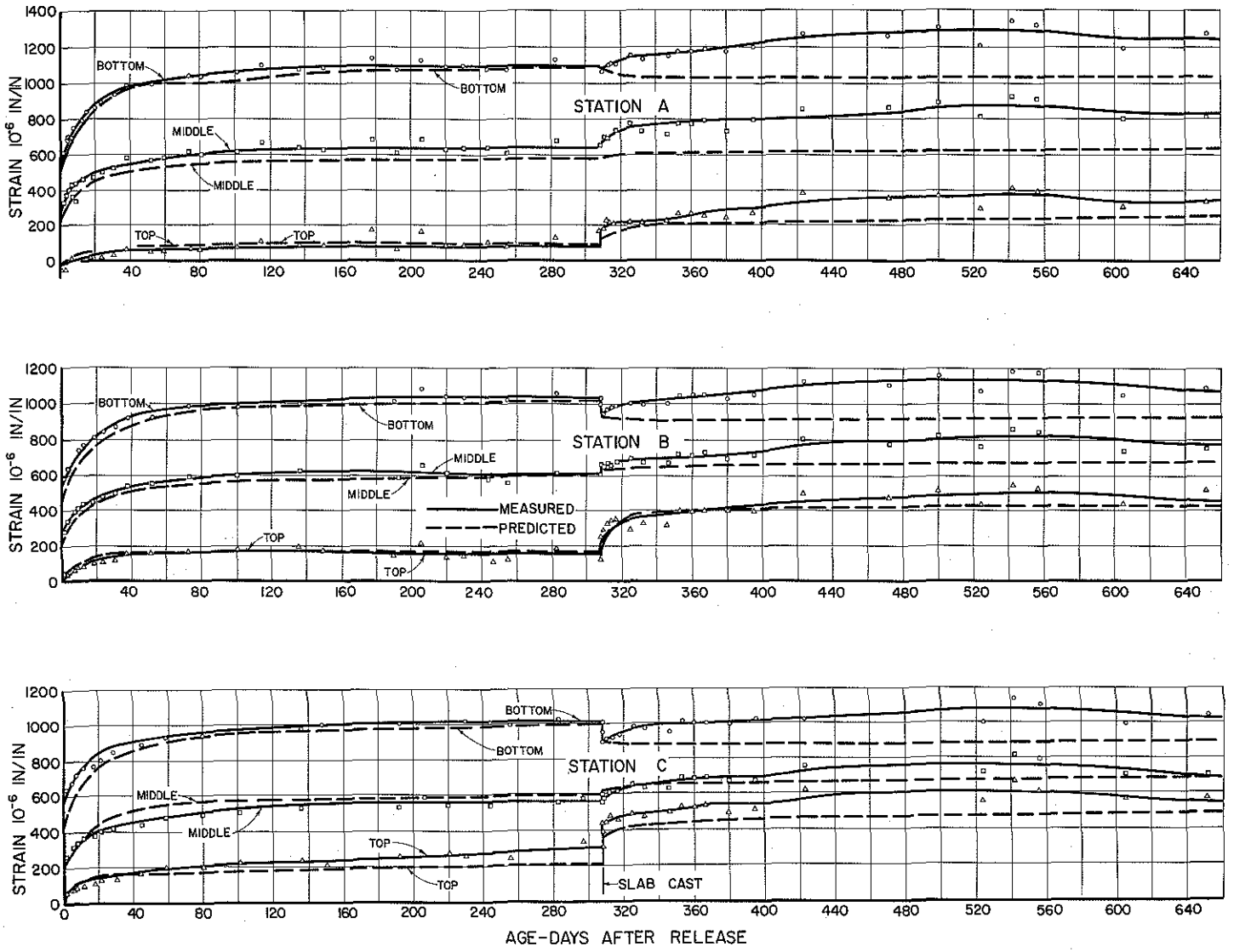

FIGURE 3-16 STRAINS IN BRIDGE BEAM LI-5 (LW)

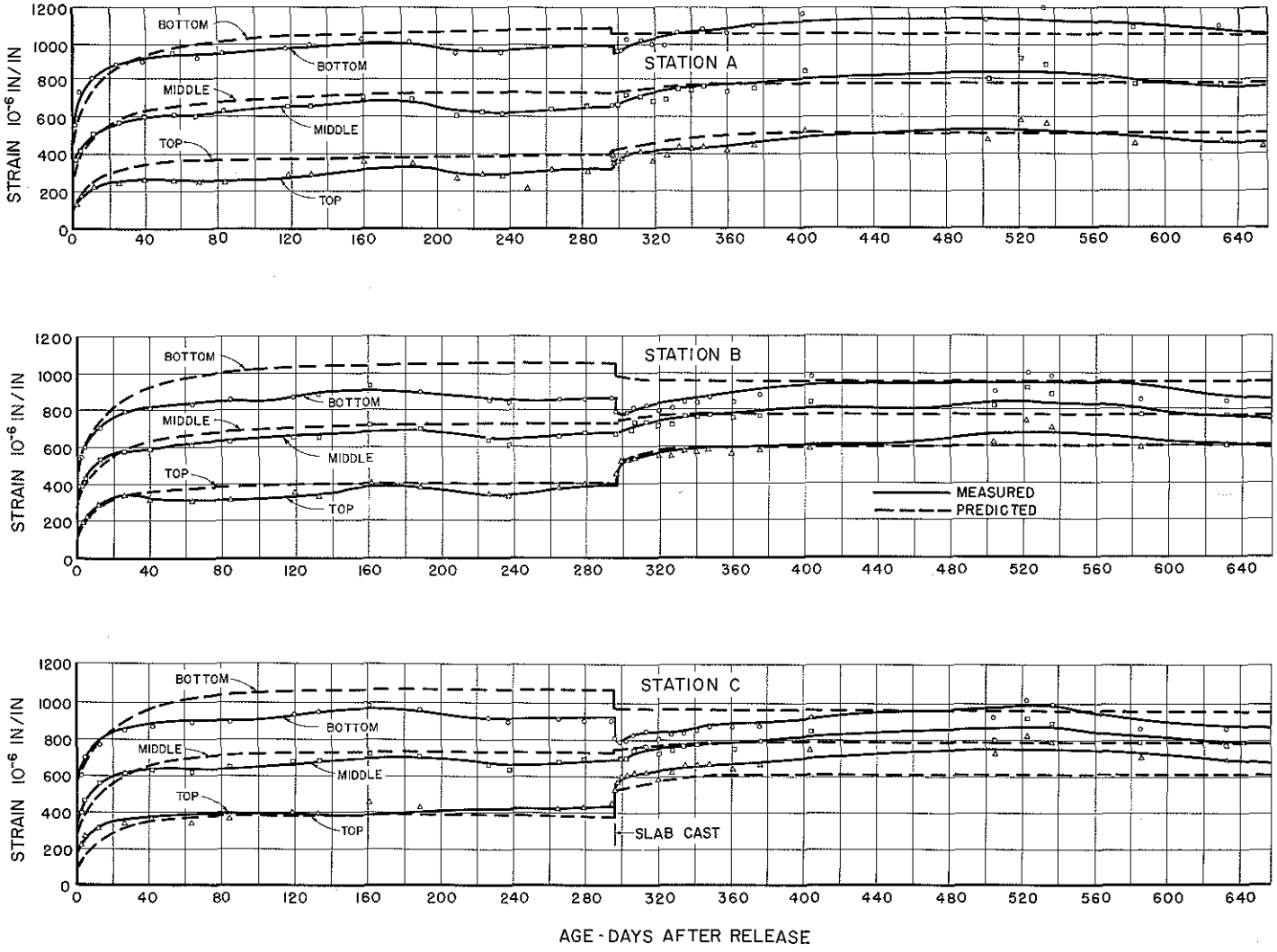

FIGURE 3-17 STRAIN IN BRIDGE BEAM L3-5 (NW)

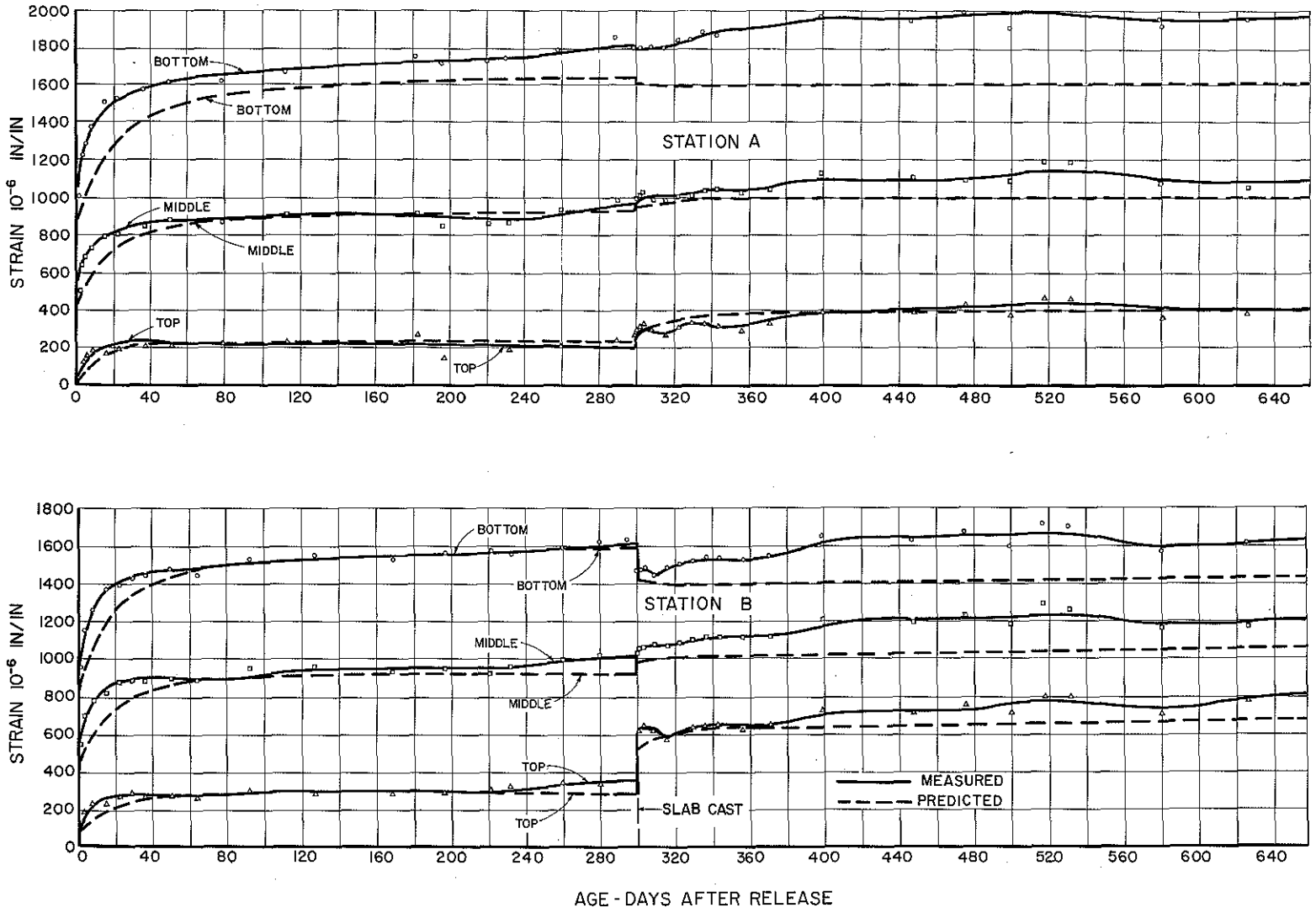

FIGURE 3-18 STRAINS IN BRIDGE BEAM L4-5 (LW)

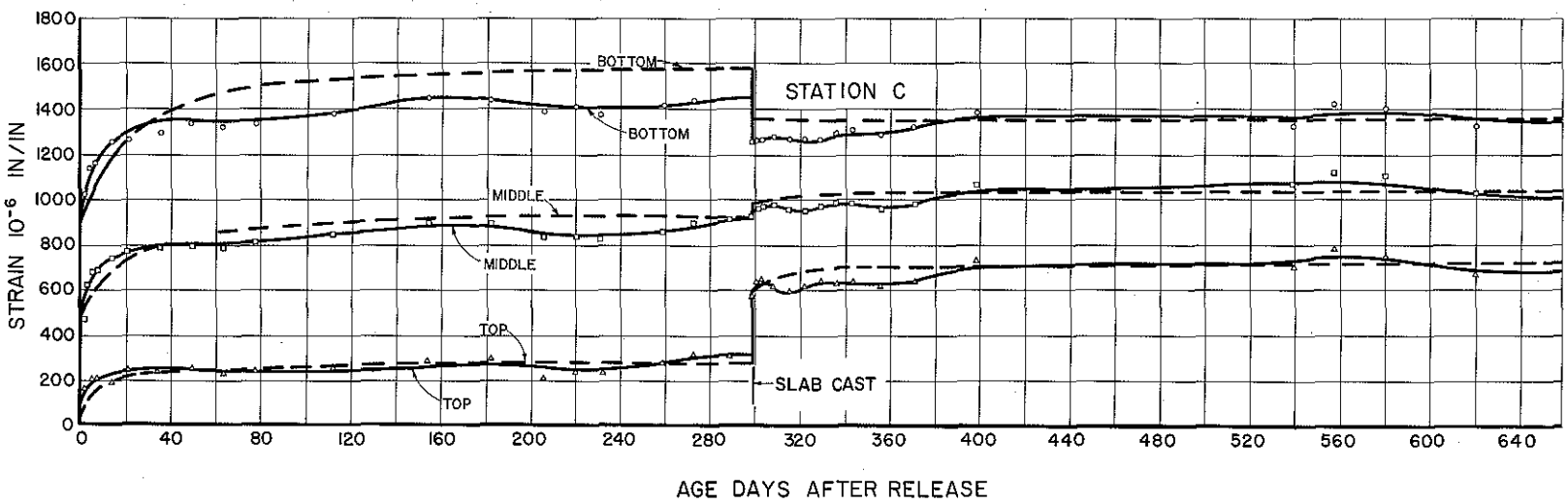

FIGURE 3-19 STRAINS IN BRIDGE BEAM L4-5 (CONT.)
(LW)

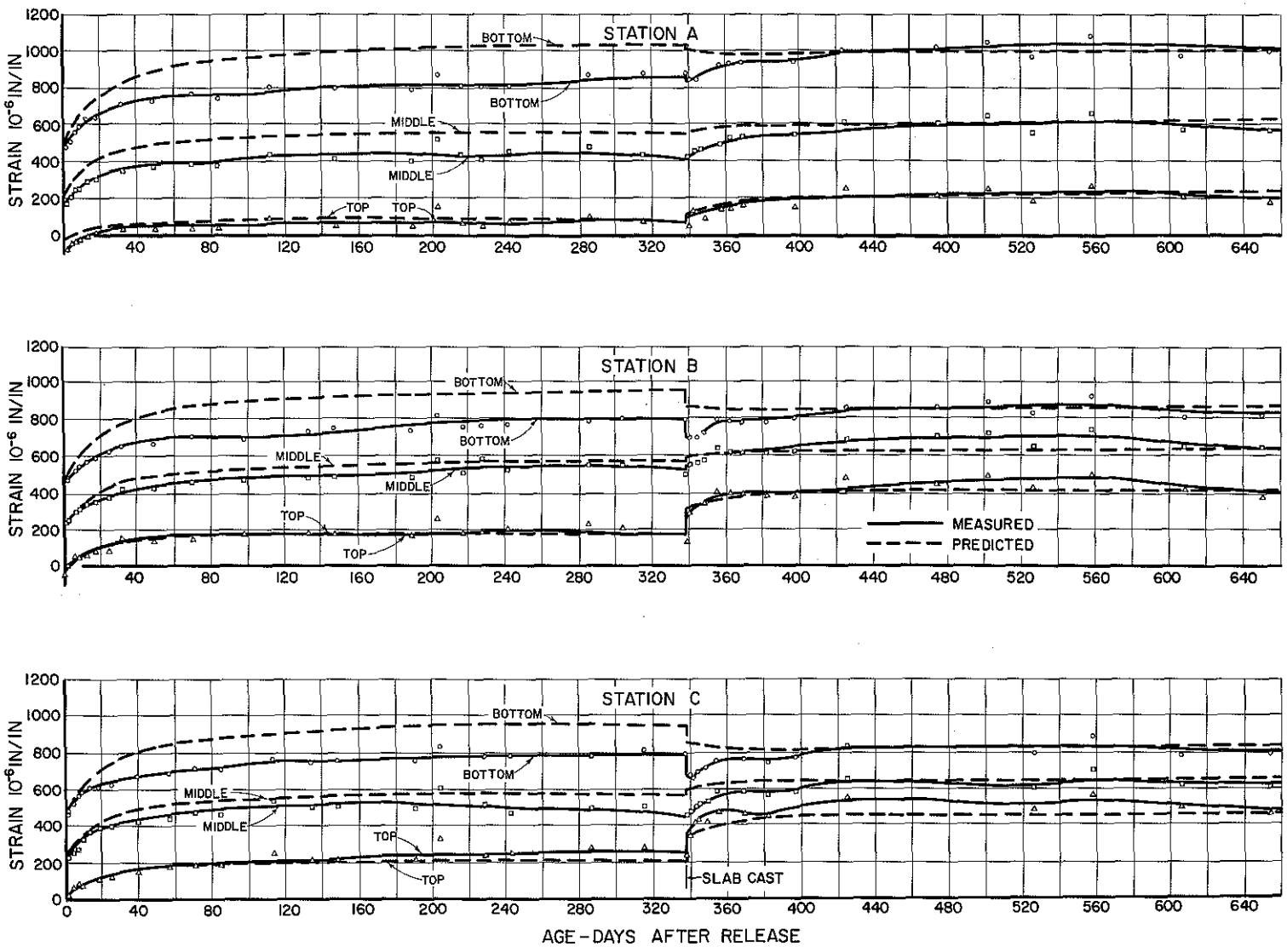

FIGURE 3-20 STRAIN IN BRIDGE BEAM RI-5 (LW)

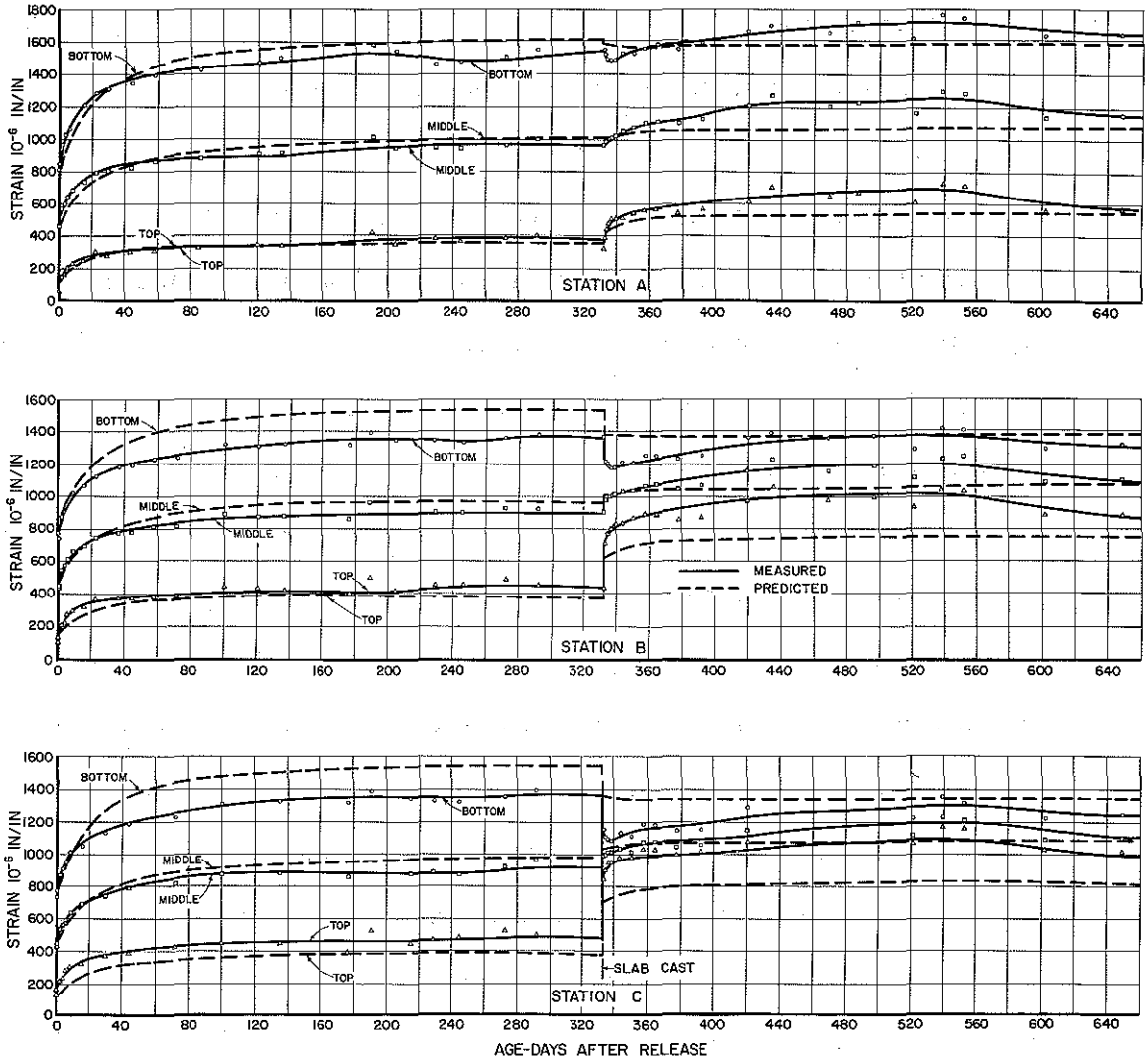

FIGURE 3-21 STRAINS IN BRIDGE BEAM R4-5 (LW)

used as a validity test of the program in Ref. 1, but deflections show better agreement. The primary use of strain measurements was made in computing prestress losses.

E. Strains in Slabs

Slab strains were due to shrinkage of slab and of beams, and to creep of beams and slabs. Because of low stresses in the slabs, little creep strain would be expected. And, as a matter of fact, if shrinkage strains from the 3 ft. square specimens are compared with their slab mate it is seen that there is little difference between the shrinkage at the bottom of the slab and that in the specimen.

The averages of the two bottom-of-slab strains are in general agreement with the readings from the top gage points in the beams. The beam gages are about 3 in. below the slab gages and the two slab gages are offset 3 in. and about 40 in. from the center line of the beam, and some small differences in strain would be evident between the beam and slab gages.

Figures 3-23 to 3-27 show that predictions of slab strains agree well with measured values, which further strengthens the validity of the overall method.

F. Deflections

Both theoretical and measured mid-span deflections of the beams are tabulated in Table 3.3. Values of release camber, taken from Ref. 1, are also shown. Values of deflection under slab load in spans L4 and R2 are subject to some question

TABLE 3.3 MID-SPAN DEFLECTIONS OF BEAMS

Item	Span	Concrete BM	Concrete Slab	Release Camber Measured (in.)	Elastic Defl Due to Slab Theory (in)	Elastic Defl Due to Slab Measured (in)	Ratio (Measured / Theory)	Δ release minus Δ slab (Net elastic defl. (in.))	Final Camber (in.)	Ratio (Final camber / Net elastic defl.)
L1-1	40	LW	LW	0.38	0.208	0.102	0.49	0.278	0.50	1.80
3	40	LW	LW	0.40	0.208	0.114	0.55	0.286	0.43	1.51
5	40	LW	LW	0.43	0.208	0.065	0.31	0.365	0.50	1.37
6	40	LW	LW	0.38	0.208	0.102	0.49	0.278	0.41	1.47
8	40	LW	LW	0.40	0.208	0.102	0.49	0.298	0.46	1.54
		Average = (0.398)			(.208)	(0.097)	(0.42)	(0.301)	(0.46)	(1.5)
L3-1	56	NW	LW	0.65	0.453	0.276	0.61	.374	0.70	1.87
3	56	NW	LW	0.58	0.453	0.325	0.72	.255	0.58	2.28
5	56	NW	LW	0.62	0.453	0.264	0.58	.356	0.58	1.63
6	56	NW	LW	0.62	0.453	0.186	0.41	.434	0.53	1.22
8	56	NW	LW	0.65	0.453	0.234	0.52	.416	0.53	1.27
		Average = (0.62)			(0.453)	(0.257)	(0.57)	(0.367)	(0.582)	(1.6)
L4-1	56	LW	LW	1.31	0.828	0.359	0.43	.951	1.49	1.57
3	56	LW	LW	1.32	0.828	0.814	0.98	.506	1.46	2.88
5	56	LW	LW	1.37	0.828	0.570 *	0.69	.800	1.62	2.03
6	56	LW	LW	1.26	0.828	0.456	0.56	.804	1.45	1.80
8	56	LW	LW	1.36	0.828	0.500	0.60	.860	1.26	1.47
		Average = (1.32)			(0.828)	(0.540)	(0.65)	(0.784)	(1.46)	(1.9)

* See pg. 58.

(Continued)

TABLE 3.3 (Con't)

R1-5	40	LW	LW	0.33	0.208	0.154	0.74	.176	0.38	2.16
R2-5	56	LW	LW	1.30	0.828	0.557*	0.67	.734	1.20	1.64
R3-5	56	NW	NW	0.64	0.453	0.234	0.52	.406	0.60	1.48
R4-5	56	LW	NW	1.12	1.035	0.666	0.64	.454	0.72	1.59

Note: Effective spans are 38'-9" and 54'-9"; wgts are 150 pcf and 120 pcf for the reinforced concretes; moduli of elasticity are 5900 ksi and 3220 ksi for NW and LW in the calculations.

* Questionable values because elevation points were cut off by construction crew during placement of the slab.

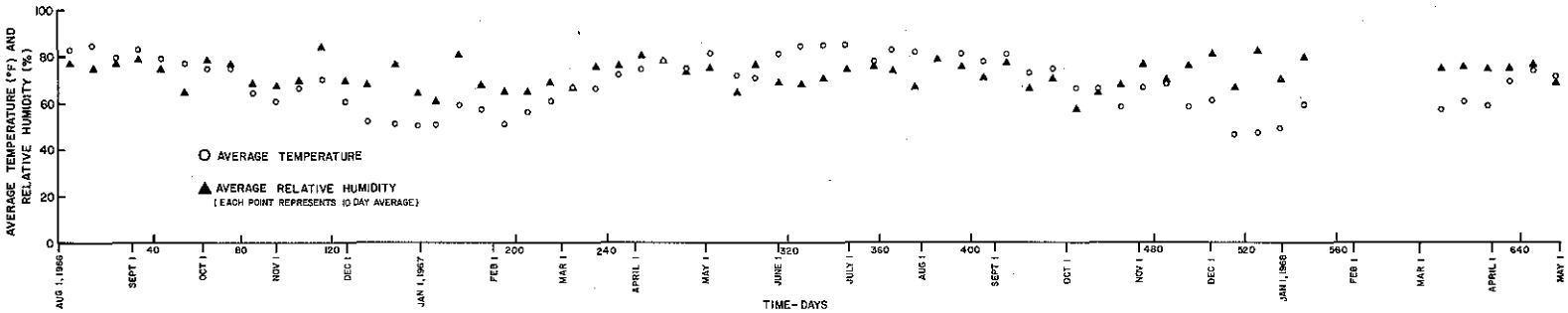

FIGURE 3-22 AVERAGE TEMPERATURE AND RELATIVE HUMIDITY AT HOUSTON, TEXAS

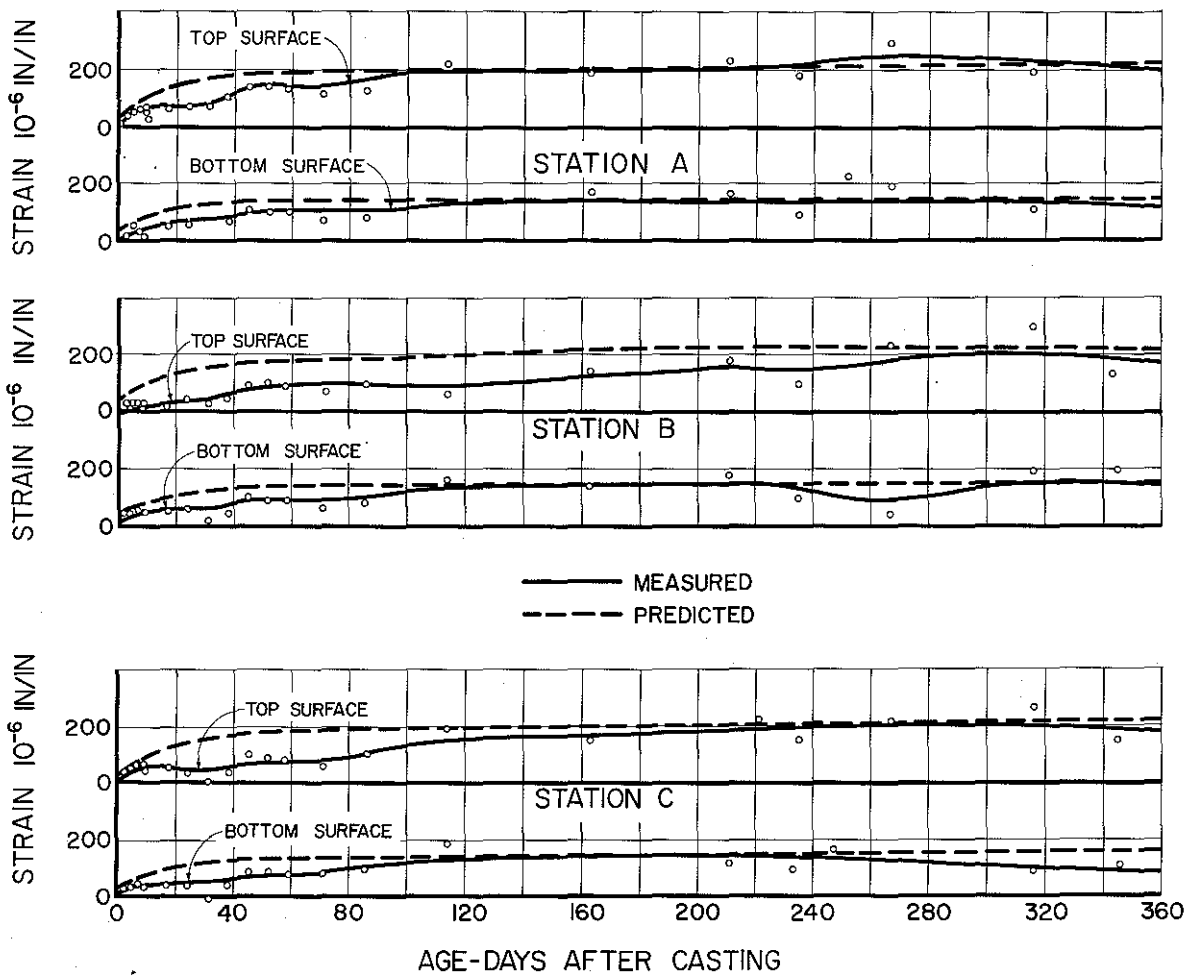

FIGURE 3-23 STRAIN IN SLAB LS-1 (LW)

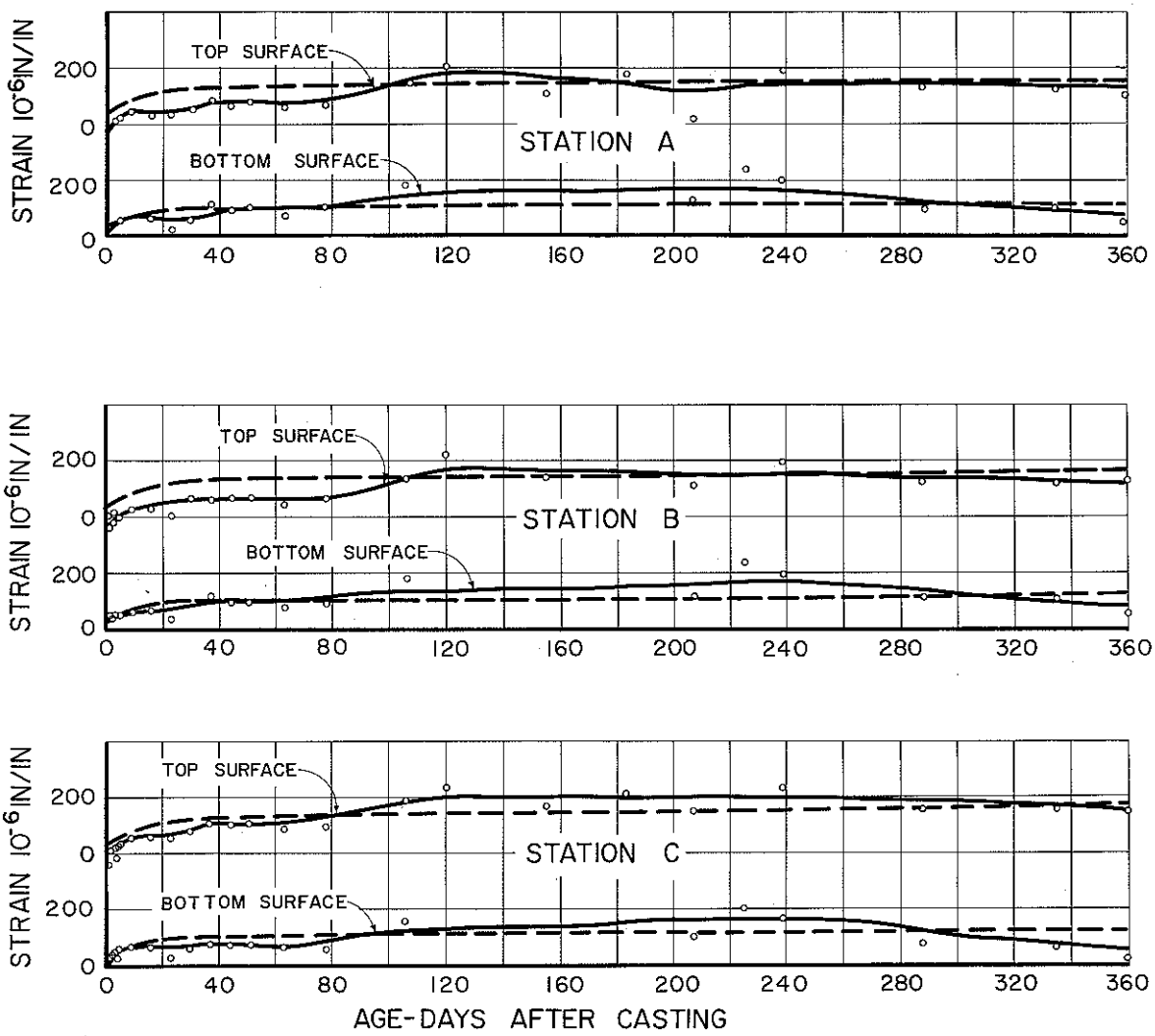

FIGURE 3-24 STRAIN IN SLAB LS-3 (LW)

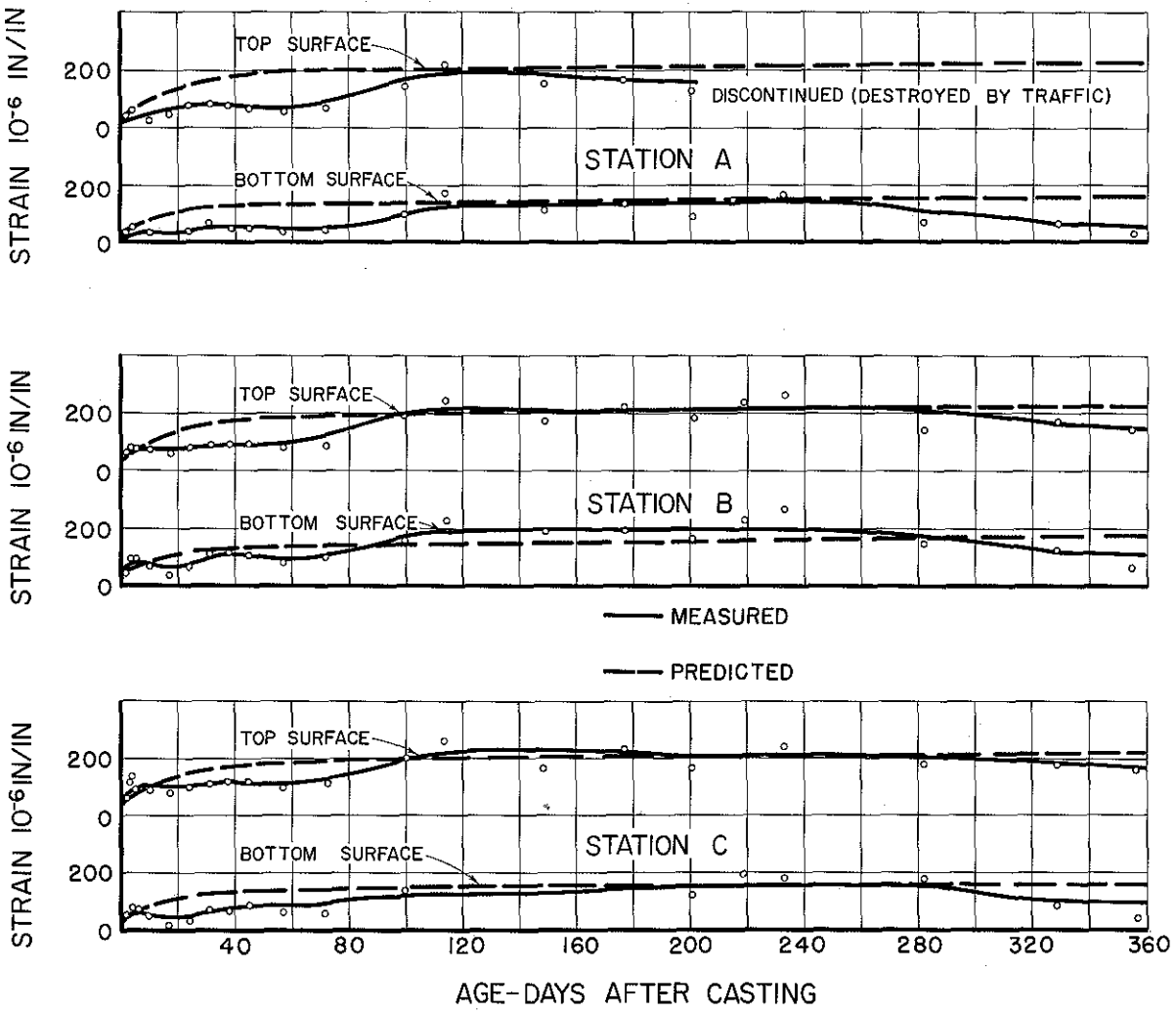

FIGURE 3-25 STRAIN IN SLAB LS—4 (LW)

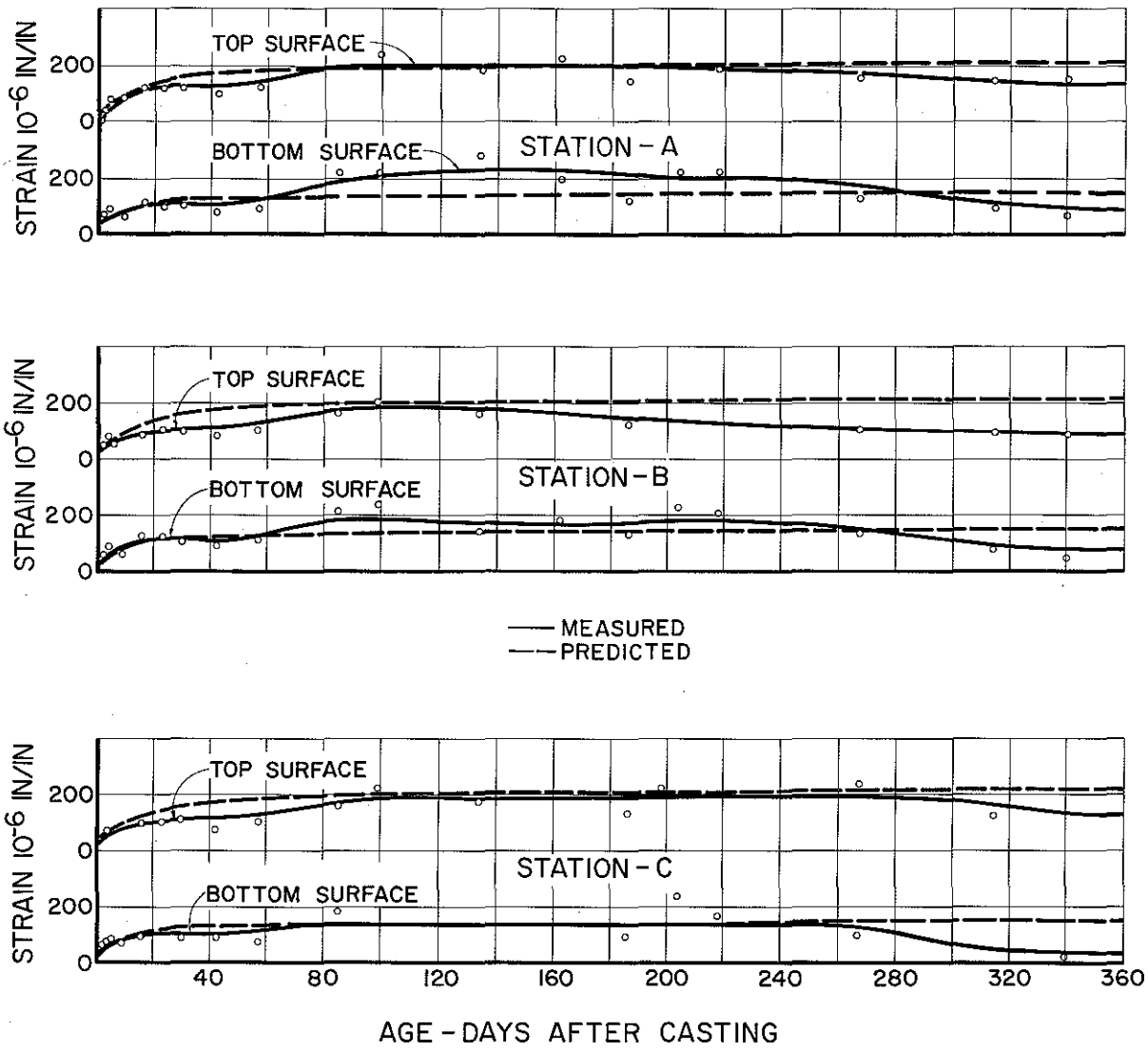

FIGURE 3-26 STRAIN IN SLAB RS-I (LW)

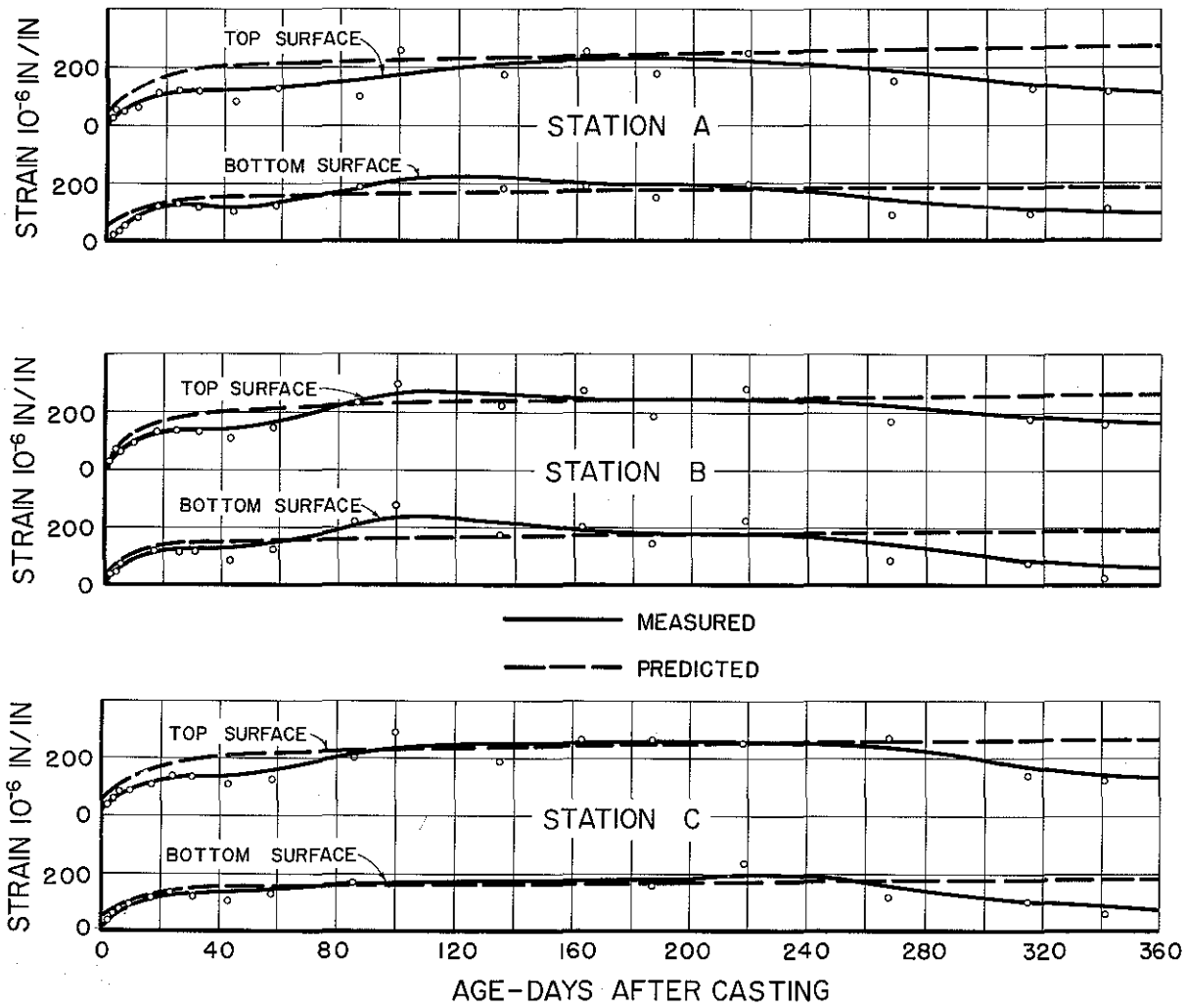

FIGURE 3-27 STRAIN IN SLAB RS-4 (NW)

because the bolts that had been used as elevation points in the beams were cut off by construction workers before elevation readings could be taken just before the slab was cast. The values shown are based on the assumption that elevations read about one week prior to casting were the same as those just before casting.

Plots of deflection versus age appear in Figs. 3-28 to 3-37 where both measured deflection and predicted deflection are shown. Predictions are based on the method explained in Ref. 1, where changes in slope of the deflected beams are computed over short lengths of beam from strains at top and bottom. The strains are taken from the function defining the curve of measured strains.

The slab forms were suspended from the beams by hangers, which is common practice in this type of construction. The beams rested on rubber pads at their end seats and they were not shored during slab casting. Deflections under the weight of plastic slab were computed on the basis of a uniformly loaded simple beam.

Agreement between predicted and measured deflections are good except for the period before casting of the slab in spans L-4 and R-2, Figs. 3-33 and 3-35, and for the complete period for span R-4, Fig. 3-37. Ref. 1 shows poor agreement, too, in spans R-2 and R-4. Beams in span R-4 remained seven days on the prestressing line before release of prestress, against one

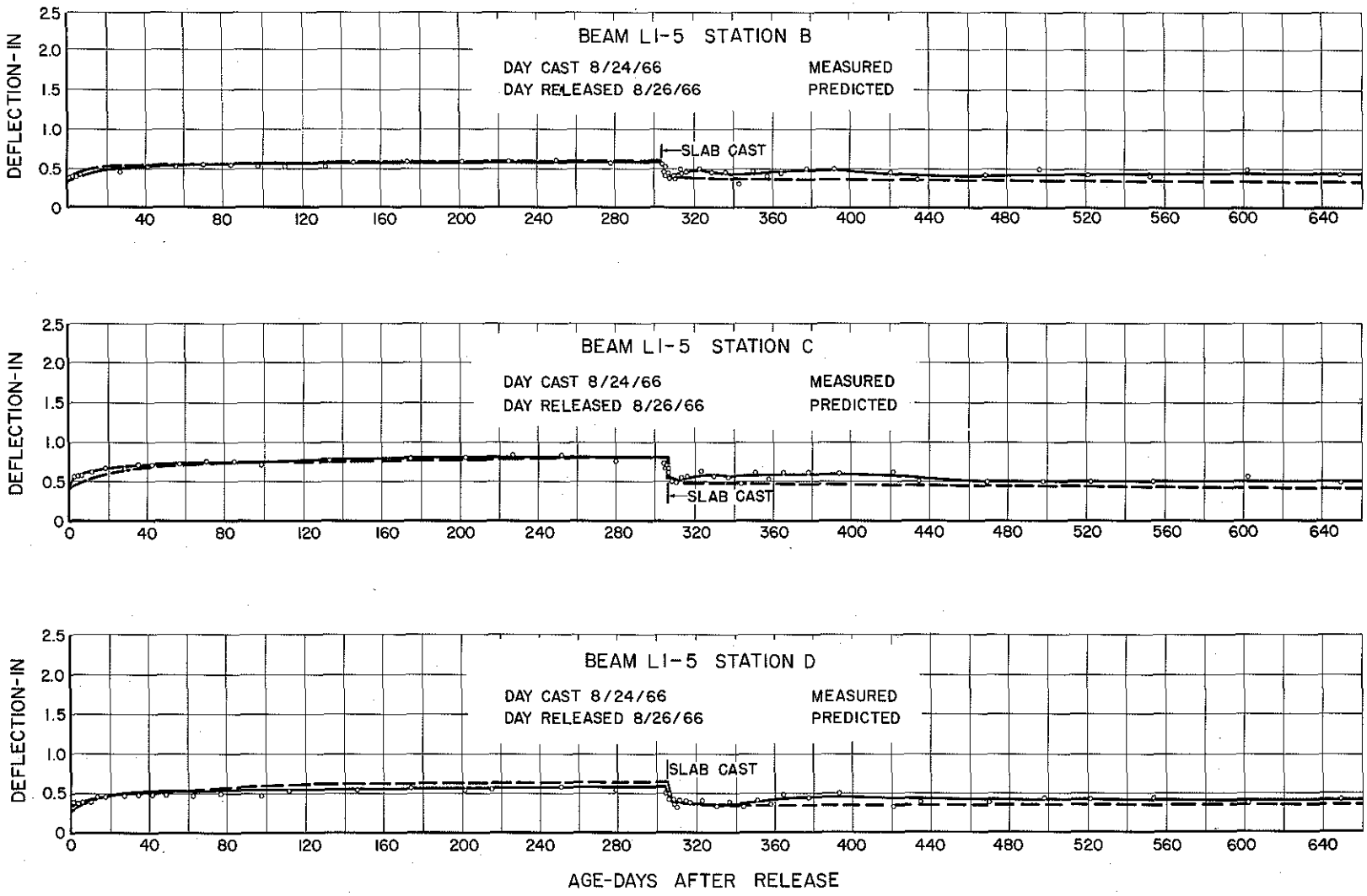

FIGURE 3-28 DEFLECTION OF BRIDGE BEAMS
LW BEAMS, LW SLAB

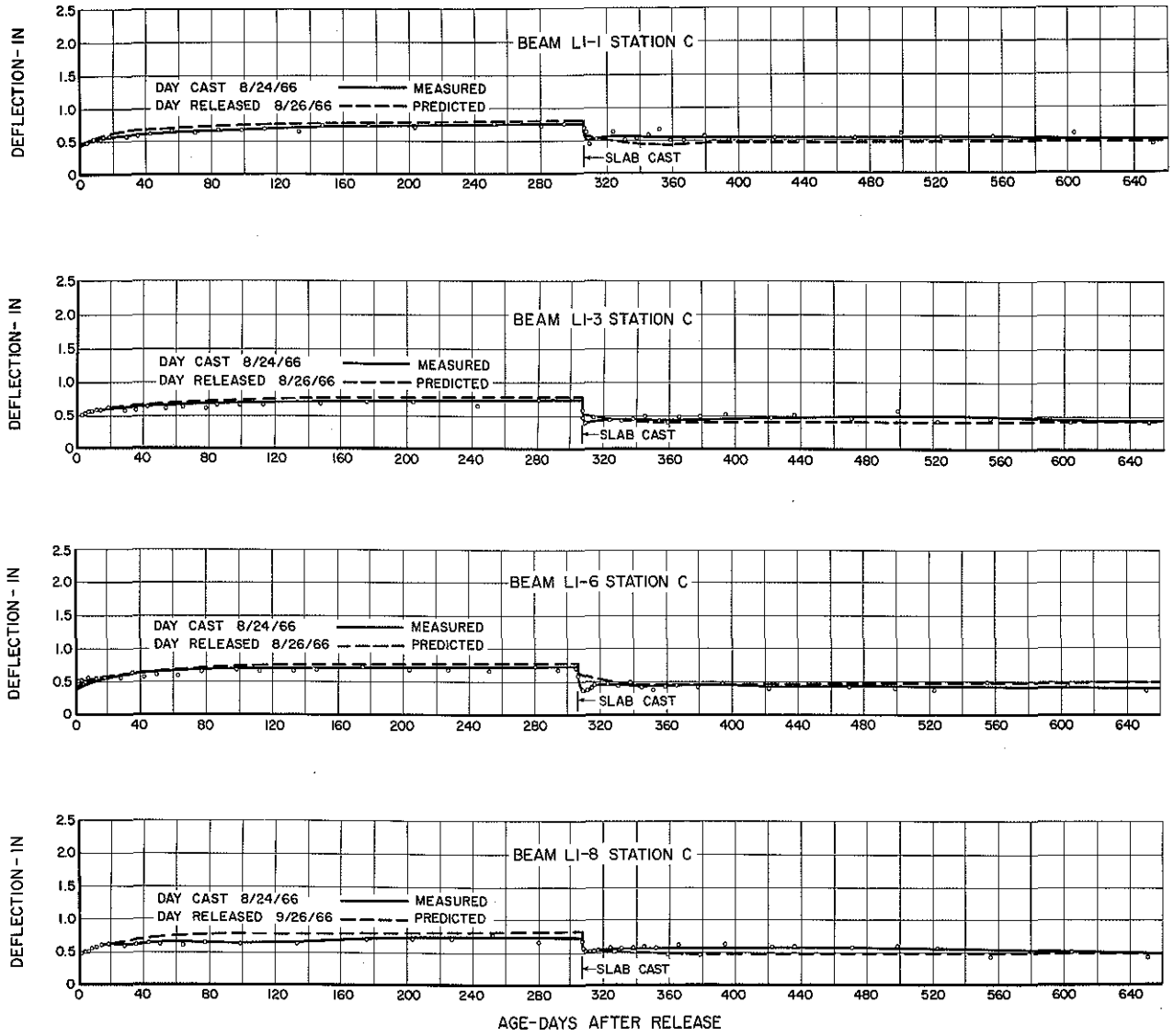

FIGURE 3-29 DEFLECTION OF BRIDGE BEAMS
LW BEAMS, LW SLAB

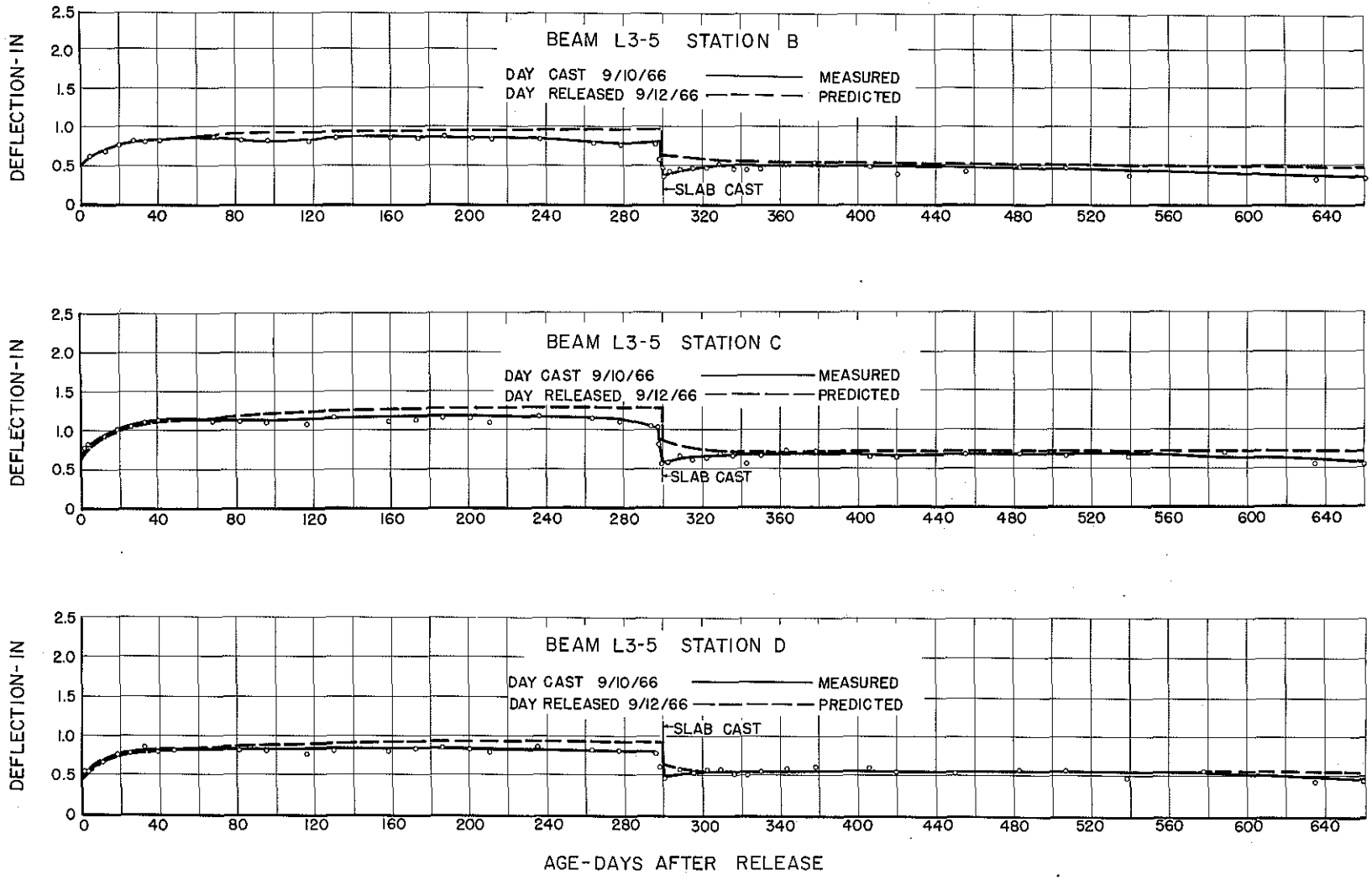

FIGURE 3-30 DEFLECTION OF BRIDGE BEAMS
NW BEAMS, LW SLAB

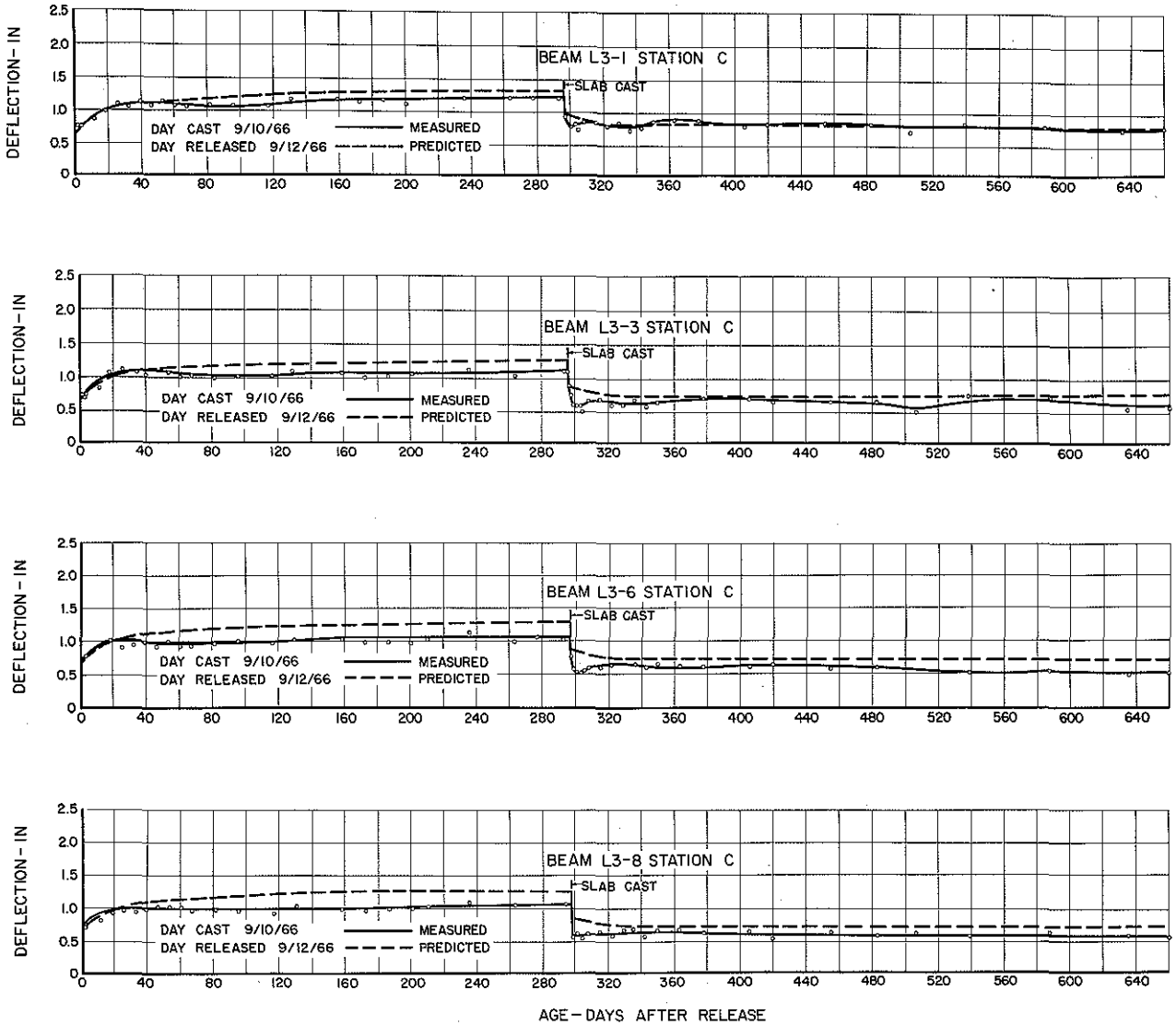

FIGURE 3-31 DEFLECTION OF BRIDGE BEAMS
NW BEAMS, LW SLAB

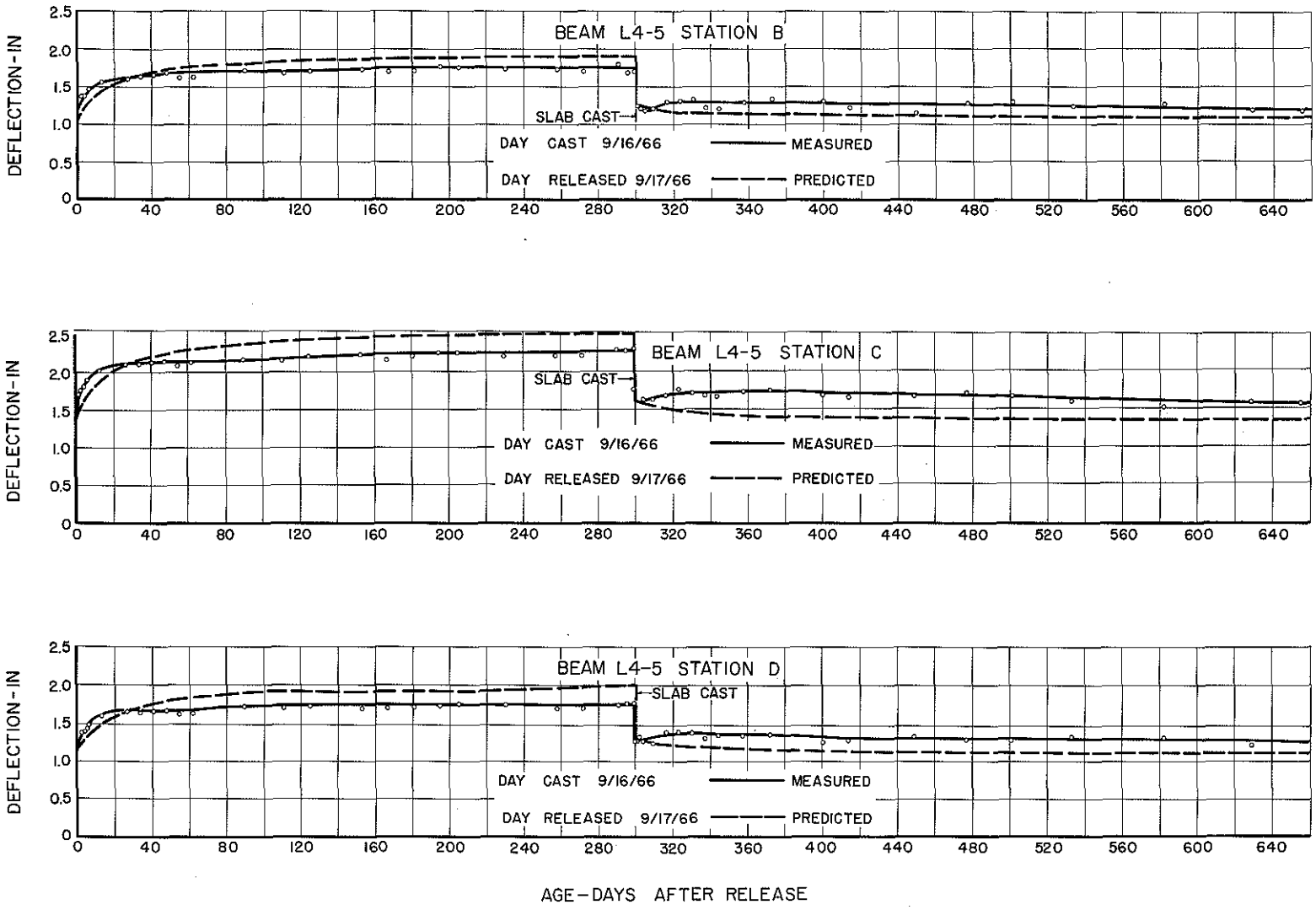

FIGURE 3-32 DEFLECTION OF BRIDGE BEAMS
LW BEAMS, LW SLAB

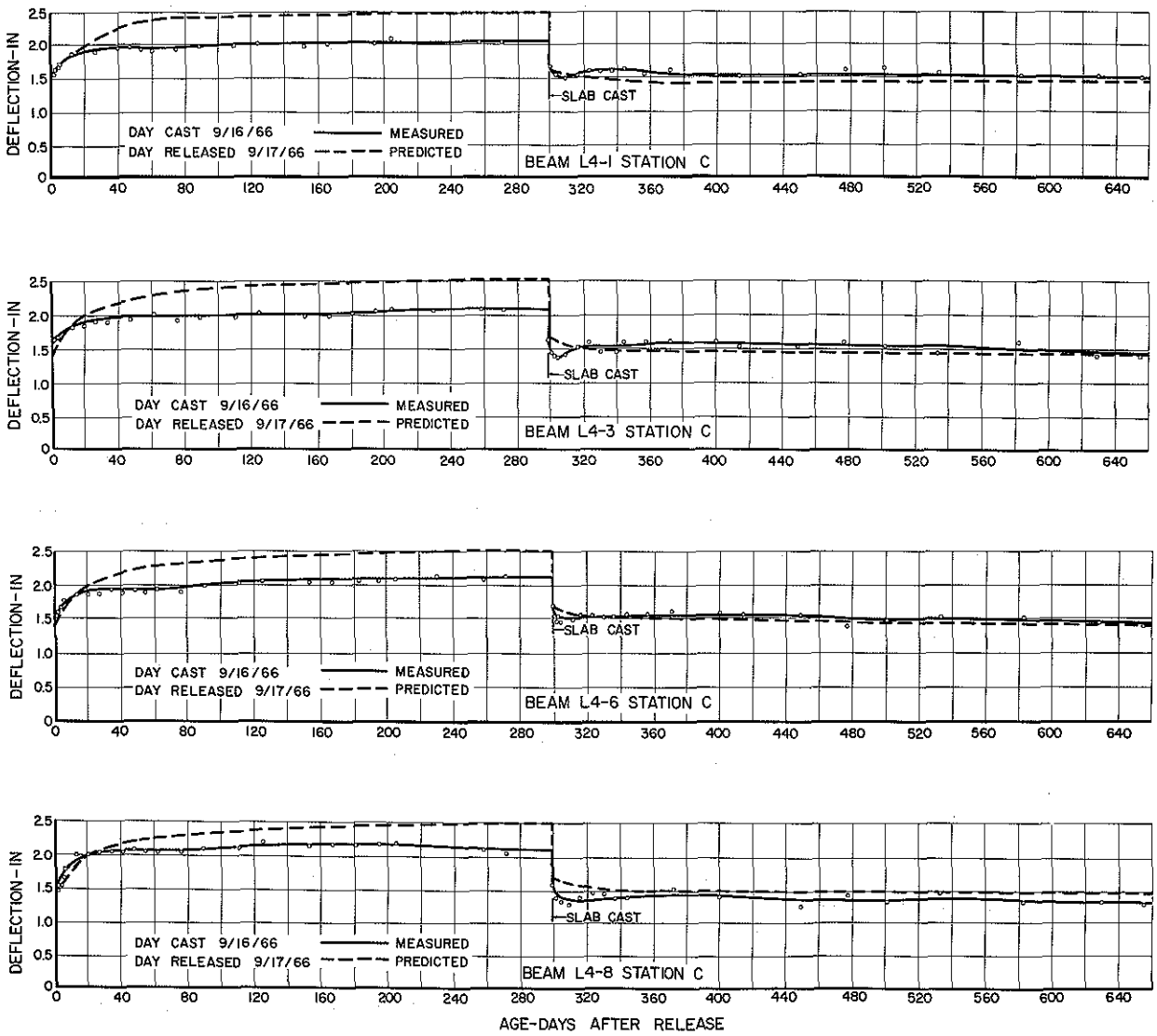

FIGURE 3-33 DEFLECTION OF BRIDGE BEAMS
LW BEAMS, LW SLAB

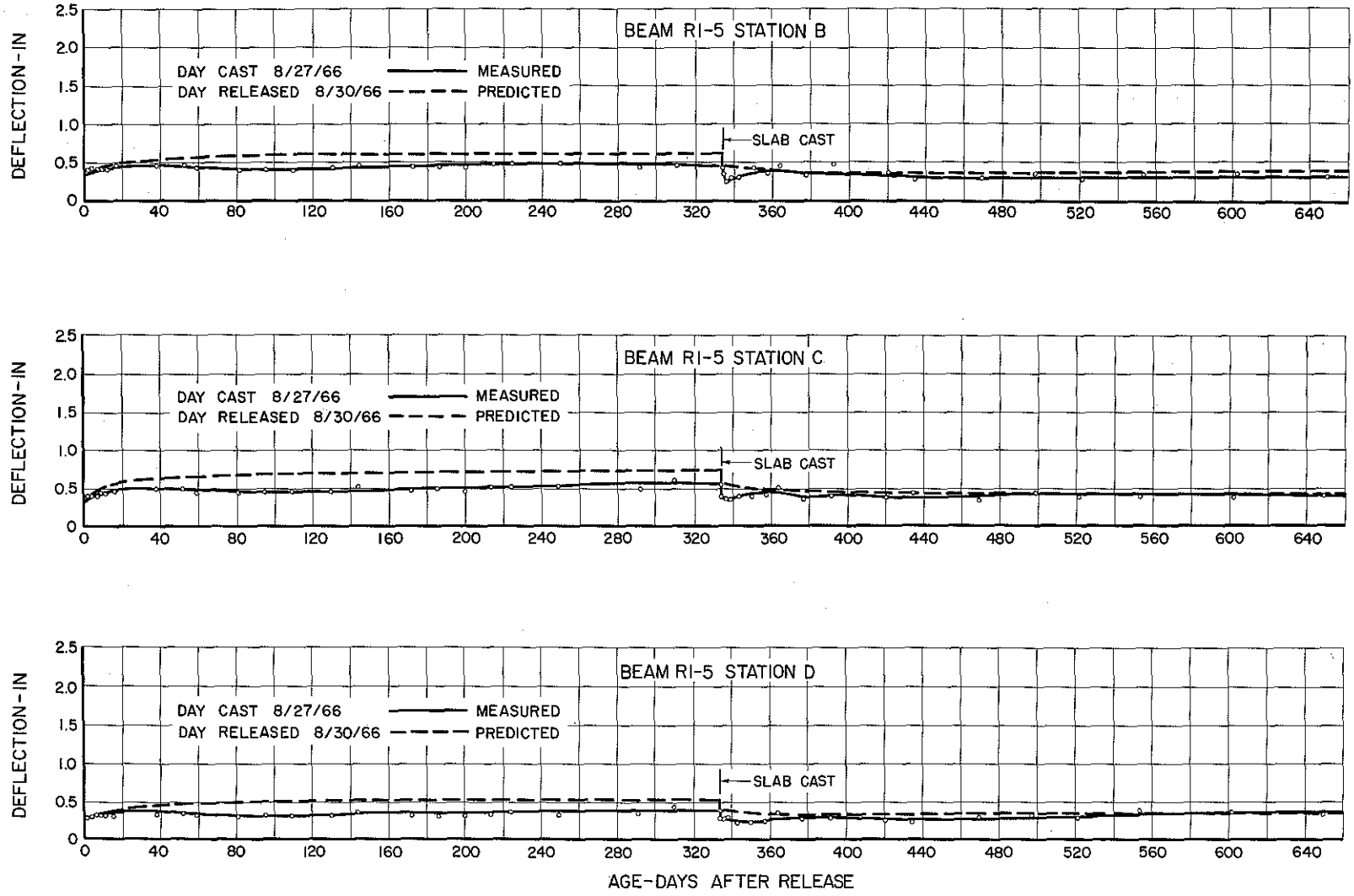

FIGURE 3-34 DEFLECTION OF BRIDGE BEAMS
LW BEAMS, LW SLAB

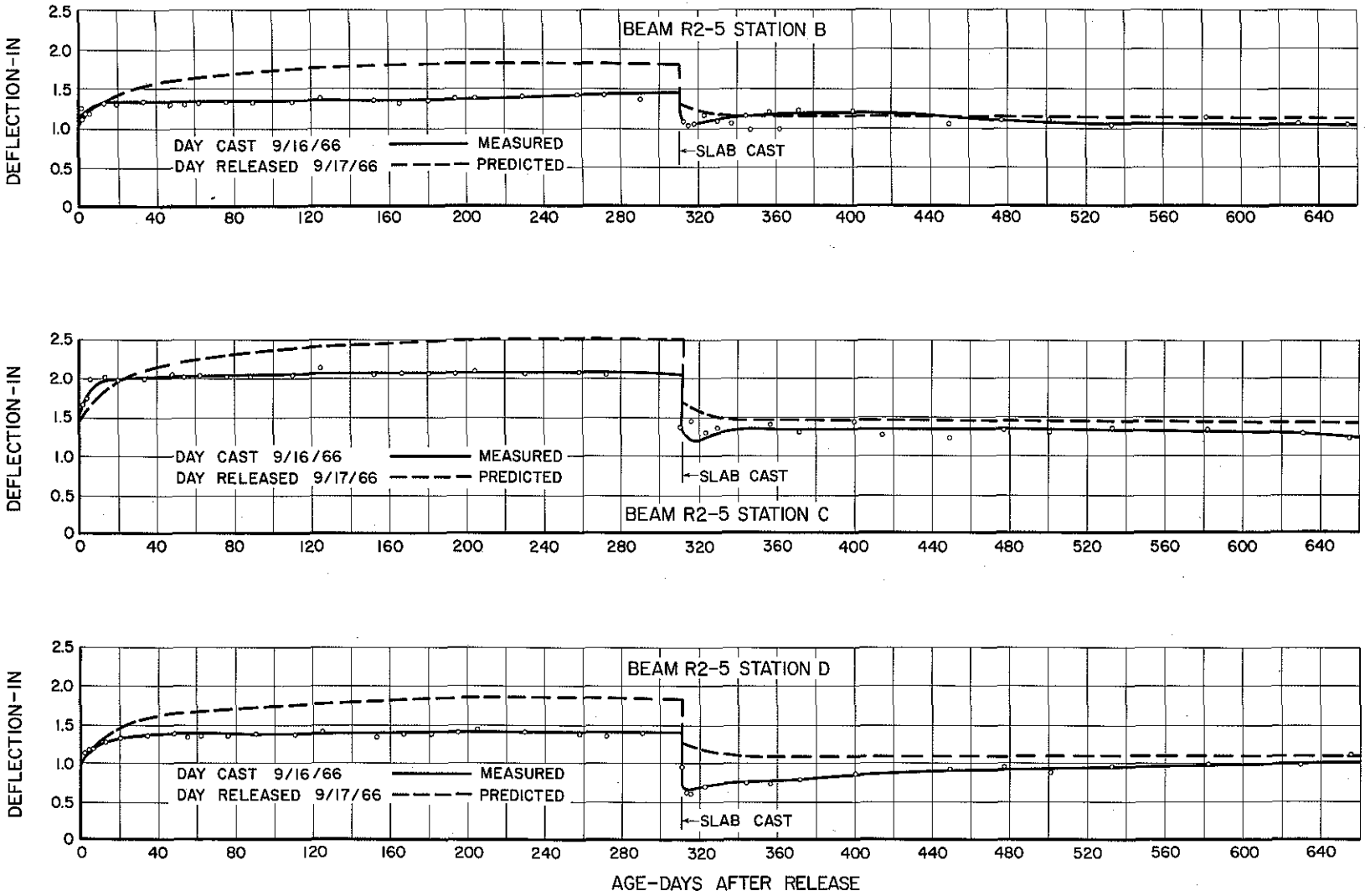

FIGURE 3-35 DEFLECTION OF BRIDGE BEAMS
LW BEAMS, LW SLAB

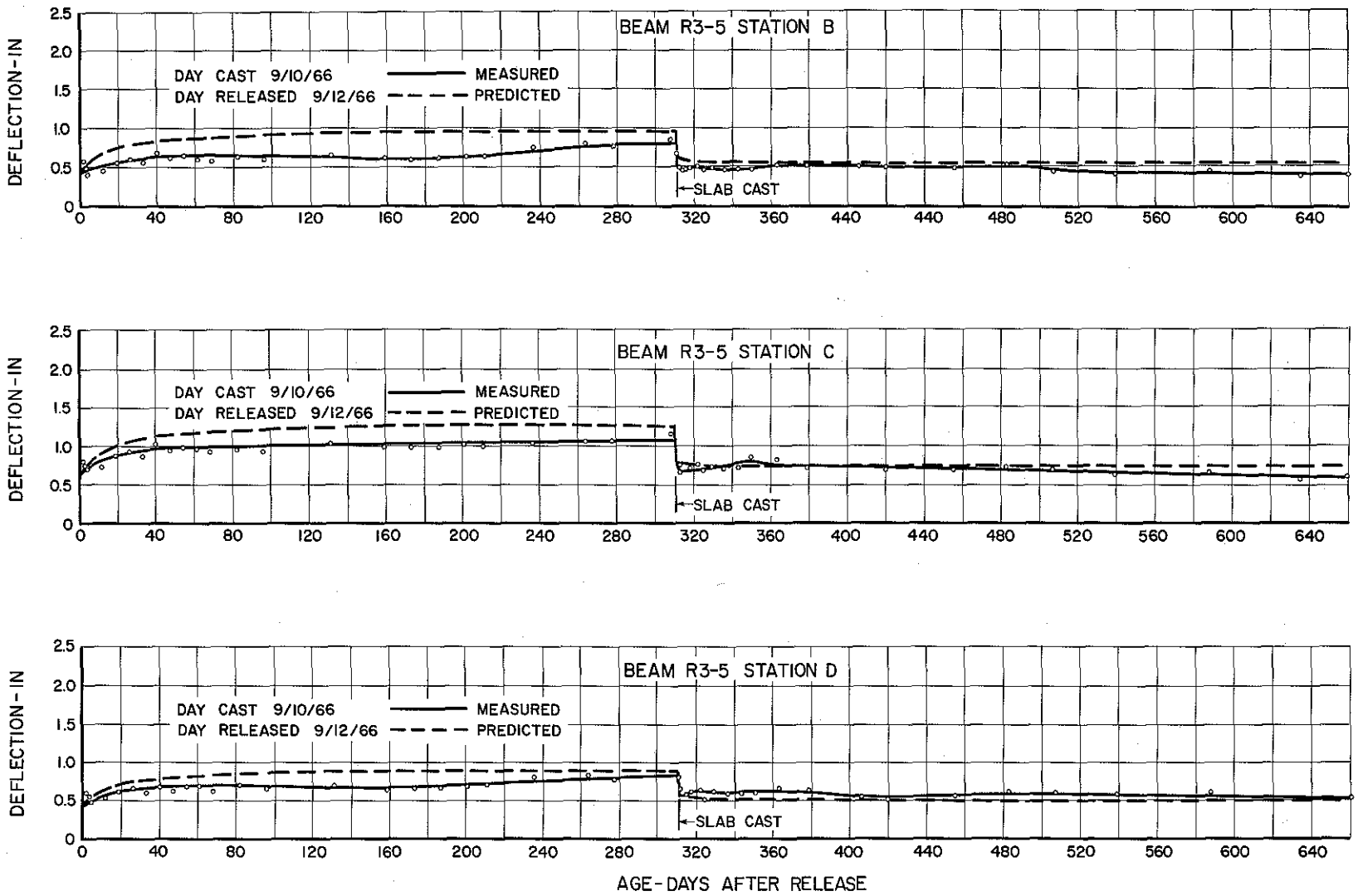

FIGURE 3-36 DEFLECTION OF BRIDGE BEAMS
NW BEAMS, NW SLAB

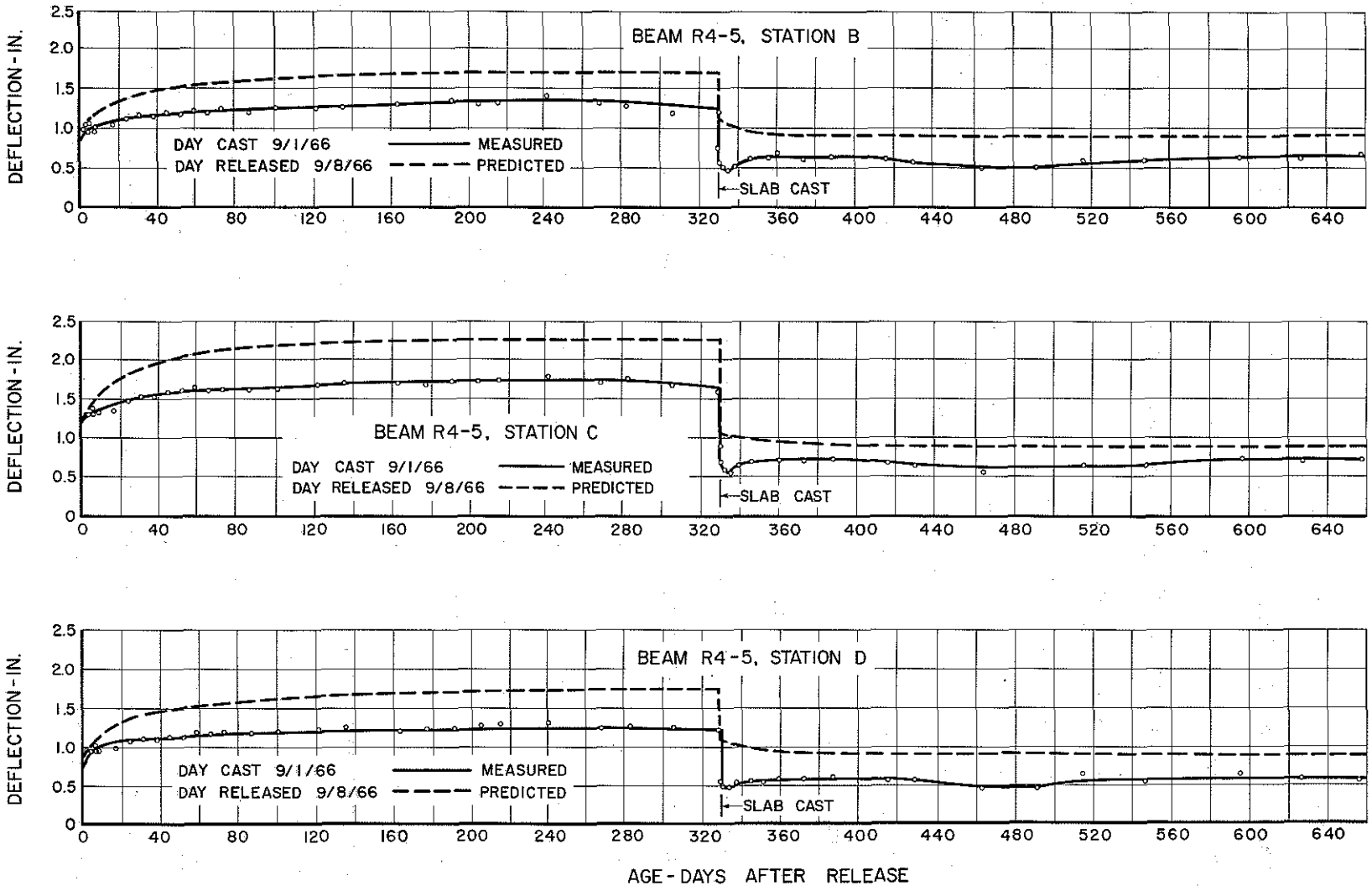

FIGURE 337 DEFLECTION OF BRIDGE BEAMS
LW BEAMS, NW SLAB

to three days for the other beams, and agreement between measured and predicted values for R-4 beams has been poor throughout.

If the curves of predicted deflections given in Ref. 1 are compared with those in this report, differences will be noted for the period from release of prestress to casting of slab. Those differences come about because the extension of data curves for creep and shrinkage extended over a much larger period in the latter report, and the function defining those strains was changed by the greater coverage of time.

The information developed in Table 3.4 is of such interest to the designer in estimating deflections to obtain the desired deck profile after the slab is cast. The measured elastic deflection at the time the slab was cast is in all cases, except for questionable reading in L4-3, much less than the value calculated from a uniformly loaded beam. The measured values come from elevation readings just before and just after casting of the slab; a period of some 4 to 6 hours elapsed between those readings. The ratio of measured to theoretical deflection at mid-span averages 0.47 in the 40 ft. LW beam L1. The corresponding value from one beam in span R1, identical to L1, was 0.75; both sets of beams carried LW slabs. The only known difference in the beams is that L1 beams were steamed and prestress was released at 2-day age whereas R1 beams were

TABLE 3.4 PRESTRESS LOSSES AT MIDSPAN

Beam	Span (ft)	Concrete		Midspan (Sta. C) Prestress Loss (% of Pre-release) (Determined from strain measurements)					Ratio of Losses ($\frac{\text{Time dependent}}{\text{Elastic}}$)
		Bm	Slab	Release (elastic)	Slab Cast (elastic)	Net elastic	Final	Time Dependent*	
L1-5	40	LW	LW	7.44	-1.57	5.87	15.93	10.06	1.71
R1-5	40	LW	LW	6.01	-1.43	4.58	14.92	10.34	2.26
L4-5	56	LW	LW	11.75	-2.97	8.78	21.83	13.05	1.49
R4-5	56	LW	NW	10.45	-2.16	8.29	20.84	12.55	1.51
L3-5	56	NW	LW	7.46	-1.46	6.00	14.57	8.57	1.43

* Final minus total elastic .

cured under wet mat and prestress was released at 3 day age. The corresponding deflection ratio for 56 ft. LW beams carrying LW slabs are 0.65 average for L4 and 0.67 for R2-5.

Normal weight beams of span L2 carrying a LW slab deflected 0.57 as much as was computed when the slab was added, and NW beam R3-5 carrying NW slab deflected 0.52 as much.

The 56 ft. LW beam carrying NW slab, R4-5, deflected 0.64 of the computed value under the weight of the plastic slab.

Summarizing the information on elastic deflection under the weight of the plastic slab, the following approximate percentages of measured to computed deflections were found:

40 ft. LW beam, LW slab	47%
56 ft. LW beam, LW slab	66%
56 ft. LW beam, NW slab	64%
56 ft. NW beam, NW slab	52%
56 ft. NW beam, LW slab	57%

The time lapse from beginning to finish of the slab pour was about 2 1/2 to 3 hours and the pour progressed smoothly from the outside of the bridge, beam #9, to the inside, beam #1. From all that is known of the history of the beams, slabs, and construction procedures nothing is known that would explain the great difference between theoretical and measured deflections.

The variation of concrete secant modulus produces some changes in deflection, but the changes are small. In Table 3.5

TABLE 3.5 CHANGES IN FINAL MIDSPAN CAMBER AND PRESTRESS LOSS WITH CHANGES IN MODULUS OF BEAM CONCRETE. (Values were computed by the step-by-step procedure given in the Appendix)

BEAM	E/E measured %	Midspan Camber (in)	Midspan Prestress Loss (%)
L3-5	80	0.699	16.05
	90	0.716	15.70
(56' NW)	100	0.732	15.42
	110	0.745	15.19
	120	0.757	15.00
L4-5	80	1.381	22.22
	90	1.405	21.80
(56' LW)	100	1.424	21.43
	110	1.439	21.12
	120	1.435	20.84

final deflections at mid-span are given for a NW and LW beam where the moduli were varied from 80% to 120% of the measured value. Determinations were made by the step-by-step method of computations outlined in the Appendix. That table shows a very small change in deflection brought about by the change in modulus. The 56 ft. NW beam changed only 0.058 in. over the 40% change in modulus, and the 56 ft. LW beam changed 0.054 in. These results indicate that the relatively small changes in concrete modulus would not produce appreciable changes in deflections.

A range of deflections, from low to high, that would result from certain incorrect values of secant modulus, shrinkage, and unit creep is shown in Fig. 3-43 for NW and LW beams.

Overestimation of deflection will result from a modulus lower than the true value and from creep and shrinkage estimates too high. Too high modulus with too low creep and shrinkage will result in underestimates of deflection. For the values used in Fig. 3-43, the modulus variation was 20% lower to 20% higher than measured modulus. Corresponding creep and shrinkage were 40% higher and 40% lower than measured. Such variations produce elastic deflections that are 20% too high or low due to modulus. Changes primarily due to creep and shrinkage occur early after release of prestress with some change noted, too, after slab placement. Most of the time dependent changes in

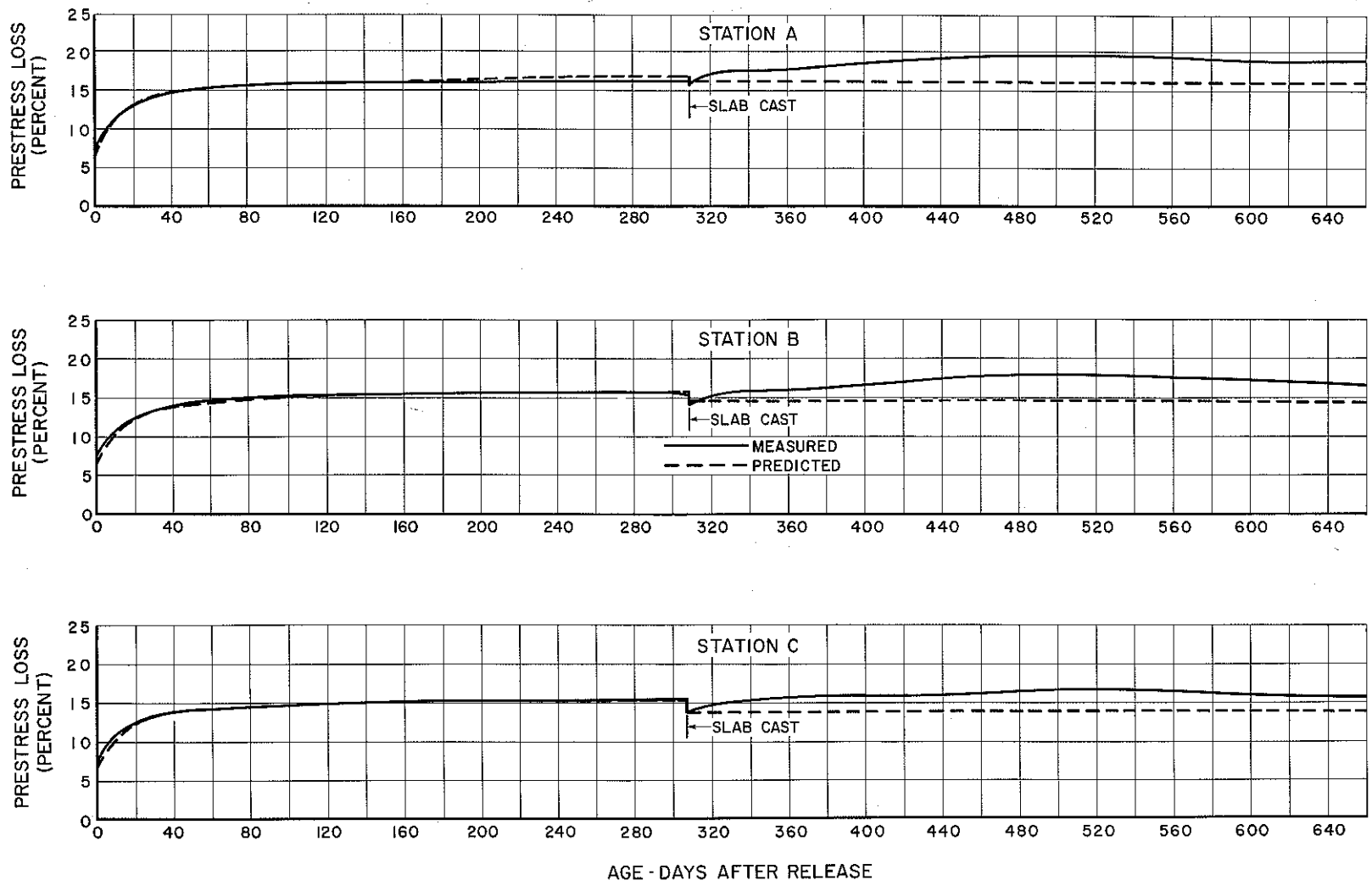

FIGURE 3-38 PRESTRESS LOSS IN BRIDGE BEAM LI-5
LW BEAM, LW SLAB

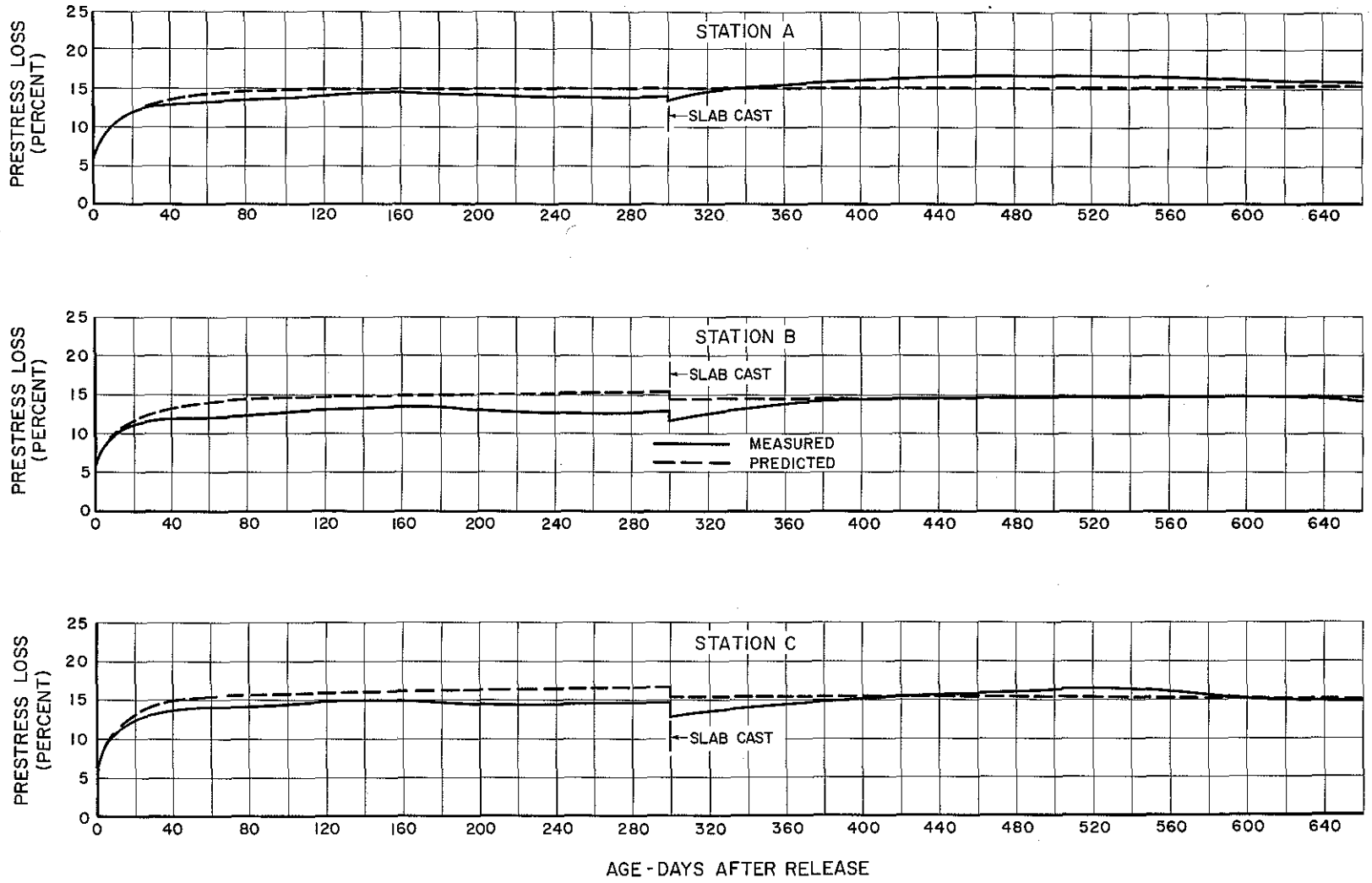

FIGURE 3-39 PRESTRESS LOSS IN BRIDGE BEAM L3-5
NW BEAM, LW SLAB

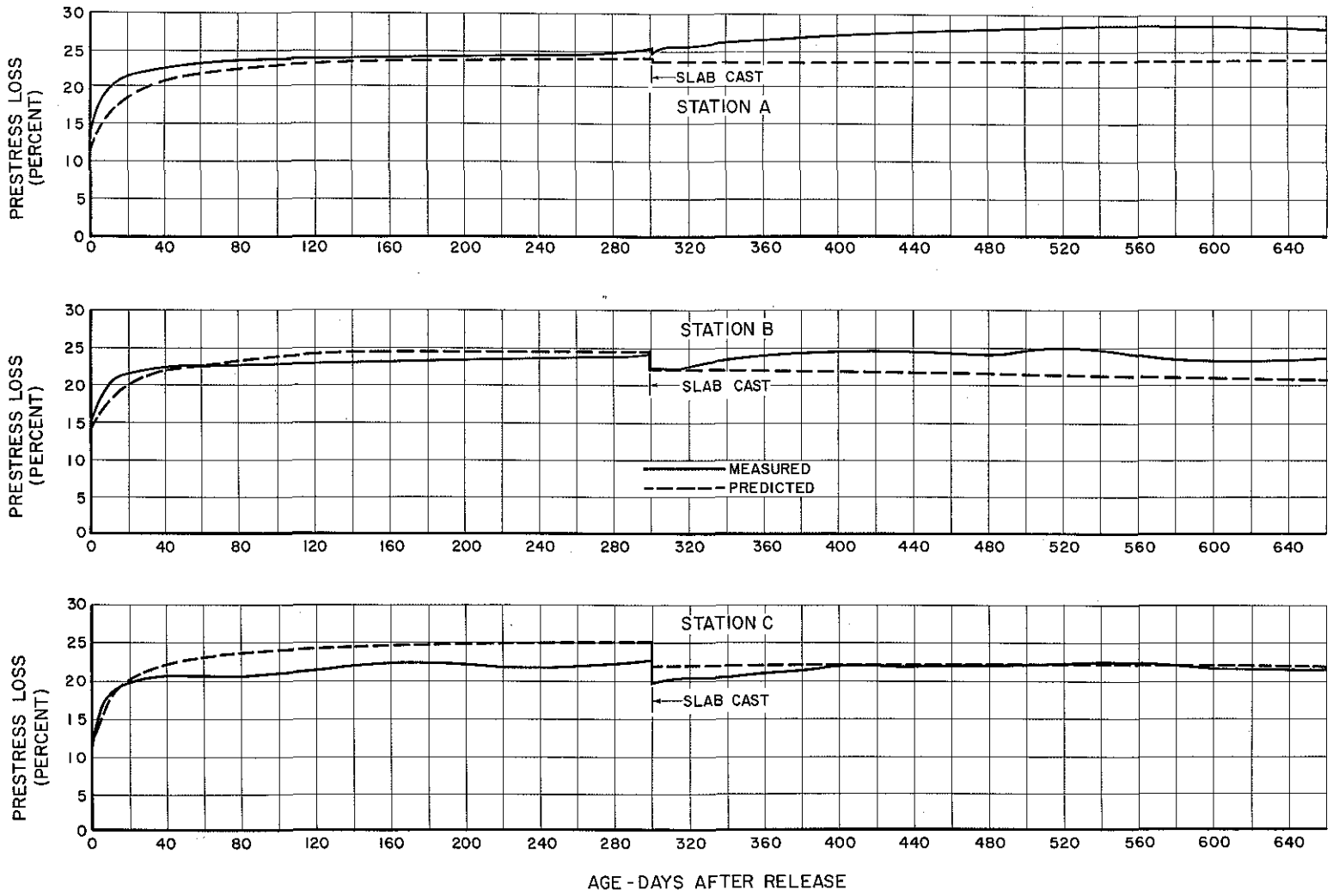

FIGURE 3-40 PRESTRESS LOSS IN BRIDGE BEAM L4-5
LW BEAM, LW SLAB

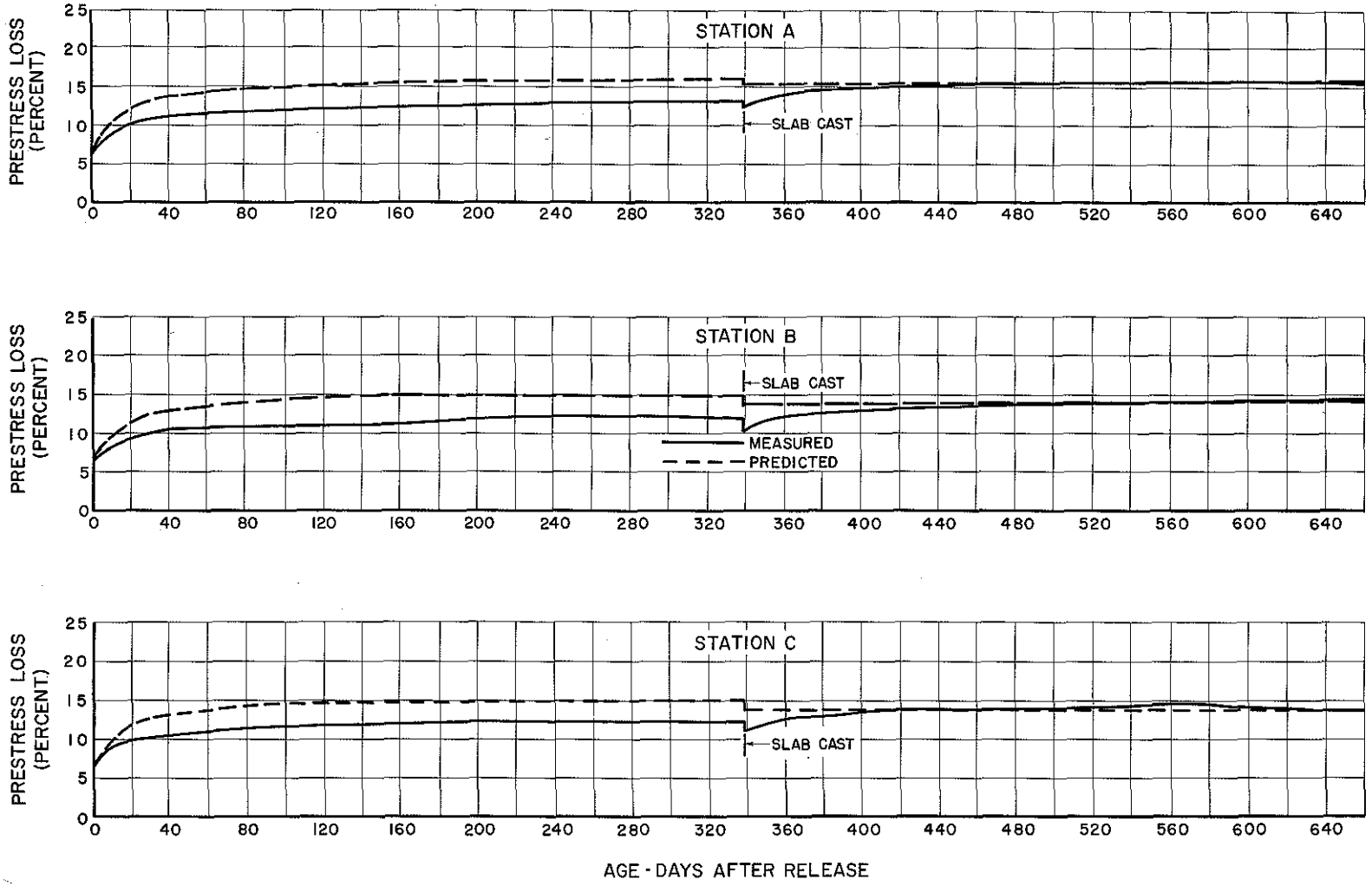

FIGURE 3-41 PRESTRESS LOSS IN BRIDGE BEAM RI-5
LW BEAM, LW SLAB

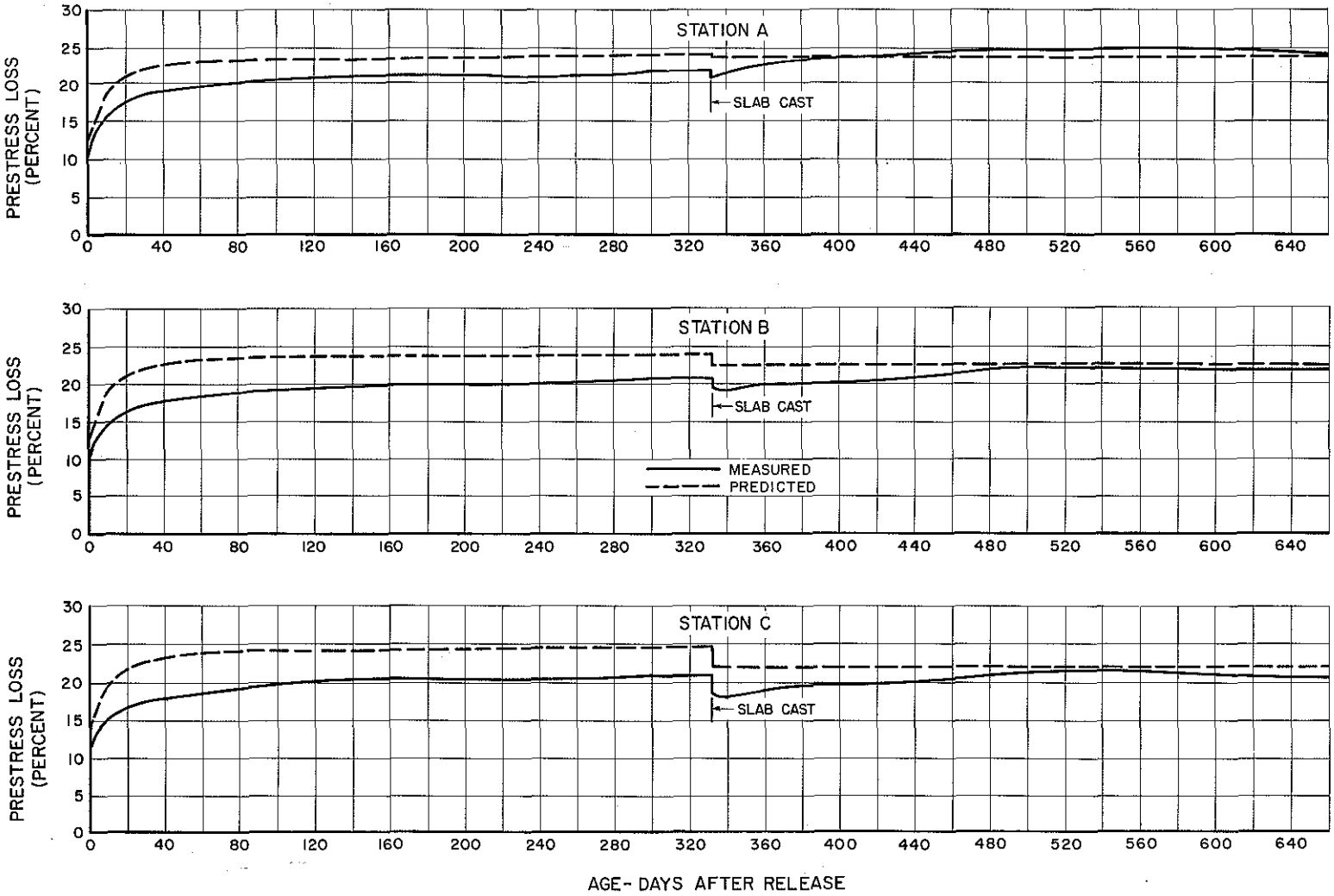

FIGURE 3-42 PRESTRESS LOSS IN BRIDGE BEAM R4-5
LW BEAM, NW SLAB

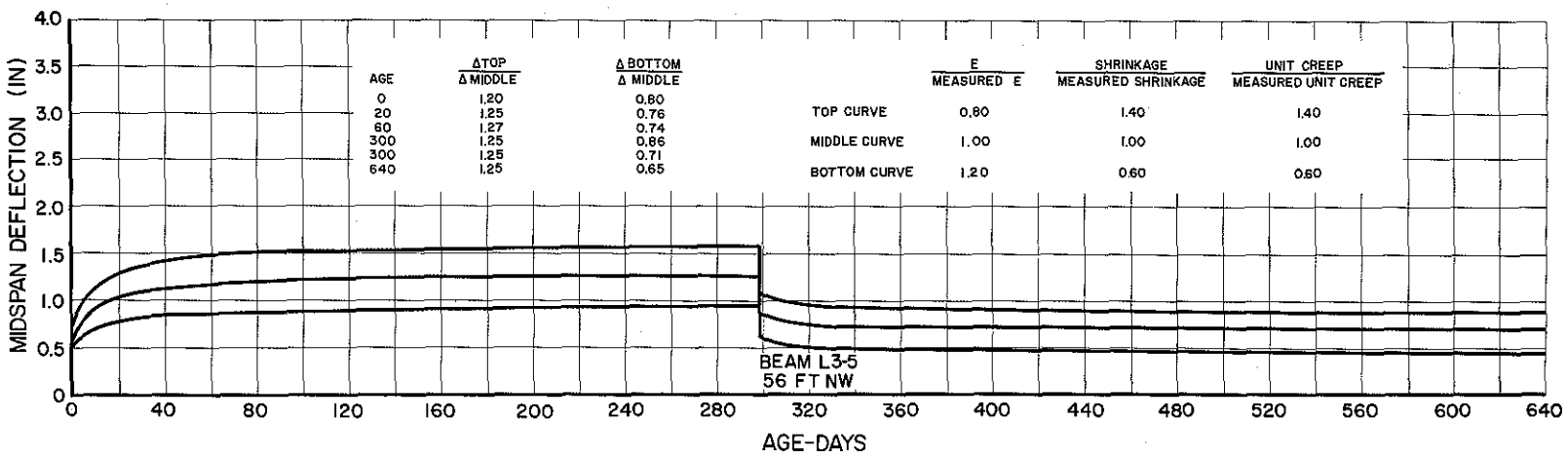

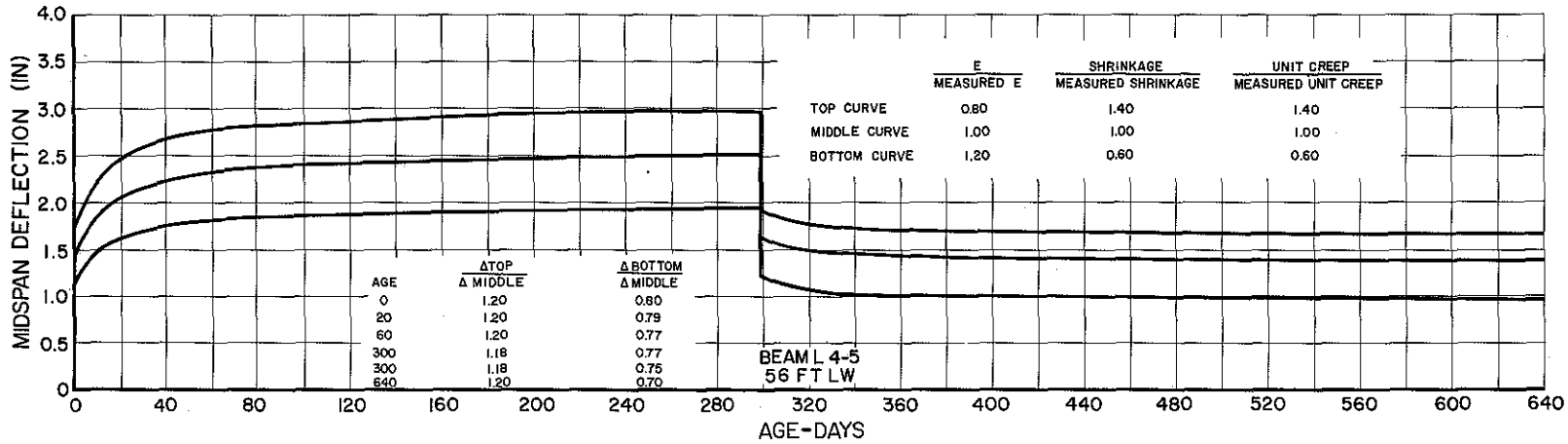

FIG. 3-43 INFLUENCE OF CHANGES IN SETS OF MODULUS, SHRINKAGE AND CREEP ON MIDSPAN DEFLECTION

Fig. 3-43 occurred within the period from release of prestress to about two months thereafter. High and low predictions vary from 126% to 65% of datum losses respectively for the NW beam, and from 121% to 69%, respectively, for the LW beam.

Sinno's studies (Ref. 6, Table 6.12) showed that changes in unit creep and shrinkage produce little change in deflections when the modulus remains unchanged. This indicates that elastic strains account for much of the change, and that can be seen in Fig. 3-43.

Modulus of elasticity predictions within 20% of actual values appear to be reasonable. Test records of creep and shrinkage for various concretes under various conditions should permit the designer to predict those values within 40% of actual values. If predictions can be made within those limits, deflections at mid-span should be within the range of 70% to 130% of theoretically exact values.

G. Prestress Loss

Prestress losses determined from measured strains in the beams extrapolated to the centroid of the prestressing steel are represented by the "MEASURED" curves in Figs. 3-38 through 3-42. Losses determined from predicted strains at cgs of the steel are represented by the "PREDICTED" curves in those figures.

The greatest variance of predictions from measured curves in the final year appear in Fig. 3-38 for beam L1-5, and Fig.

3-40 for beam L4-5. There is generally good agreement at the end of the test period, although differences occur in some cases over periods between the beginning and the end.

The loss at mid-span, station C, was about the same value at the end of tests as it was before the slab was cast. There was generally a little increase in losses, after slab casting, at beam end, station A, and quarter span, station B.

Mid-span prestress losses are tabulated in Table 3.4. Elastic losses occurred at release of prestress and elastic increases occurred when the slabs were cast. The algebraic sum of those two values has been designated as net elastic loss.

Terminal date losses in the 40 ft. LW beams at mid-span were approximately 15%, and in the 56 ft. LW beams, approximately 21%. The 56 ft. NW beam showed 14 1/2% loss at mid-span. Table 3.5 shows very minor changes in losses with changes in concrete modulus.

Time dependent losses, final minus net elastic loss, were 10% for 40 ft. LW beams, 13% for 56 ft. LW beams, and 8 1/2% for 56 ft. NW beams. The ratios of time dependent to net elastic losses averaged about 2.0 for 40 ft. LW beams, 1.5 for 56 ft. LW beams, and 1.4 for 56 ft. NW beams. Corresponding ratios of final to release losses can be found from values in Table 3.4 to be 2.3, 1.9, and 1.9, respectively.

Final losses may be closely approximated as 2 times the elastic losses at release for both concretes in the longer beams, and at about 2.3 for the shorter span LW beams.

A range of prestress losses based on prediction of secant modulus, shrinkage, and creep values from too high to too low are shown for a NW and a LW beam in Fig. 3-44. Data for the curves in that figure were developed in a way similar to that used for the deflection study. The datum values, the middle curves in the figure, were based on measured values of secant modulus, shrinkage, and unit creep. A low modulus, 80% of measured, and high shrinkage and creep, 140% of measured, produced the high loss curves. The low loss curve came from modulus of 120% of measured, and shrinkage and creep at 60% of measured. Losses ranged between the limits of 68% to 131% of theoretically correct values for the NW beam, and from 73% to 126% for the LW beam.

It is tempting to compare span ratios with prestress loss ratios, although there is little data on which to make the comparisons. The ratio of long to short span, 56/40, is 1.4 whereas the ratio of final losses in corresponding spans for LW beams is 21.33/15.42, or 1.38 -- almost the same.

The practice that some designers follow in estimating total losses to be about 15% and 20%, respectively for NW and LW, appears, from these results, to be a good one.

3.8 Conclusions

Results of tests made on the full size highway bridge made of pretensioned prestressed beams and cast in place slabs show that:

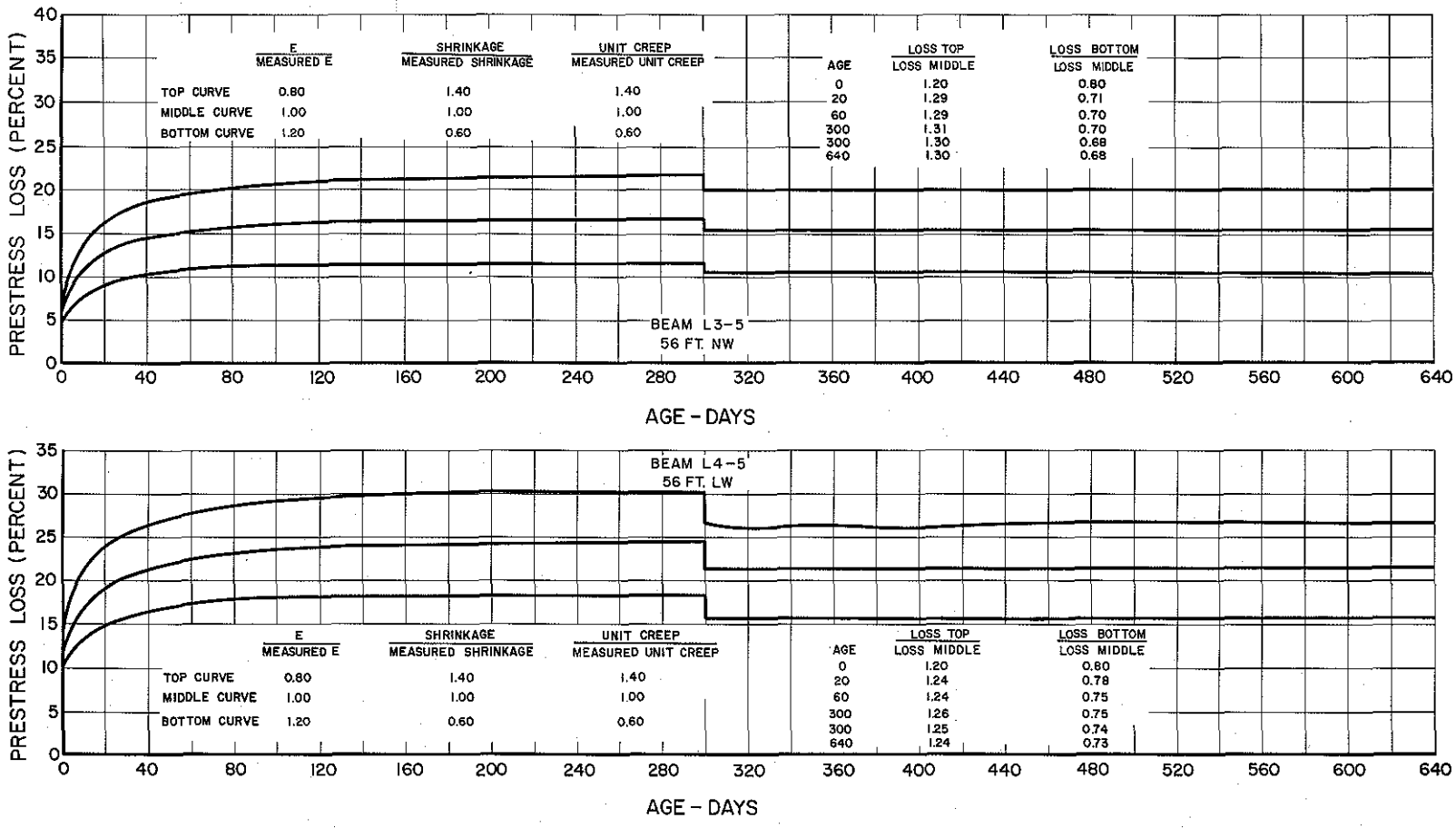

FIGURE 3-44 INFLUENCE OF CHANGES IN SETS OF MODULUS, SHRINKAGE, AND CREEP ON PRESTRESS LOSS AT MIDSPAN

A. Time dependent camber and prestress lossed in prestressed beams can be closely predicted provided that accurate shrinkage and creep data are available.

B. The gains in time dependent camber and prestress loss in beams 10 months old at slab casting were very small for the period between slab casting and termination of tests, a period of about one year.

C. The measured elastic deflection of prestressed beams under the weight of the plastic slab was just a little over one-half the deflection computed by theory.

D. The total final beam camber at mid-span was about 1.6 and 1.9 times the net elastic camber (due to release of prestress and casting of the deck slab) for 56 ft. NW and LW beams, respectively.

E. The time dependent prestress loss was approximately 1.5 times the net elastic loss (due to prestress release and casting of the deck slab) in 56 ft. NW and LW beams. It was higher for the 40 ft. beams.

F. The theoretical effect of over and under estimates of elastic modulus, shrinkage, and creep may be computed by the step-by-step procedure outlined in the report. The most severe combination of 20% error in modulus and 40% error in creep and in shrinkage resulted in approximately 30% error in mid-span deflection and prestress loss.

CHAPTER 4

SUMMARY AND CONCLUSIONS

4.1 The Objectives of the Overall Program

The development of a method that would enable one to predict creep, camber, and prestress loss in pretensioned prestressed lightweight concrete bridge beams was the primary objective of the study.

A secondary objective was the comparison of deflections and prestress losses in draped strand prestressed beams with those of straight strand beams.

In addition to those objectives, it was desirable to gather information on the behavior of full size prestressed concrete beams. That information would include values of camber prestress loss, creep, and shrinkage of beams of a lightweight concrete and a normal weight concrete.

A final objective was to study the creep behavior of the composite prestressed concrete beam - cast in place reinforced concrete slab full size highway bridge.

4.3 The Program

Laboratory tests in the early stages proved the method of prediction to be a valid one and pilot tests on instrumentation on a full size bridge proved the instrumentation plan to be workable.

The main test program called for instrumentation of five full size pretensioned prestressed beams from which strains and elevations were read from the day of casting until they reached an age of 660 days. At approximately 300-day age the beams were erected in the bridge, and

the deck slab was cast. Strain and elevation readings from the slab and beams continued from that age to termination of the program.

Creep and shrinkage data collected from control specimens were used in a program for predicting strain, camber, and prestress loss in the beams and slabs. No relaxation of steel was included.

Four full size pretensioned prestressed concrete bridge beams were cast and instrumented to compare the behavior of draped strand beams with that of straight strand beams. Two normal weight beams were used, one with draped strand and the other with straight strands. Two similar beams of lightweight concrete were used.

4.3 The Conclusions

A. The step-by-step method produces reliable predictions of camber and prestress losses in pretensioned prestressed concrete beams. Control creep, shrinkage, and modulus of elasticity representative of the prototype specimen should be used in the program.

B. At release of prestress there was good agreement between computed and measured camber. The 40 ft. LW beams cambered approximately 0.40 in. at mid-span when prestress was released. The 56 ft. LW beams averaged approximately 1.32 in. mid-span camber at release, and the NW beams 0.62 in. There was excellent agreement between computed and measured camber at release.

C. When the slab was placed, beam age approximately 300 days, computed elastic deflections, due to the plastic slab, were much greater in all beams than measured values. The ratios of measured

to computed mid-span deflections due to that cause were 0.47 for 40 ft. LW, 0.65 for 56 ft. LW, and 0.57 for 56 ft. NW. Modulus of elasticity measurements up to 90 day age indicated no great change in early modulus values. Size effects and possibly the wetting of the top of the beams worked toward holding these deflections to low values.

D. The ratio of 660 day camber, in the beam-slab bridge, to the net measured elastic deflection under prestress release and slab casting, was 1.5 for the 40 ft. LW beams, 1.9 for the 56 ft. LW beams, and 1.6 for the 56 ft. HW beams.

E. Ratios of time dependent prestress losses to elastic prestress losses varied with the type of concrete, curing of beams, and combinations of beam and slab concretes. The ratios for the 56 ft. beams varied from 1.43 to 1.51.

F. Prestress losses, or percentages of the pre-release stress in strands, were approximately 15% for 40 ft. LW beams; 21% for 56 ft. LW beams; and 14 1/2% for 56 ft. NW beams, all at mid-span at 660-day age.

G. Changes in elastic modulus of plus or minus 20%, with no changes in creep or shrinkage, caused less than plus or minus 1% change in prestress loss in theoretical calculations. Those changes do, however, cause changes in elastic deflections in amounts proportional to the change in the modulus.

H. Severe divergences in creep and shrinkage from actual (datum) values in combination with 20% change in modulus of elasticity, from its actual value, cause variations from datum values of deflections and prestress losses.

Based on datum values computed from actual moduli, creep, and shrinkage, errors in estimations of those parameters would cause deflections and prestress losses at mid-span shown below:

Decrease E to 80% of datum and increase creep and shrinkage to 140% of datum:

Beam	Deflection (% datum)	Prestress Loss (% datum)
56 ft. NW	126	131
56 ft. LW	119	124

Increase E to 120% of datum and decrease creep and shrinkage to 60% of datum:

Beam	Deflection (% datum)	Prestress Loss (% datum)
56 ft. NW	65	68
56 ft. LW	70	73

I. There was little difference in prestress loss in draped strand and blanketed strand 50 ft. beams at 140 day age. Camber ratios of the blanketed strand beams to those of the draped strand beams were 0.57 for NW beams and 0.62 for LW beams, respectively.

REFERENCES

1. Furr, Howard L. and Raouf Sinno. "Creep in Prestressed Lightweight Concrete," Research Report 69-2, Study 2-5-63-69, Texas Transportation Institute, Texas A&M University, College Station, Texas. October 1967.

2. Torben C. Hansen and Alan H. Matlock, "Influence of Size and Shape of Member on the Shrinkage and Creep of Concrete," Journal of the American Concrete Institute, February 1946, Proceeding v. 63, page 267.

3. Dan E. Branson, "Time-Dependent Effects in Composite Concrete Beams," Journal of the American Concrete Institute, February 1964, Proc. v. 61, No. 2, pp 213-230.

4. Abul Hasnat, Behavior of Prestressed Composite T-Beams of Lightweight Aggregate Concrete, Ph.D. Dissertation, Texas A&M University, College Station, Texas, January 1965 (101 pages).

5. ACI Standard Building Code Requirements for Reinforced Concrete (ACI 318-63), American Concrete Institute, Detroit, Michigan, 1963.

6. Raouf Sinno, The Time Dependent Deflections of Prestressed Concrete Bridge Beams, Ph.D. Dissertation, Texas A&M University, College Station, Texas, January 1968 (178 pages).

APPENDIX

DETAILED FLOW DIAGRAM FOR PREDICTING PRESTRESSED BEAM CAMBER, PRESTRESS LOSS, AND STRAINS

Symbols for Computer Program

ID	Project identification
IDB	Beam identification
ENER	Moment of inertia of beam gross section ($in.^4$)
CGC	Distance from bottom of beam to the centroid of the gross section (in.)
D	Overall depth of beam (in.)
UW	Weight per lineal ft. of beam (lb./ft.)
AC	Gross area of beam cross section ($in.^2$)
XL	Beam span C-L of supports (ft.)
H	Distance from mid-span to hold-down point (ft.)
STNO	Number of prestressing tendons
AST	Area of one prestressing tendon ($in.^2$)
ED	Eccentricity of effective prestressing strands at end support (dist. from CGC to CGS) (in.)
EM	Eccentricity of effective prestressing strands at mid-span (in.)
PS	Anchorage force per tendon (lb.)
EC	Modulus of elasticity of beam concrete (ksi)
ES	Modulus of elasticity of prestressing steel (ksi)
EA, EB, EX	Distance from mid-span to station A, B, X (ft.)
ASH	Shrinkage strain for beam concrete at infimite time (microinches per in.)
BSH	Age at which 50% of ASH develops (days)
ACR	Creep strain in beam concrete at infinite time (microinches per in.)

BCR	Age at which 50% of ACR develops (days)
XN	Length of time increment (days)
XNT	Length of prediction period (days)
XLX	Number of strain increments
XA, XB, XC	Distance from center of support to stations A, B, C (ft.)
GT	Distance from top of beam to top gage point (in.)
GB, GM	Distance from bottom of beam to bottom gage point and middle gage point, respectively (in.)
XINC	Time duration from day of casting of beam to day of prestress release (days)
W	Width of slab for one beam (flange width) (ft.)
T	Thickness of slab (in.)
UWS	Weight per lineal ft. at slab width W (lb./ft.)
ECSL	Modulus of elasticity for slab concrete (ksi)
ASHSL	Shrinkage strain in slab concrete at infinite time (microinches per in.)
BSHSL	Age at which 50% of ASHSL develops (days)
ACRSL	Creep strain in slab concrete at infinite time (microinches per in.)
BCRSL	Age at which 50% of ACRSL develops (days)
XCAST	Age of beams when slabs were cast (days)
INCSL	Time duration of free shrinkage of slab between casting date and date when it is assumed to be effective in transmitting shrinkage induced stress to beam (days)

KIF — Integer control which directs the program to include or not to include camber and/or strain

KIF = 1 -- program predicts camber

KIF = 2 -- program predicts strains

KIF = 3 -- program predicts camber and strains

PROGRAM FOR PREDICTING STRESSES, STRAINS, AND CAMBER IN PRESTRESSED CONCRETE BEAM AND IN COMPOSITE REINFORCED CONCRETE SLAB WITH PRESTRESSED CONCRETE BEAM

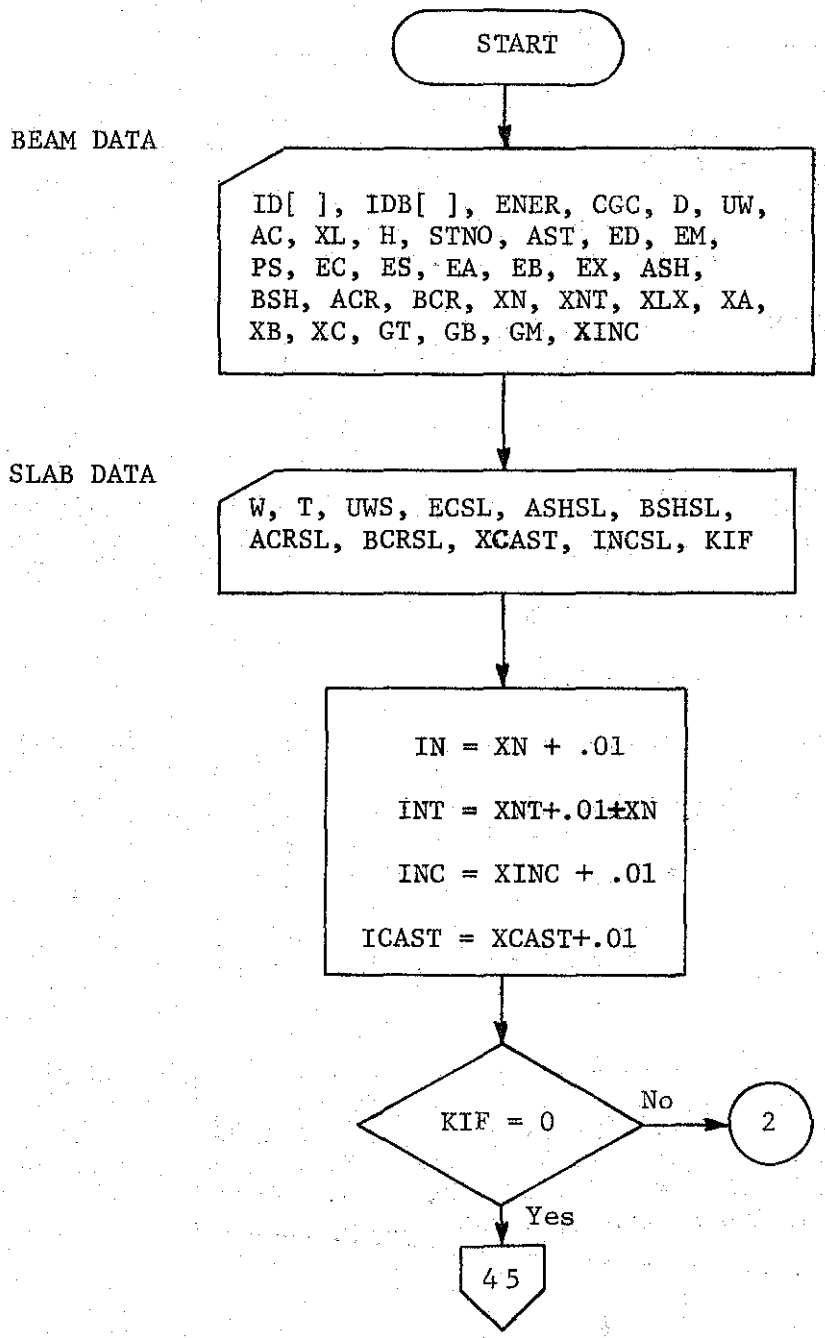

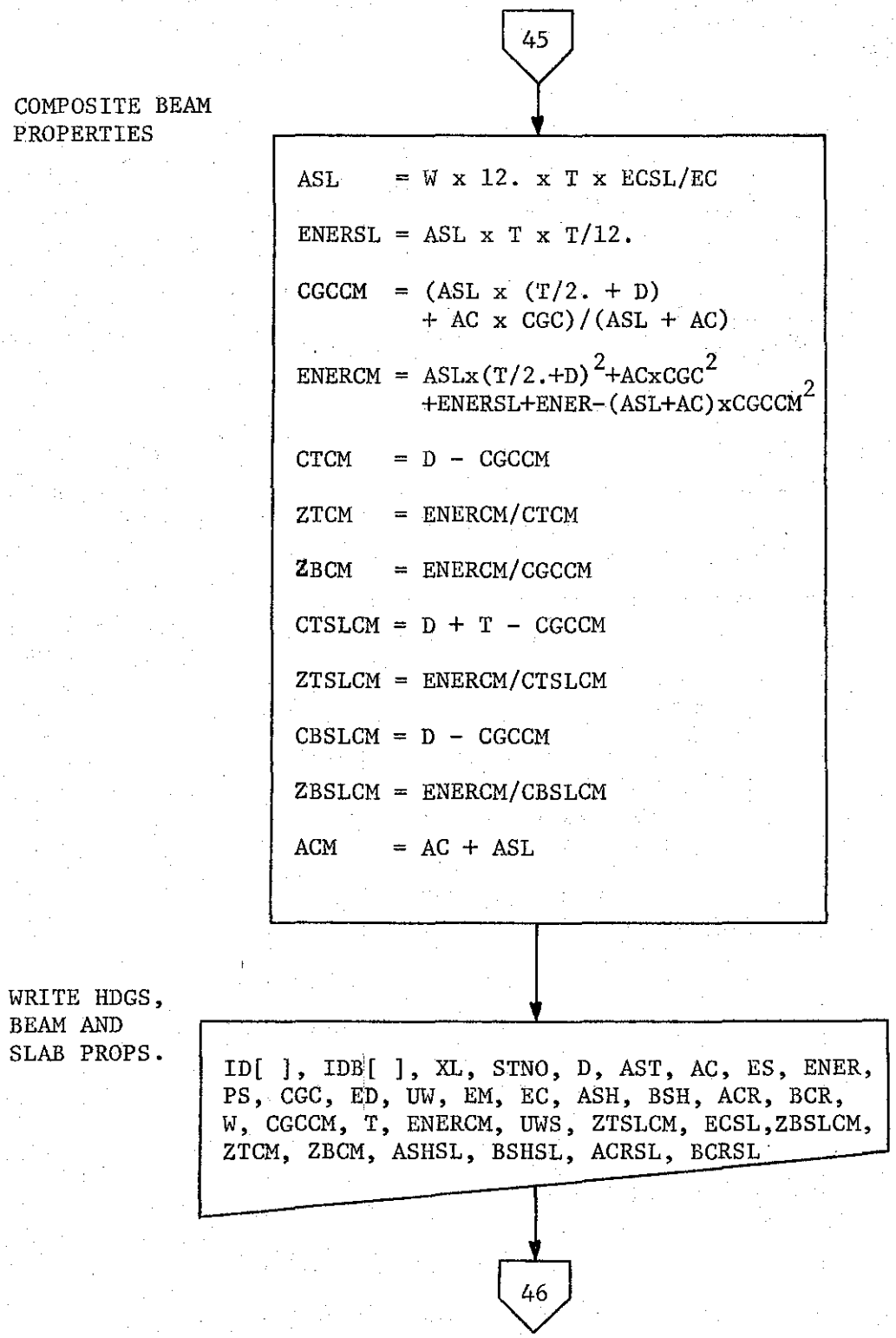
45
COMPOSITE BEAM PROPERTIES
ASL = W x 12. x T x ECSL/EC
ENERSL = ASL x T x T/12.
CGCCM = (ASL x (T/2. + D) + AC x CGC)/(ASL + AC)
ENERCM = ASLx(T/2.+D)2+ACxCGC2 +ENERSL+ENER-(ASL+AC)xCGCCM2
CTCM = D - CGCCM
ZTCM = ENERCM/CTCM
ZBCM = ENERCM/CGCCM
CTSLCM = D + T - CGCCM
ZTSLCM = ENERCM/CTSLCM
CBSLCM = D - CGCCM
ZBSLCM = ENERCM/CBSLCM
ACM = AC + ASL
WRITE HDGS, BEAM AND SLAB PROPS.
ID[ ], IDB[ ], XL, STNO, D, AST, AC, ES, ENER, PS, CGC, ED, UW, EM, EC, ASH, BSH, ACR, BCR, W, CGCCM, T, ENERCM, UWS, ZTSLCM, ECSL,ZBSLCM, ZTCM, ZBCM, ASHSL, BSHSL, ACRSL, BCRSL
46

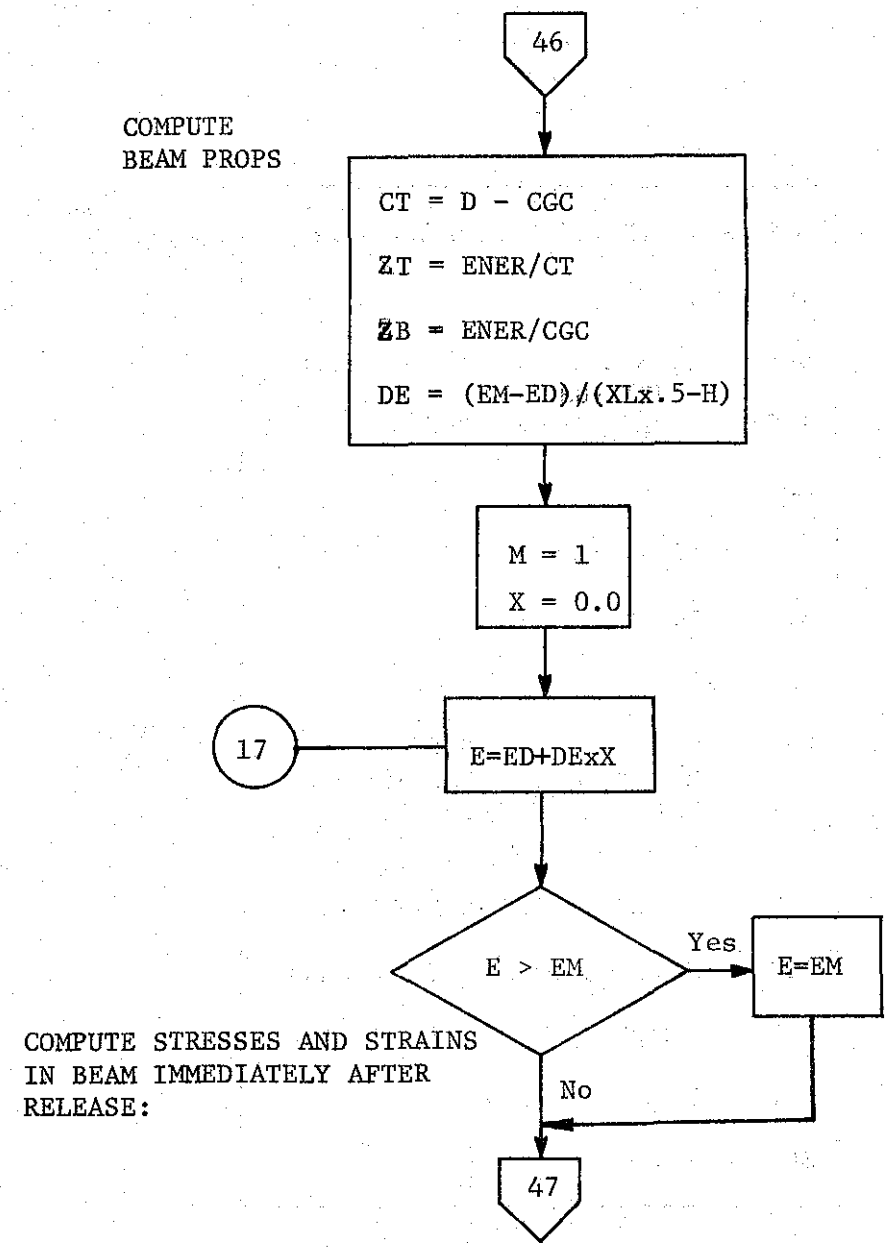
46
COMPUTE
BEAM PROPS
CT = D - CGC
ZT = ENER/CT
ZB = ENER/CGC
DE = (EM-ED)/(XLx.5-H)
M = 1
X = 0.0
17
E=ED+DExX
E > EM
Yes
E=EM
No
COMPUTE STRESSES AND STRAINS
IN BEAM IMMEDIATELY AFTER
RELEASE:
47

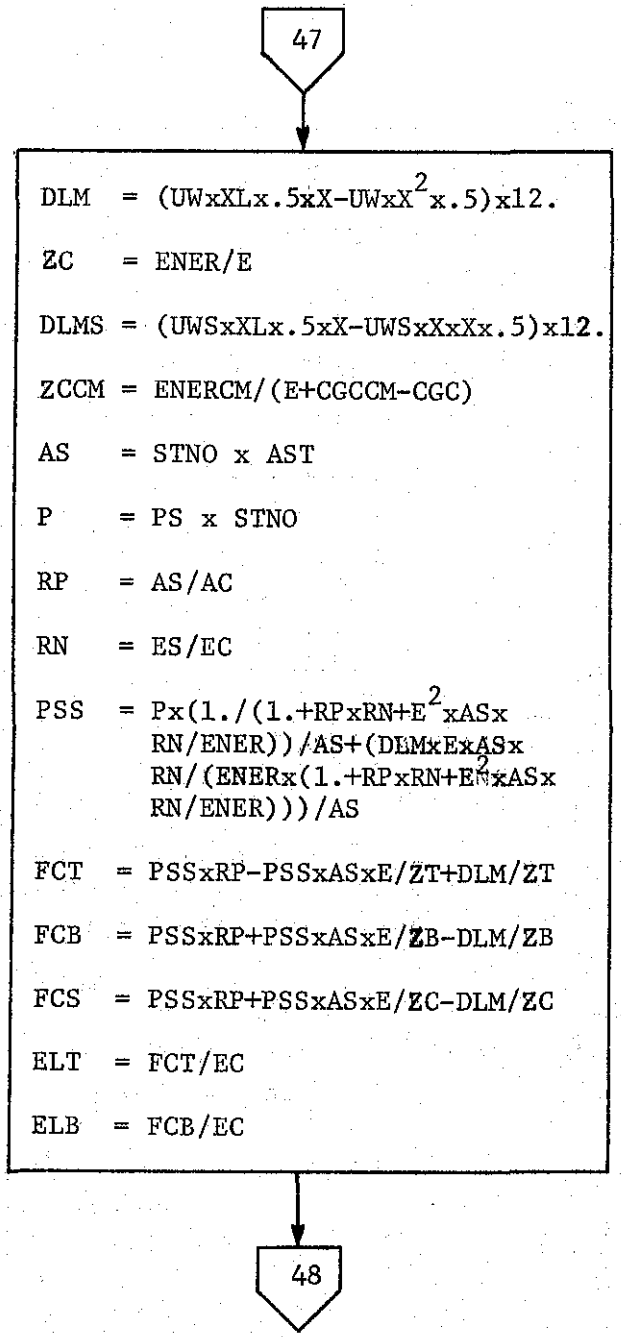
47
DLM = (UWxXLx.5xX-UWxX^2x.5)x12.
ZC = ENER/E
DLMS = (UWSxXLx.5xX-UWSxXxXx.5)x12.
ZCCM = ENERCM/(E+CGCCM-CGC)
AS = STNO x AST
P = PS x STNO
RP = AS/AC
RN = ES/EC
PSS = Px(1./(1.+RPxRN+E^2xASx RN/ENER))/AS+(DLMxExASx RN/(ENERx(1.+RPxRN+E^2xASx RN/ENER)))/AS
FCT = PSSxRP-PSSxASxE/ZT+DLM/ZT
FCB = PSSxRP+PSSxASxE/ZB-DLM/ZB
FCS = PSSxRP+PSSxASxE/ZC-DLM/ZC
ELT = FCT/EC
ELB = FCB/EC
48

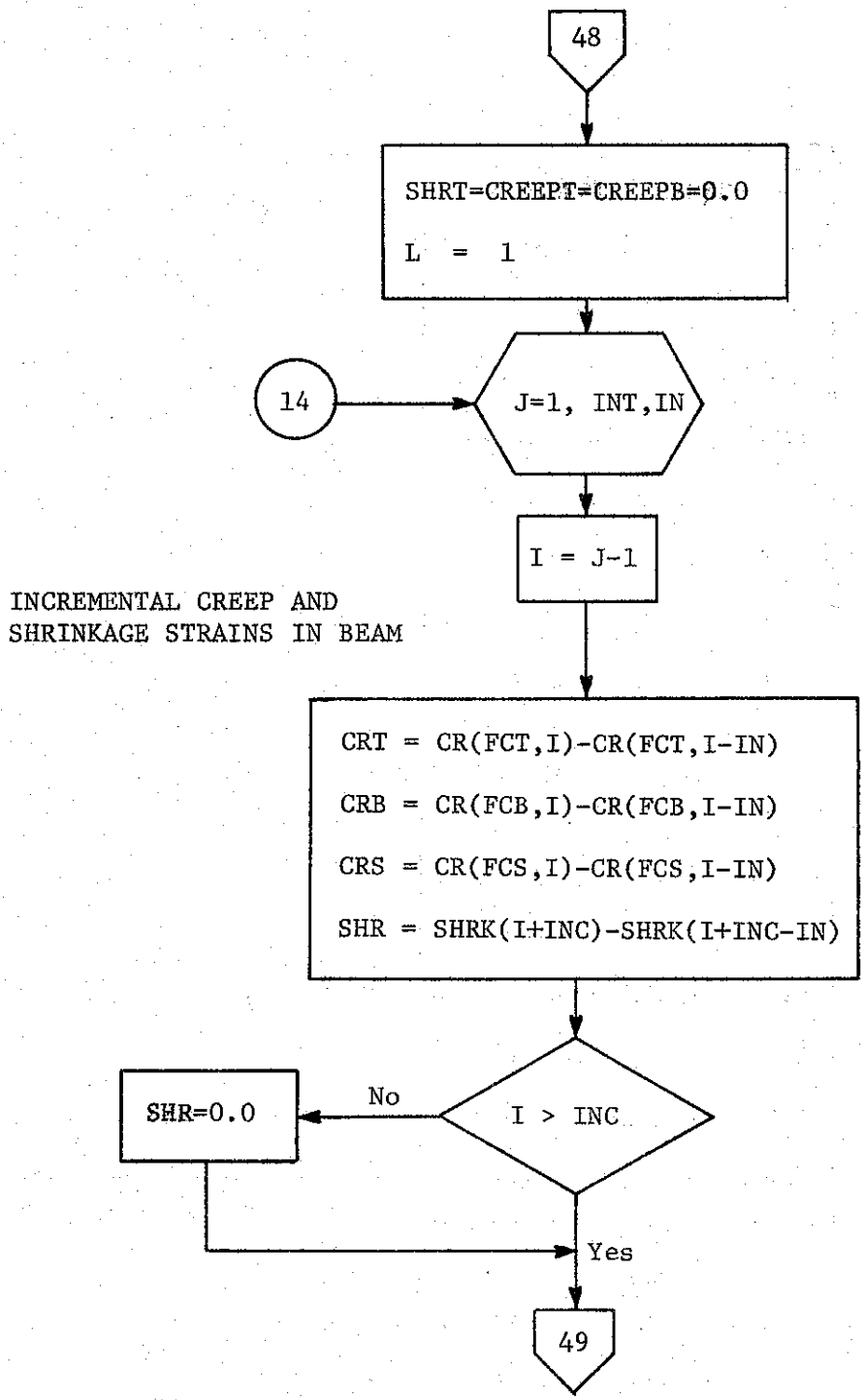
48
SHRT=CREEPT=CREEPB=0.0
L = 1
14
J=1, INT,IN
I = J-1
INCREMENTAL CREEP AND
SHRINKAGE STRAINS IN BEAM
CRT = CR(FCT,I)-CR(FCT,I-IN)
CRB = CR(FCB,I)-CR(FCB,I-IN)
CRS = CR(FCS,I)-CR(FCS,I-IN)
SHR = SHRK(I+INC)-SHRK(I+INC-IN)
I > INC
No
SHR=0.0
Yes
49

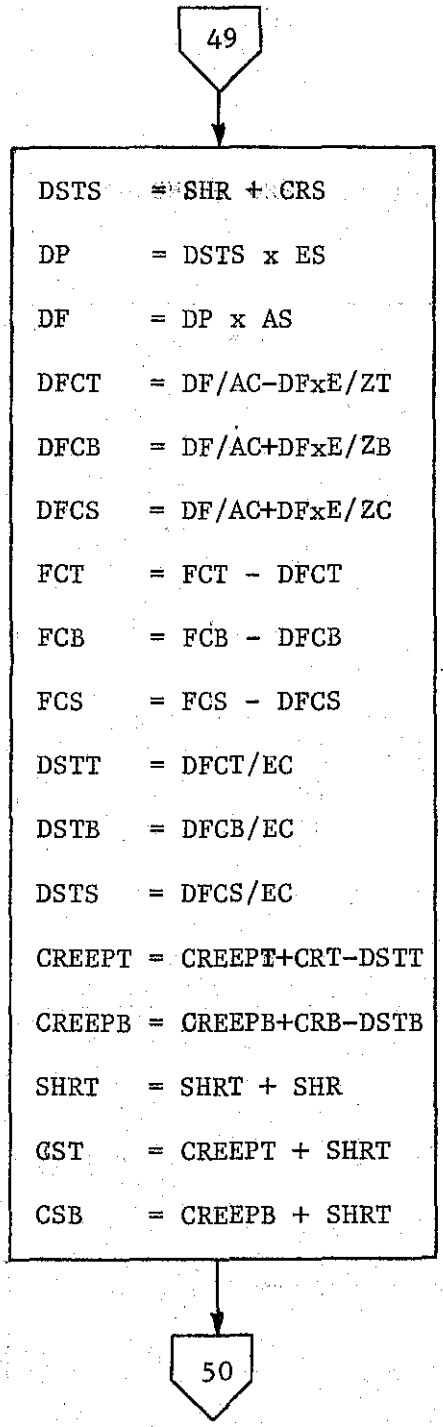
49
DSTS = SHR + CRS
DP = DSTS x ES
DF = DP x AS
DFCT = DF/AC-DFxE/ZT
DFCB = DF/AC+DFxE/ZB
DFCS = DF/AC+DFxE/ZC
FCT = FCT - DFCT
FCB = FCB - DFCB
FCS = FCS - DFCS
DSTT = DFCT/EC
DSTB = DFCB/EC
DSTS = DFCS/EC
CREEPT = CREEPT+CRT-DSTT
CREEPB = CREEPB+CRB-DSTB
SHRT = SHRT + SHR
GST = CREEPT + SHRT
CSB = CREEPB + SHRT
50

TOTAL STRAINS AND ROTATION
OF INCREMENTAL LENGTH
OF BEAM

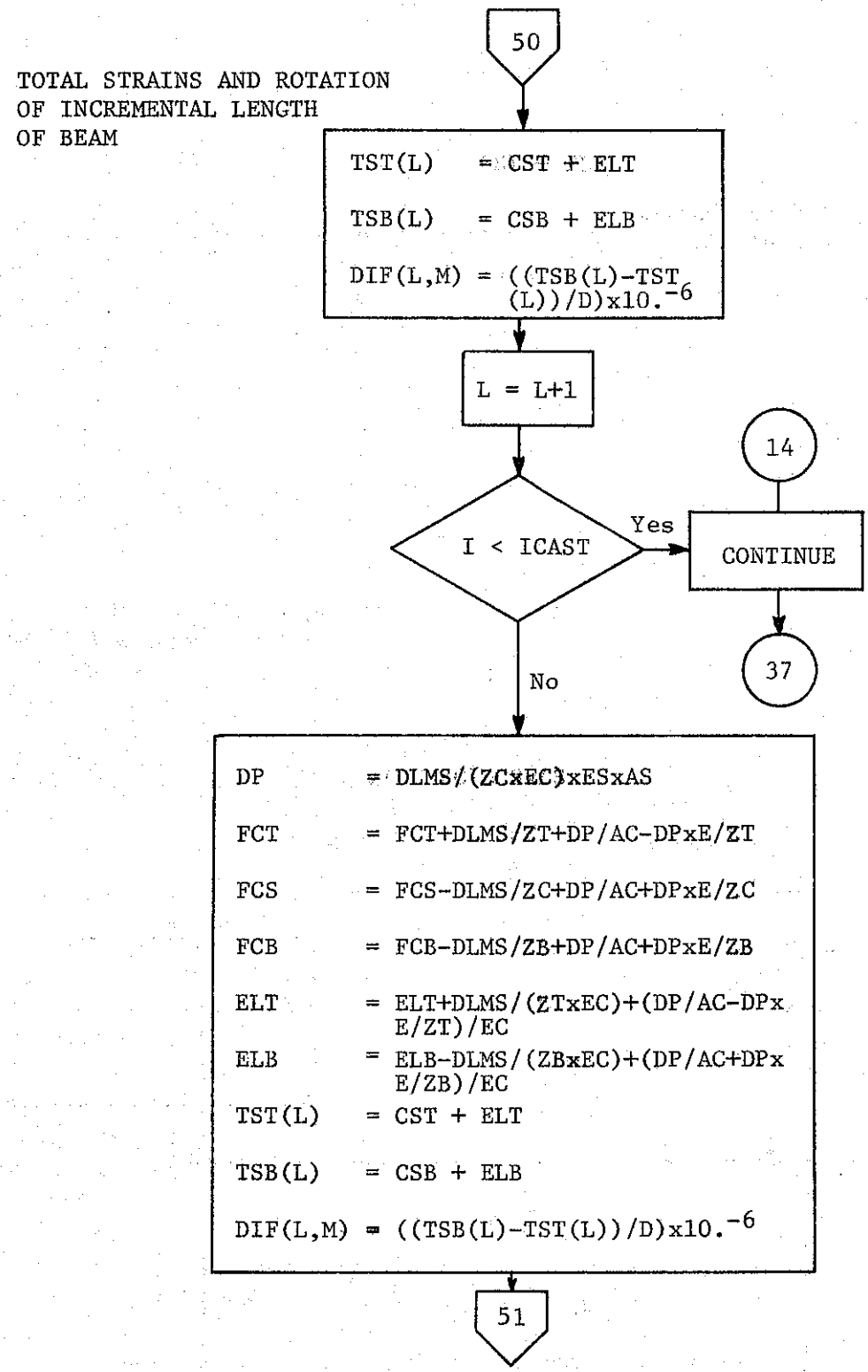

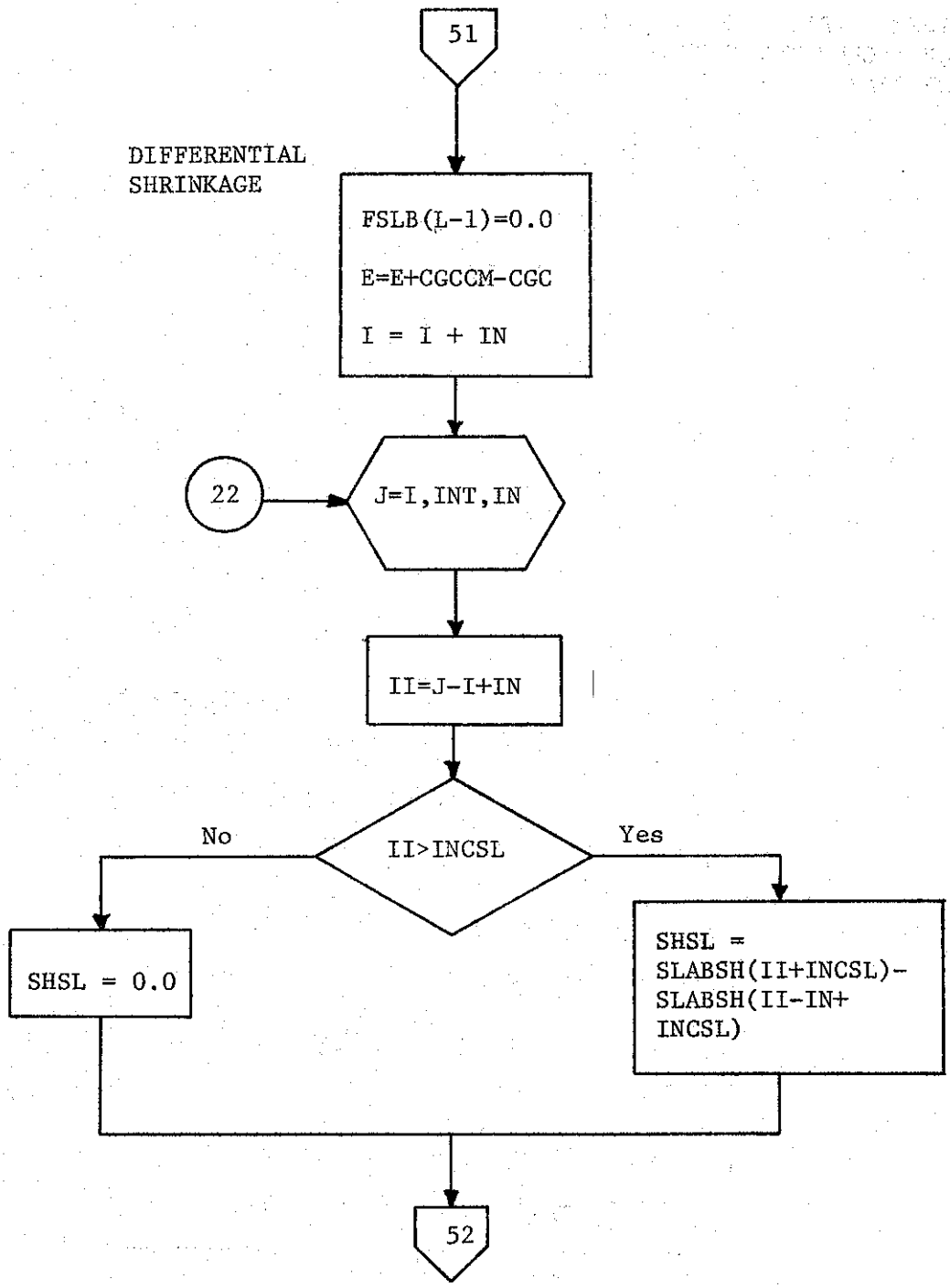
51
DIFFERENTIAL SHRINKAGE
FSLB(L-1)=0.0
E=E+CGCCM-CGC
I = I + IN
22
J=I,INT,IN
II=J-I+IN
II>INCSL
No
Yes
SHSL = 0.0
SHSL = SLABSH(II+INCSL)-SLABSH(II-IN+INCSL)
52

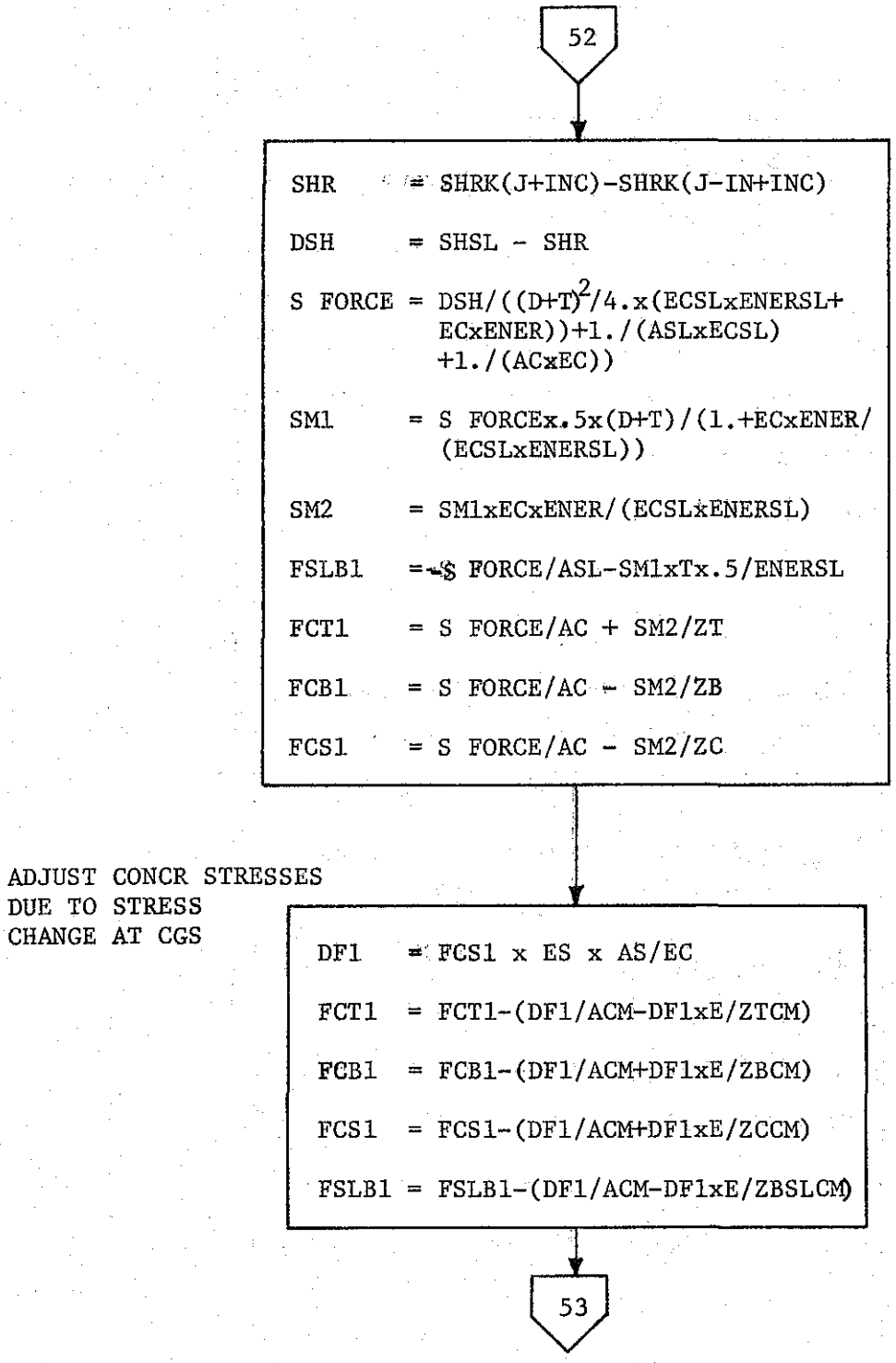
52
SHR = SHRK(J+INC)-SHRK(J-IN+INC)
DSH = SHSL - SHR
S FORCE = DSH/((D+T)**2/4.x(ECSLxENERSL+ ECxENER))+1./(ASLxECSL) +1./(ACxEC))
SM1 = S FORCEx.5x(D+T)/(1.+ECxENER/ (ECSLxENERSL))
SM2 = SM1xECxENER/(ECSLxENERSL)
FSLB1 = S FORCE/ASL-SM1xTx.5/ENERSL
FCT1 = S FORCE/AC + SM2/ZT
FCB1 = S FORCE/AC - SM2/ZB
FCS1 = S FORCE/AC - SM2/ZC
ADJUST CONCR STRESSES DUE TO STRESS CHANGE AT CGS
DF1 = FCS1 x ES x AS/EC
FCT1 = FCT1-(DF1/ACM-DF1xE/ZTCM)
FCB1 = FCB1-(DF1/ACM+DF1xE/ZBCM)
FCS1 = FCS1-(DF1/ACM+DF1xE/ZCCM)
FSLB1 = FSLB1-(DF1/ACM-DF1xE/ZBSLCM)
53

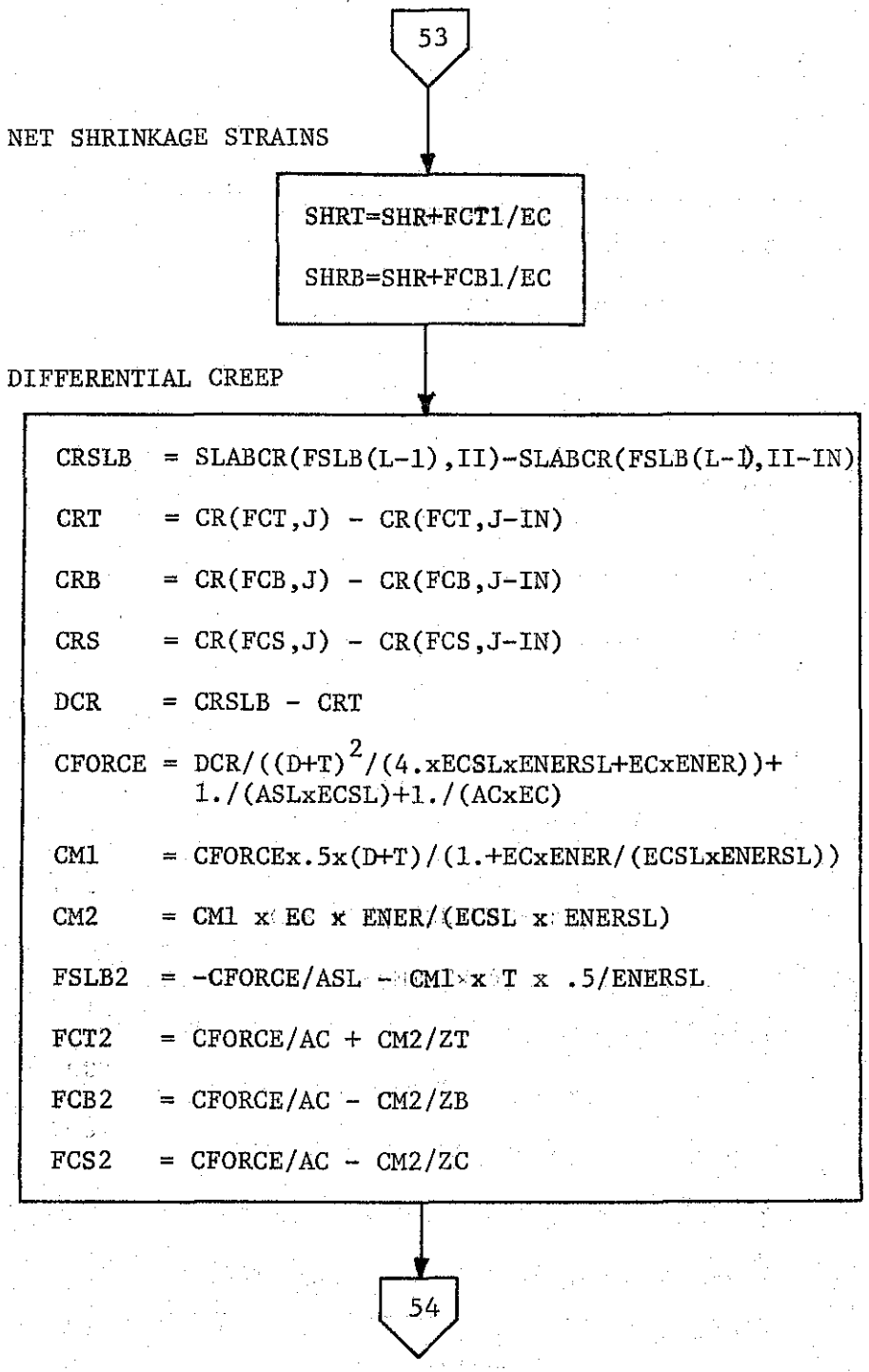
53
NET SHRINKAGE STRAINS
SHRT=SHR+FCT1/EC
SHRB=SHR+FCB1/EC
DIFFERENTIAL CREEP
CRSLB = SLABCR(FSLB(L-1),II)-SLABCR(FSLB(L-1),II-IN)
CRT = CR(FCT,J) - CR(FCT,J-IN)
CRB = CR(FCB,J) - CR(FCB,J-IN)
CRS = CR(FCS,J) - CR(FCS,J-IN)
DCR = CRSLB - CRT
CFORCE = DCR/((D+T)**2/(4.xECSLxENERSL+ECxENER))+
1./(ASLxECSL)+1./(ACxEC)
CM1 = CFORCEx.5x(D+T)/(1.+ECxENER/(ECSLxENERSL))
CM2 = CM1 x EC x ENER/(ECSL x ENERSL)
FSLB2 = -CFORCE/ASL - CM1 x T x .5/ENERSL
FCT2 = CFORCE/AC + CM2/ZT
FCB2 = CFORCE/AC - CM2/ZB
FCS2 = CFORCE/AC - CM2/ZC
54

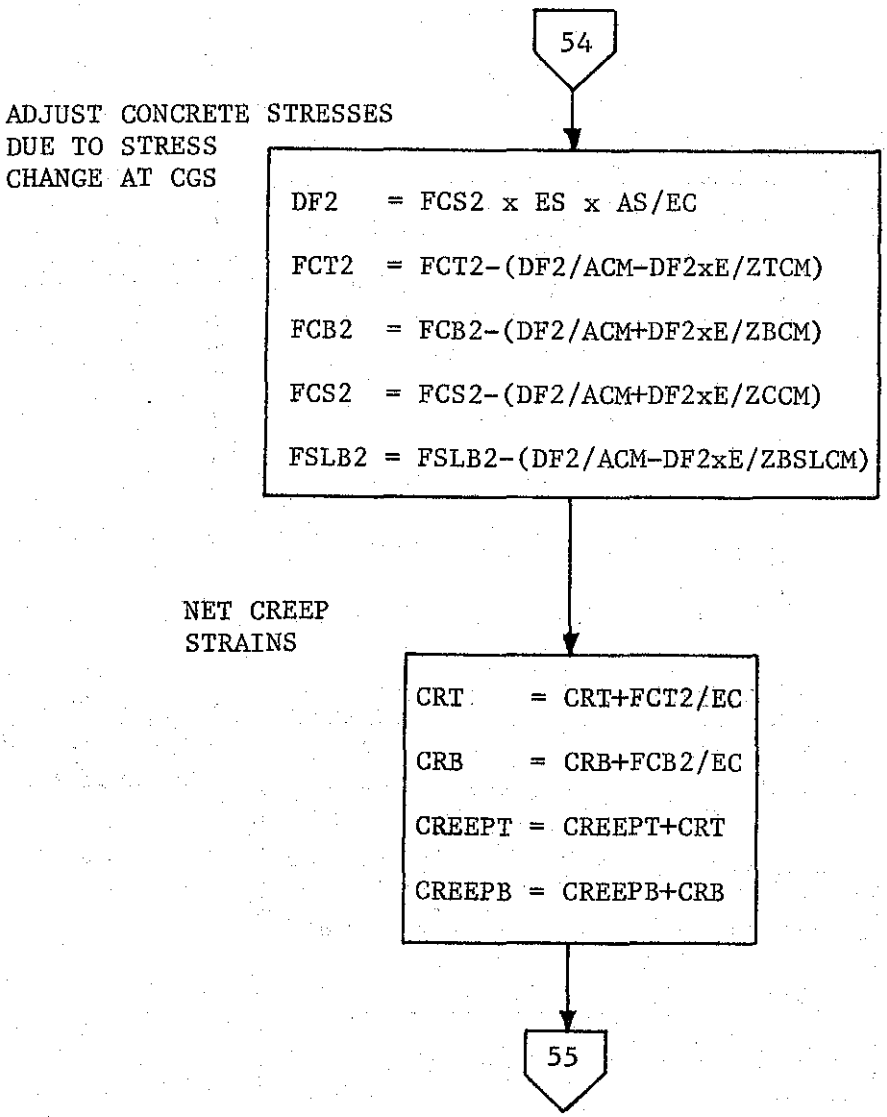
54
ADJUST CONCRETE STRESSES
DUE TO STRESS
CHANGE AT CGS
DF2 = FCS2 x ES x AS/EC
FCT2 = FCT2-(DF2/ACM-DF2xE/ZTCM)
FCB2 = FCB2-(DF2/ACM+DF2xE/ZBCM)
FCS2 = FCS2-(DF2/ACM+DF2xE/ZCCM)
FSLB2 = FSLB2-(DF2/ACM-DF2xE/ZBSLCM)
NET CREEP
STRAINS
CRT = CRT+FCT2/EC
CRB = CRB+FCB2/EC
CREEPT = CREEPT+CRT
CREEPB = CREEPB+CRB
55

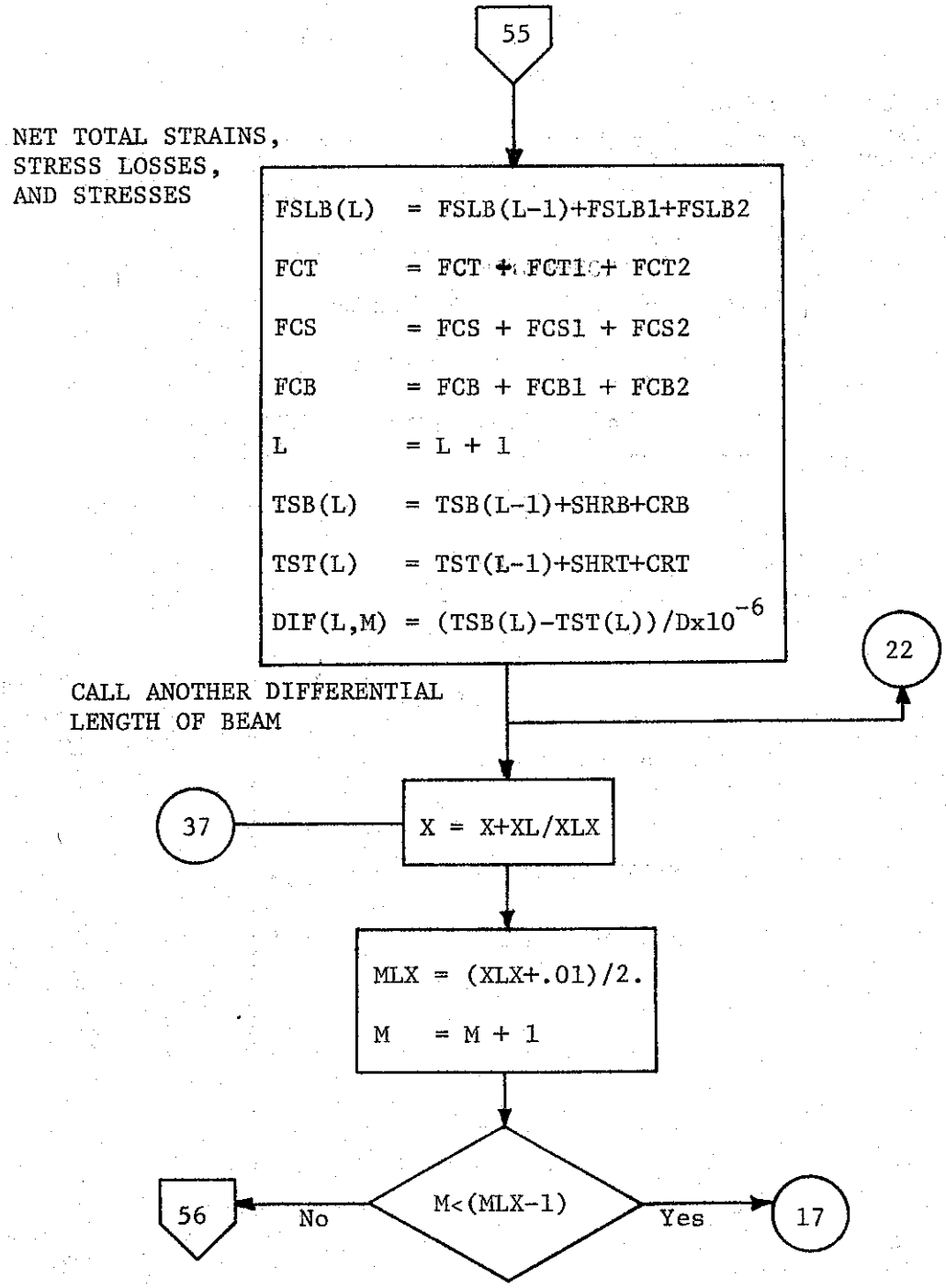
55
NET TOTAL STRAINS,
STRESS LOSSES,
AND STRESSES
FSLB(L) = FSLB(L-1)+FSLB1+FSLB2
FCT = FCT + FCT1 + FCT2
FCS = FCS + FCS1 + FCS2
FCB = FCB + FCB1 + FCB2
L = L + 1
TSB(L) = TSB(L-1)+SHRB+CRB
TST(L) = TST(L-1)+SHRT+CRT
DIF(L,M) = (TSB(L)-TST(L))/Dx10^-6
22
CALL ANOTHER DIFFERENTIAL
LENGTH OF BEAM
37
X = X+XL/XLX
MLX = (XLX+.01)/2.
M = M + 1
M<(MLX-1)
No
Yes
56
17

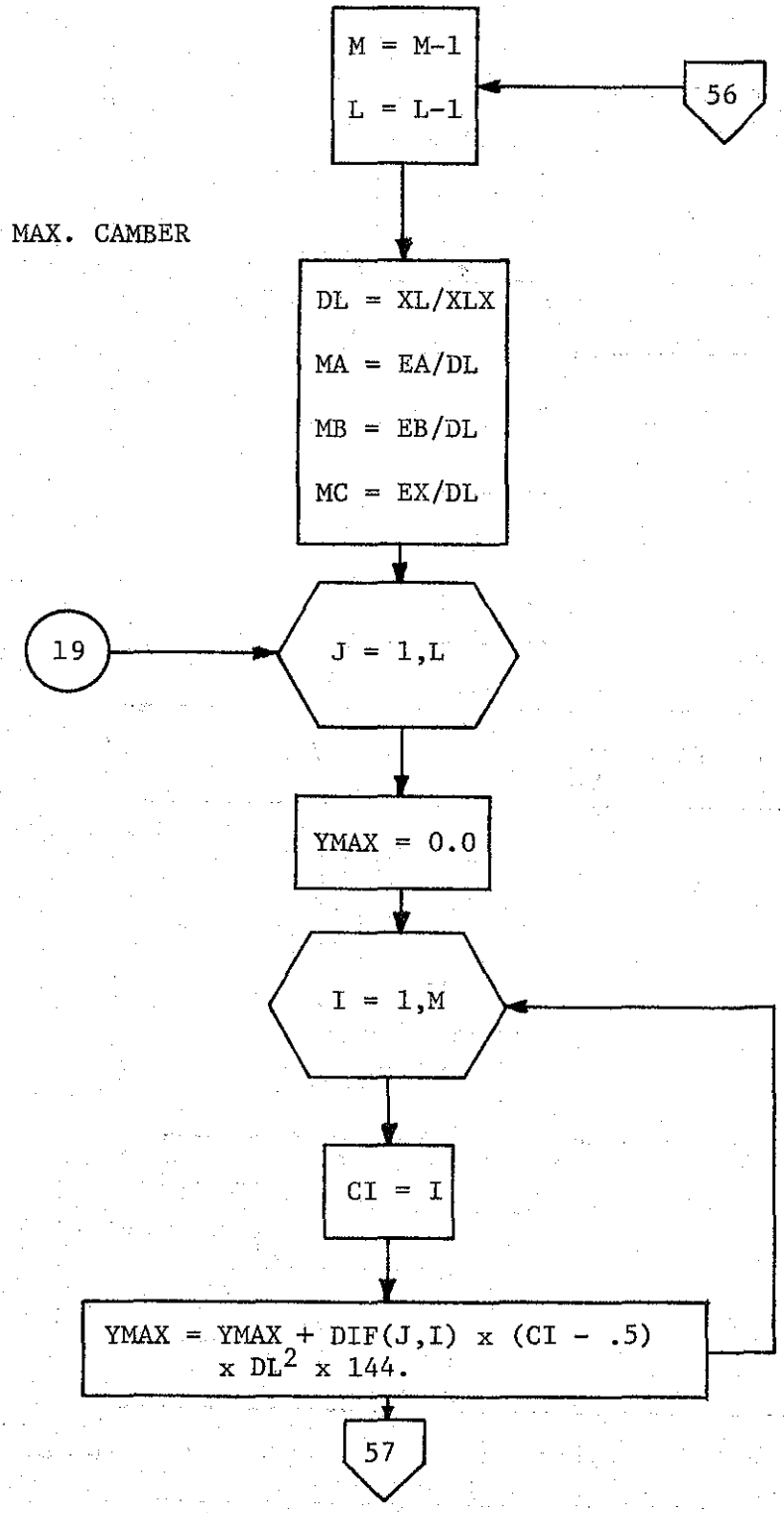
M = M-1
L = L-1
56
MAX. CAMBER
DL = XL/XLX
MA = EA/DL
MB = EB/DL
MC = EX/DL
19
J = 1,L
YMAX = 0.0
I = 1,M
CI = I
YMAX = YMAX + DIF(J,I) x (CI - .5)
x DL2 x 144.
57

CAMBER AT THREE
OTHER POINTS

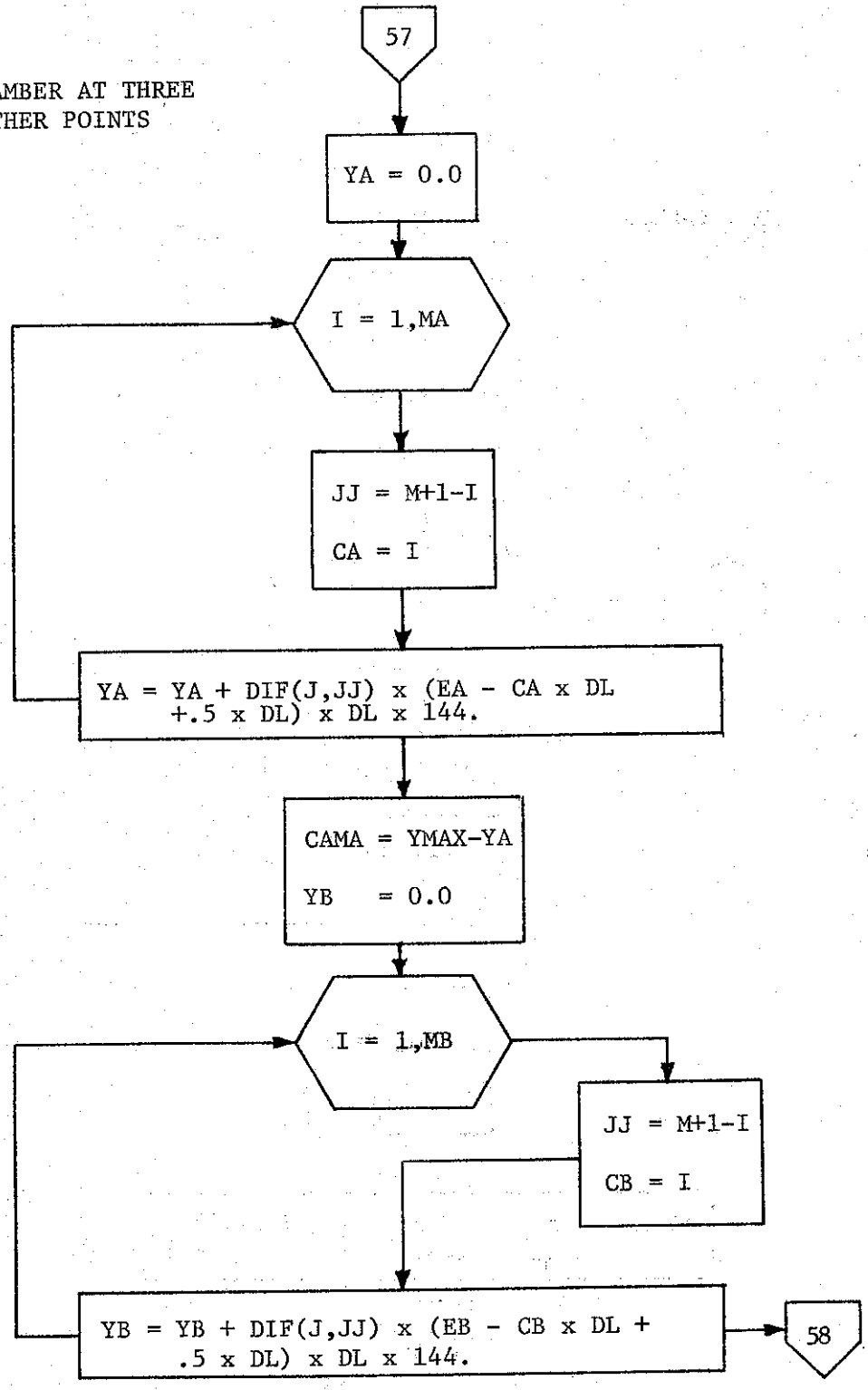

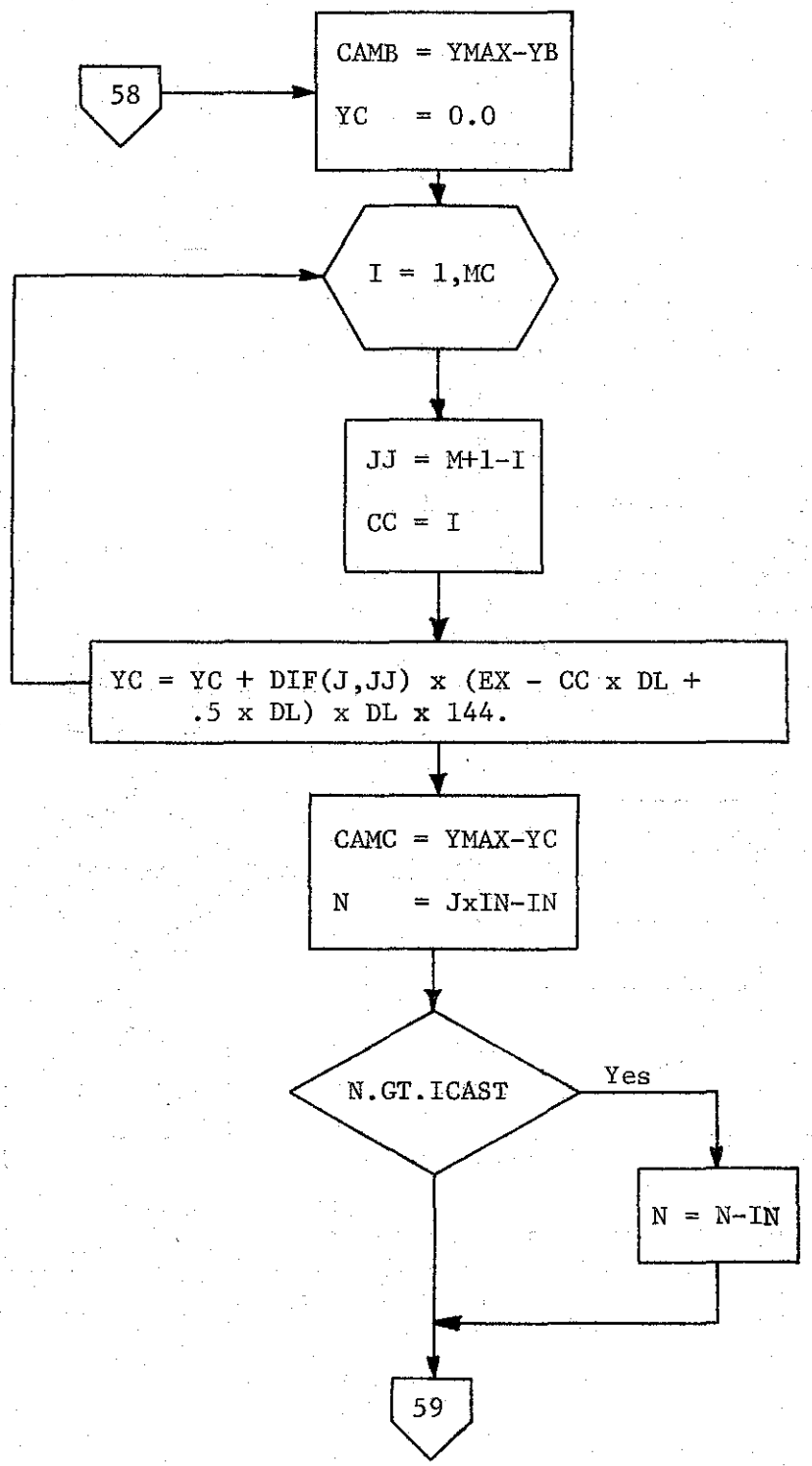
58
CAMB = YMAX-YB
YC = 0.0
I = 1,MC
JJ = M+1-I
CC = I
YC = YC + DIF(J,JJ) x (EX - CC x DL +
.5 x DL) x DL x 144.
CAMC = YMAX-YC
N = JxIN-IN
N.GT.ICAST
Yes
N = N-IN
59

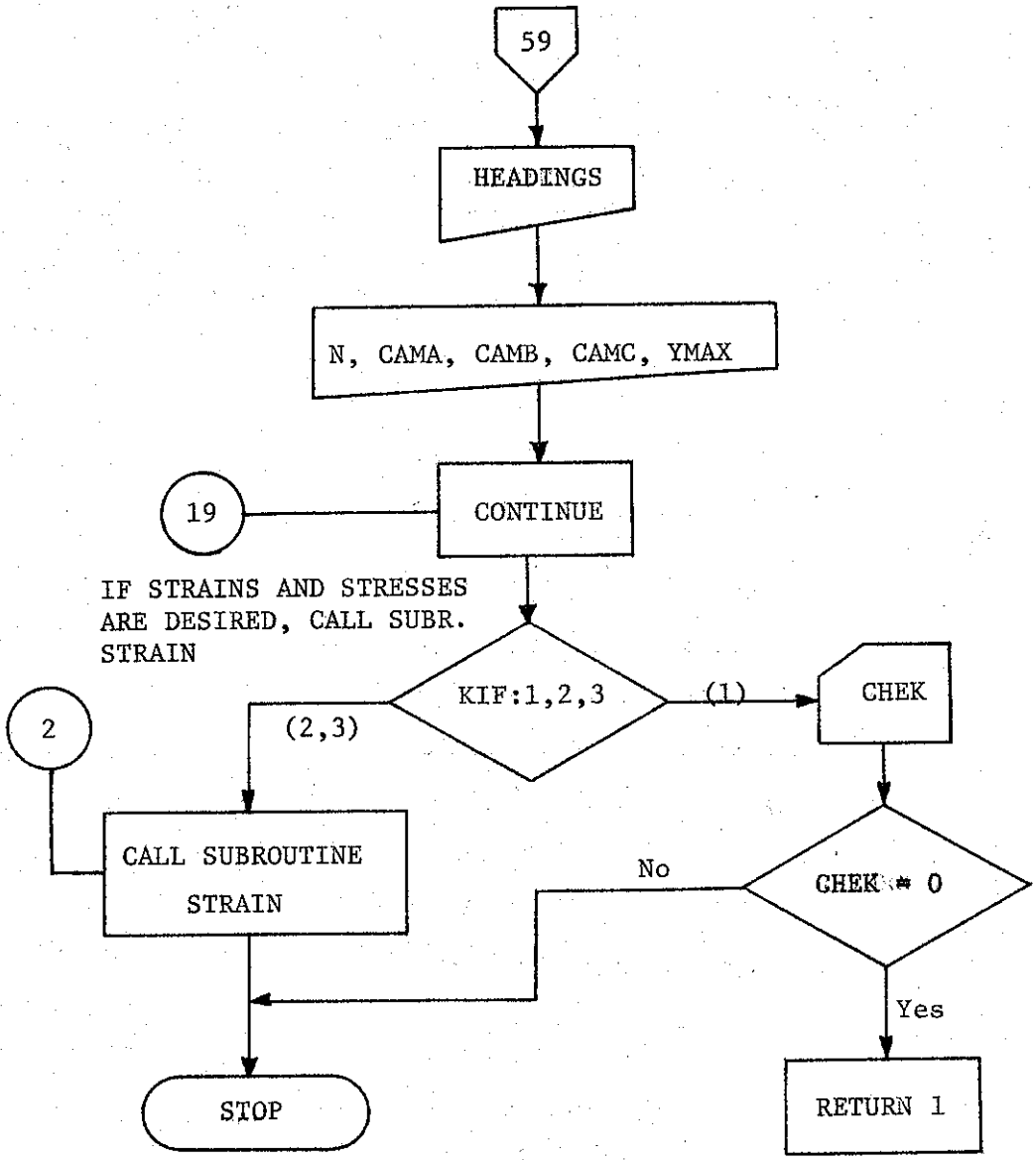
59
HEADINGS
N, CAMA, CAMB, CAMC, YMAX
19
CONTINUE
IF STRAINS AND STRESSES ARE DESIRED, CALL SUBR. STRAIN
KIF:1,2,3
(1)
CHEK
(2,3)
2
CALL SUBROUTINE STRAIN
No
CHEK .# 0
Yes
STOP
RETURN 1

```
SUBROUTINE STRAIN (AC, XL, XA, XB, XC, GT, GB, GM, ENER, CGC, D, UW, EC, STNO,
       AST, ED, EM, PS, ES, IN, INT, INC, H, W, T, UWS, ECSL, ICAST, INCSL, ID,
       IDB)

DIMENSION  ID(  ), IDB(  ), TST(  ), TSM(  ), TSB(  ), TSS(  ), STLOSS(  ),
       TSLT(  ), TSLB(  ), FSLT(  ), FSLB(  )

COMMON   ASH, BSH, ACR, BCR, ASHSL, BSHSL, ACRSL, BCRSL
```

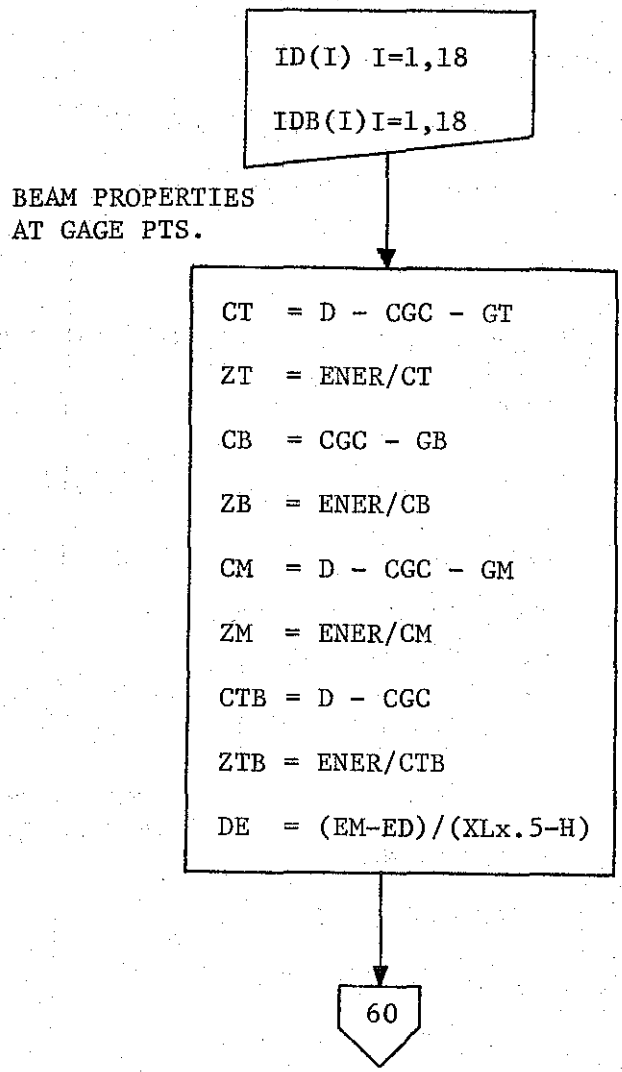

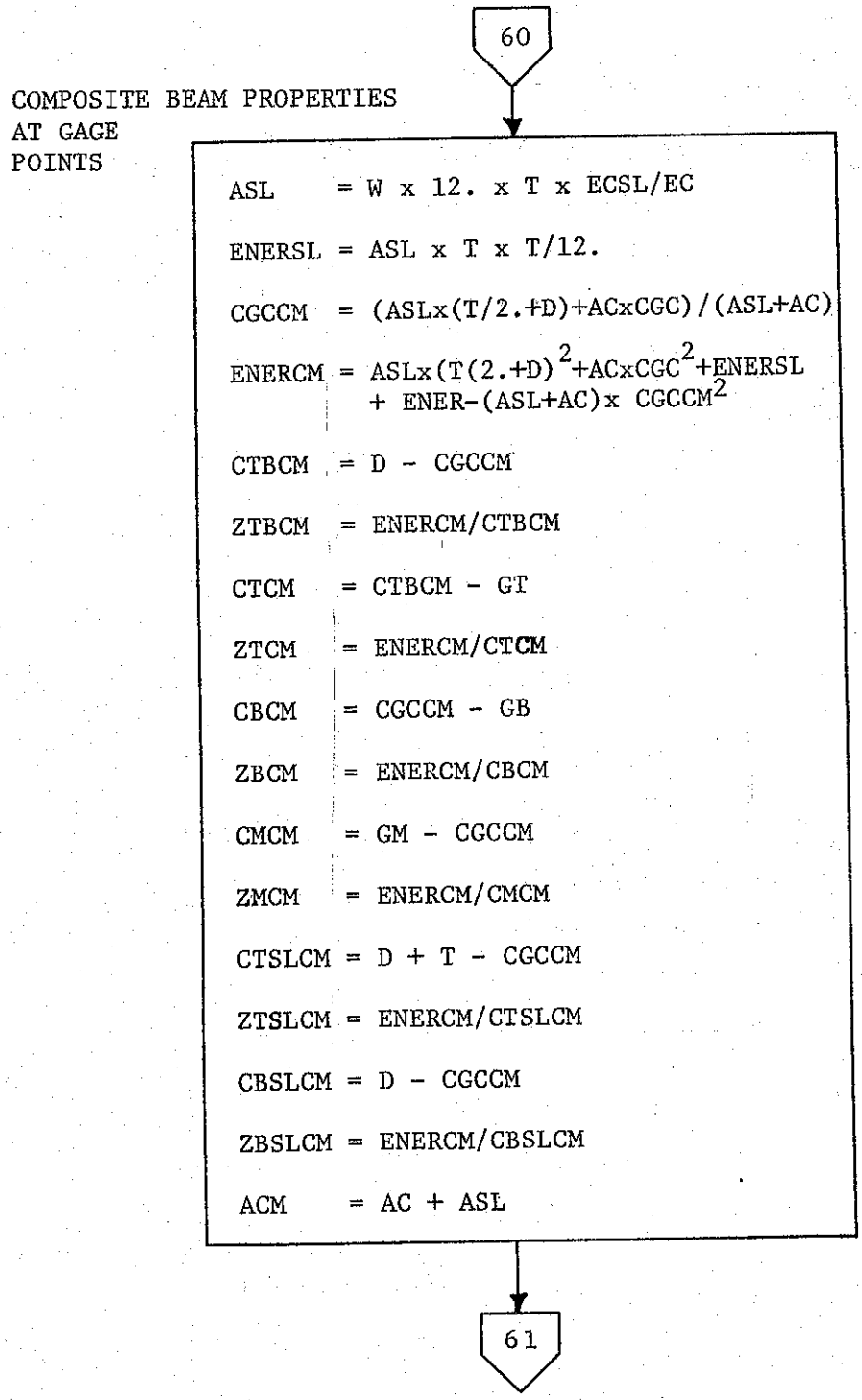
60
COMPOSITE BEAM PROPERTIES AT GAGE POINTS
ASL = W x 12. x T x ECSL/EC
ENERSL = ASL x T x T/12.
CGCCM = (ASLx(T/2.+D)+ACxCGC)/(ASL+AC)
ENERCM = ASLx(T(2.+D)2+ACxCGC2+ENERSL + ENER-(ASL+AC)x CGCCM2
CTBCM = D - CGCCM
ZTBCM = ENERCM/CTBCM
CTCM = CTBCM - GT
ZTCM = ENERCM/CTCM
CBCM = CGCCM - GB
ZBCM = ENERCM/CBCM
CMCM = GM - CGCCM
ZMCM = ENERCM/CMCM
CTSLCM = D + T - CGCCM
ZTSLCM = ENERCM/CTSLCM
CBSLCM = D - CGCCM
ZBSLCM = ENERCM/CBSLCM
ACM = AC + ASL
61

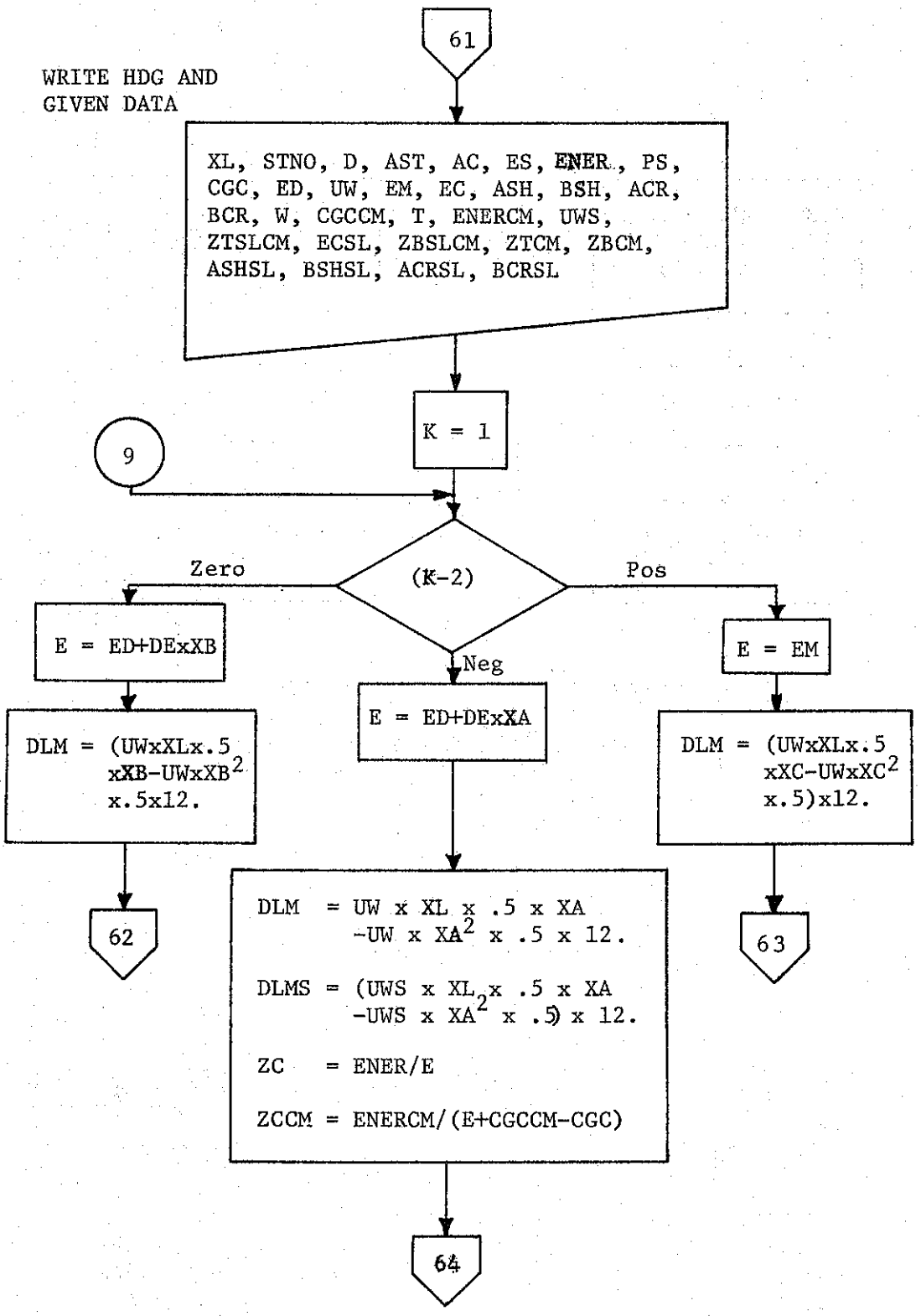
61
WRITE HDG AND GIVEN DATA
XL, STNO, D, AST, AC, ES, ENER, PS, CGC, ED, UW, EM, EC, ASH, BSH, ACR, BCR, W, CGCCM, T, ENERCM, UWS, ZTSLCM, ECSL, ZBSLCM, ZTCM, ZBCM, ASHSL, BSHSL, ACRSL, BCRSL
K = 1
9
(K-2)
Zero
Neg
Pos
E = ED+DExXB
E = ED+DExXA
E = EM
DLM = (UWxXLx.5 xXB-UWxXB2 x.5x12.
DLM = UW x XL x .5 x XA -UW x XA2 x .5 x 12.
DLMS = (UWS x XL2x .5 x XA -UWS x XA2 x .5) x 12.
ZC = ENER/E
ZCCM = ENERCM/(E+CGCCM-CGC)
DLM = (UWxXLx.5 xXC-UWxXC2 x.5)x12.
62
63
64

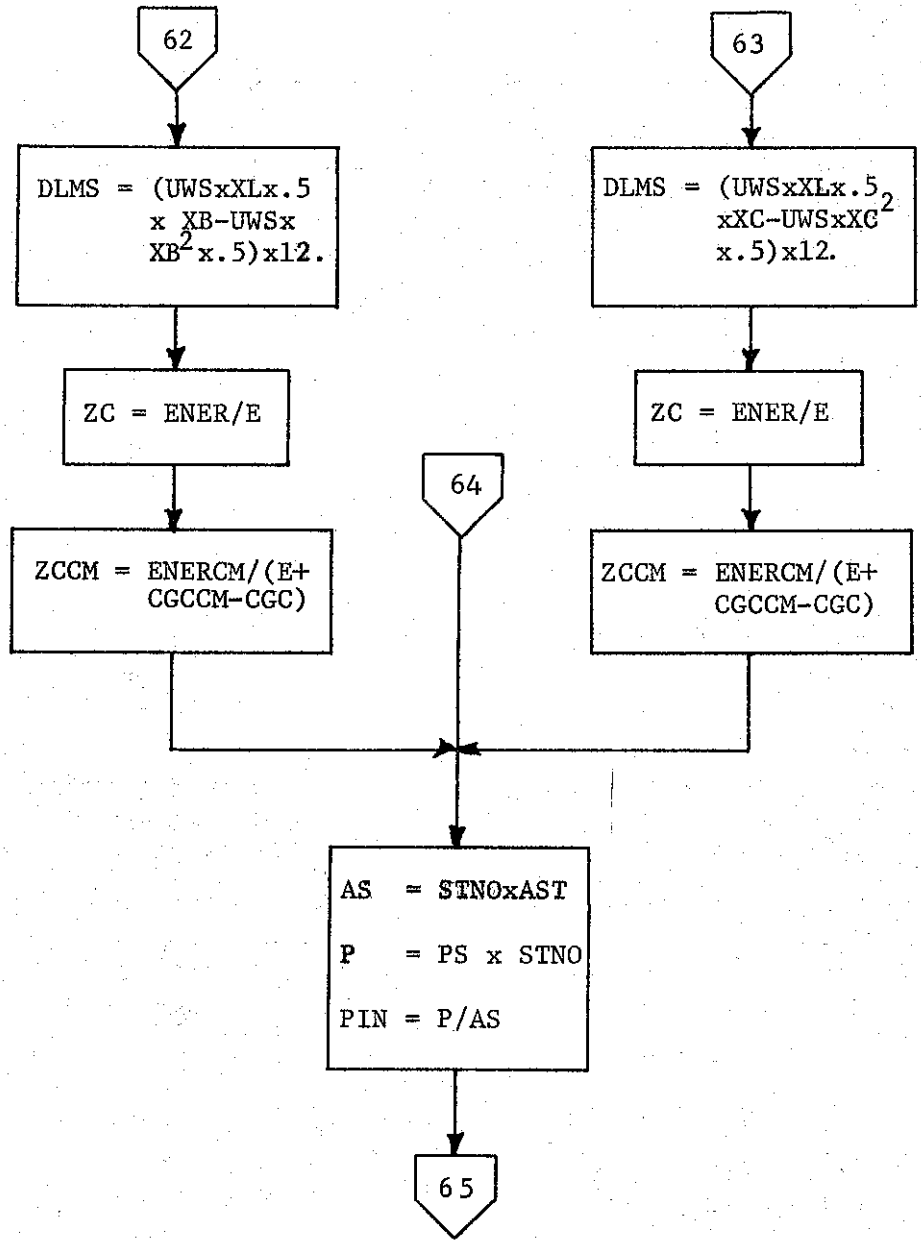
62
63
DLMS = (UWSxXLx.5 x XB-UWSx XB2 x.5)x12.
DLMS = (UWSxXLx.5 xXC-UWSxXC2 x.5)x12.
ZC = ENER/E
ZC = ENER/E
64
ZCCM = ENERCM/(E+ CGCCM-CGC)
ZCCM = ENERCM/(E+ CGCCM-CGC)
AS = STNOxAST
P = PS x STNO
PIN = P/AS
65

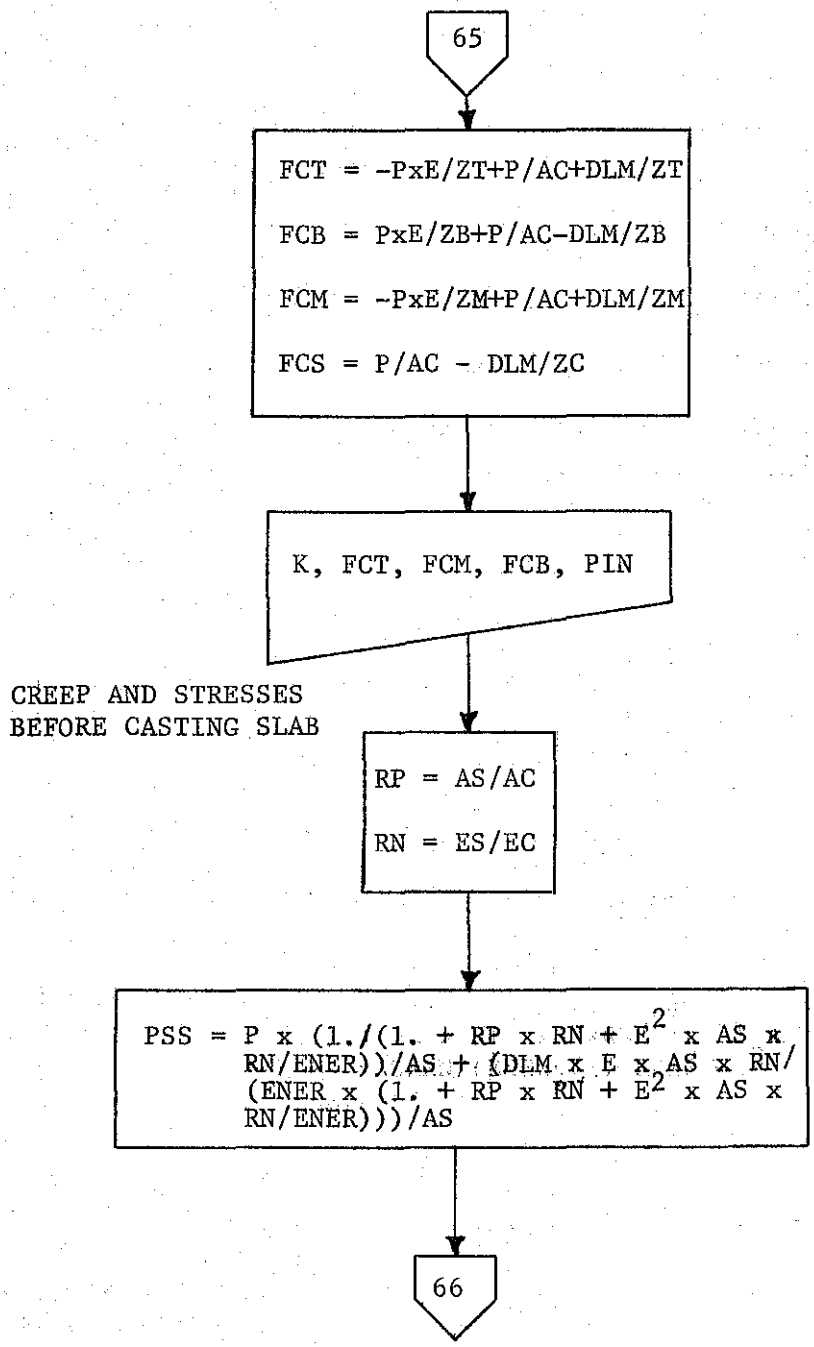
65
FCT = -PxE/ZT+P/AC+DLM/ZT
FCB = PxE/ZB+P/AC-DLM/ZB
FCM = -PxE/ZM+P/AC+DLM/ZM
FCS = P/AC - DLM/ZC
K, FCT, FCM, FCB, PIN
CREEP AND STRESSES
BEFORE CASTING SLAB
RP = AS/AC
RN = ES/EC
PSS = P x (1./(1. + RP x RN + E2 x AS x
RN/ENER))/AS + (DLM x E x AS x RN/
(ENER x (1. + RP x RN + E2 x AS x
RN/ENER)))/AS
66

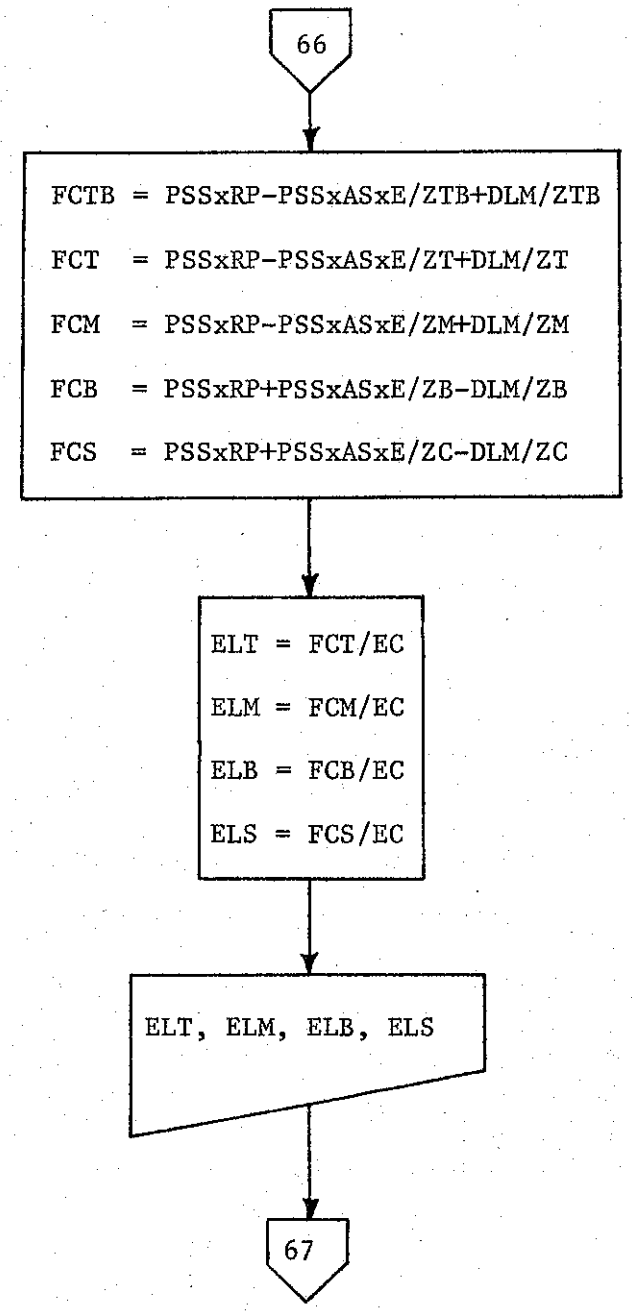
66
FCTB = PSSxRP-PSSxASxE/ZTB+DLM/ZTB
FCT = PSSxRP-PSSxASxE/ZT+DLM/ZT
FCM = PSSxRP-PSSxASxE/ZM+DLM/ZM
FCB = PSSxRP+PSSxASxE/ZB-DLM/ZB
FCS = PSSxRP+PSSxASxE/ZC-DLM/ZC
ELT = FCT/EC
ELM = FCM/EC
ELB = FCB/EC
ELS = FCS/EC
ELT, ELM, ELB, ELS
67

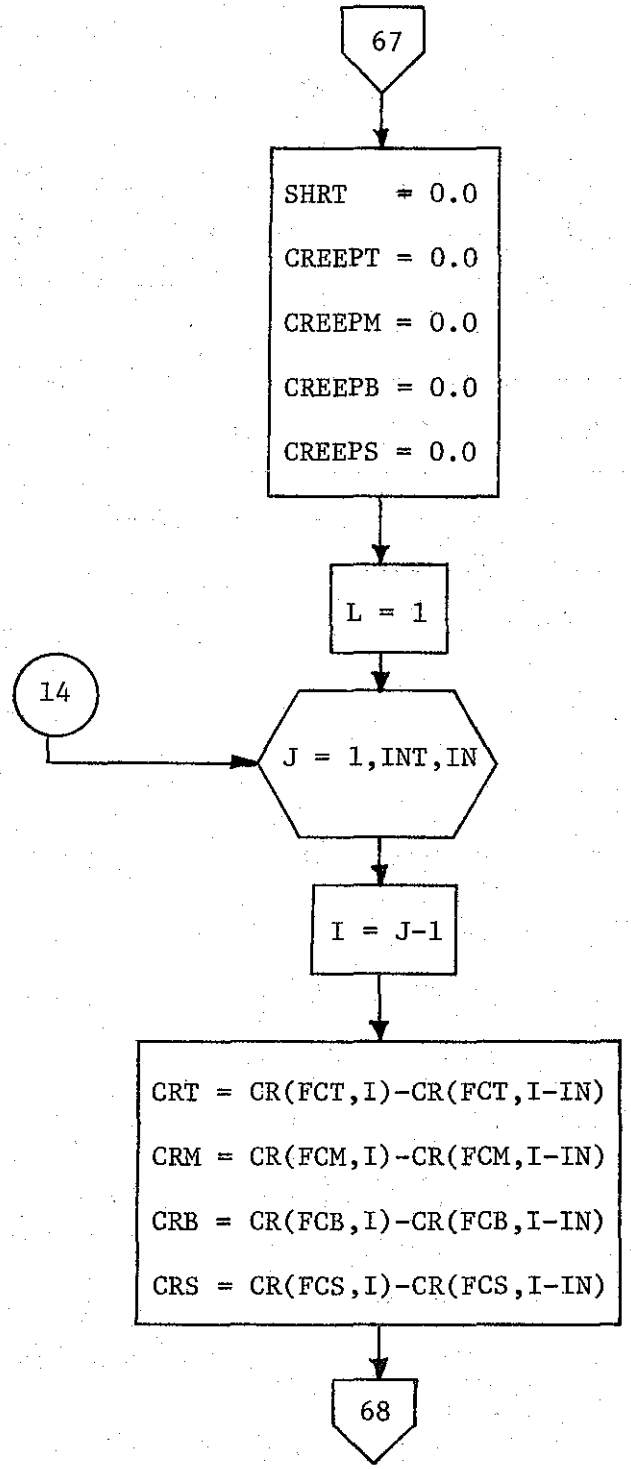
67
SHRT = 0.0
CREEPT = 0.0
CREEPM = 0.0
CREEPB = 0.0
CREEPS = 0.0
L = 1
14
J = 1,INT,IN
I = J-1
CRT = CR(FCT,I)-CR(FCT,I-IN)
CRM = CR(FCM,I)-CR(FCM,I-IN)
CRB = CR(FCB,I)-CR(FCB,I-IN)
CRS = CR(FCS,I)-CR(FCS,I-IN)
68

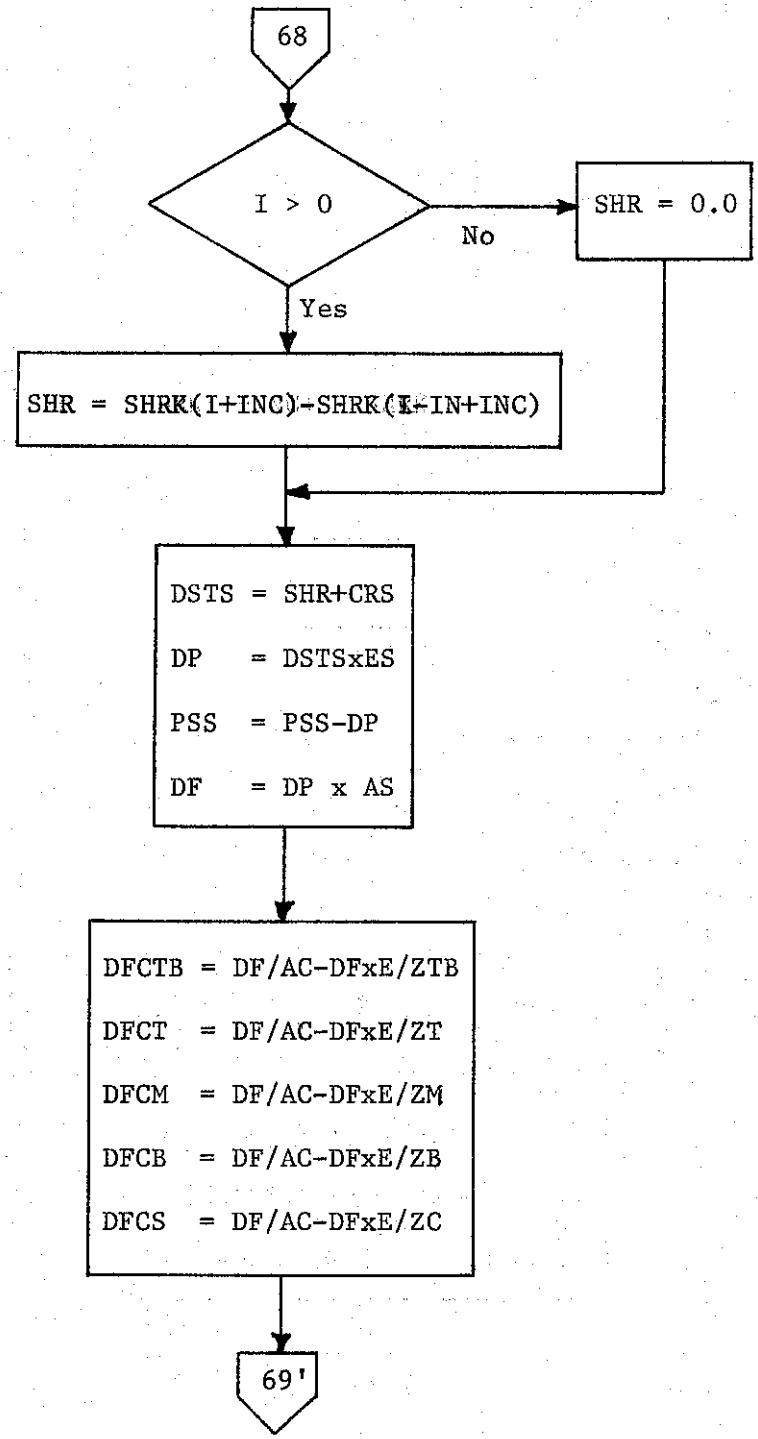
68
I > 0
No
SHR = 0.0
Yes
SHR = SHRK(I+INC)-SHRK(I-IN+INC)
DSTS = SHR+CRS
DP = DSTSxES
PSS = PSS-DP
DF = DP x AS
DFCTB = DF/AC-DFxE/ZTB
DFCT = DF/AC-DFxE/ZT
DFCM = DF/AC-DFxE/ZM
DFCB = DF/AC-DFxE/ZB
DFCS = DF/AC-DFxE/ZC
69'

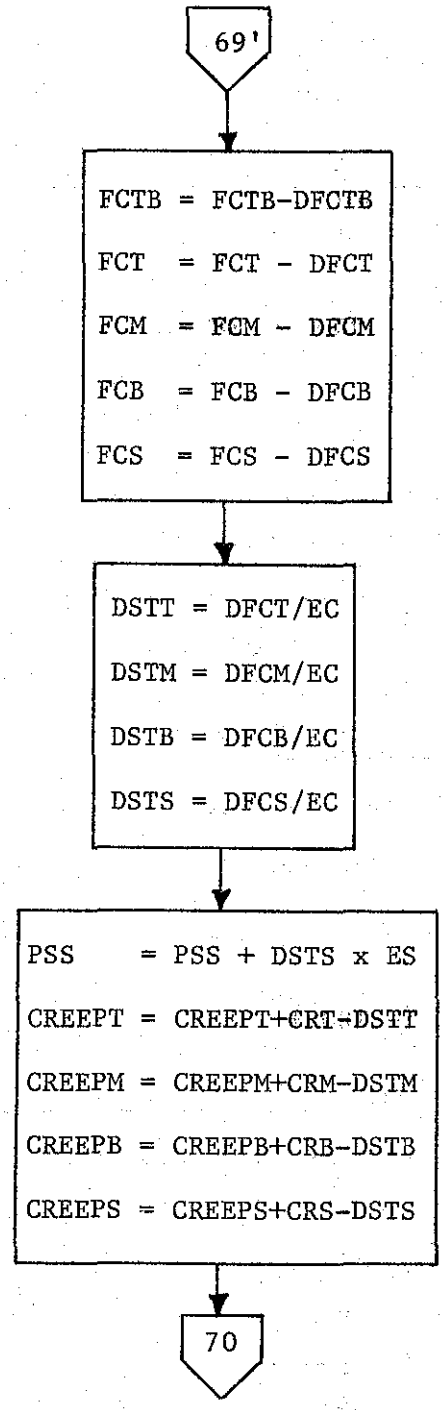
69'
FCTB = FCTB-DFCTB
FCT = FCT - DFCT
FCM = FCM - DFCM
FCB = FCB - DFCB
FCS = FCS - DFCS
DSTT = DFCT/EC
DSTM = DFCM/EC
DSTB = DFCB/EC
DSTS = DFCS/EC
PSS = PSS + DSTS x ES
CREEPT = CREEPT+CRT-DSTT
CREEPM = CREEPM+CRM-DSTM
CREEPB = CREEPB+CRB-DSTB
CREEPS = CREEPS+CRS-DSTS
70

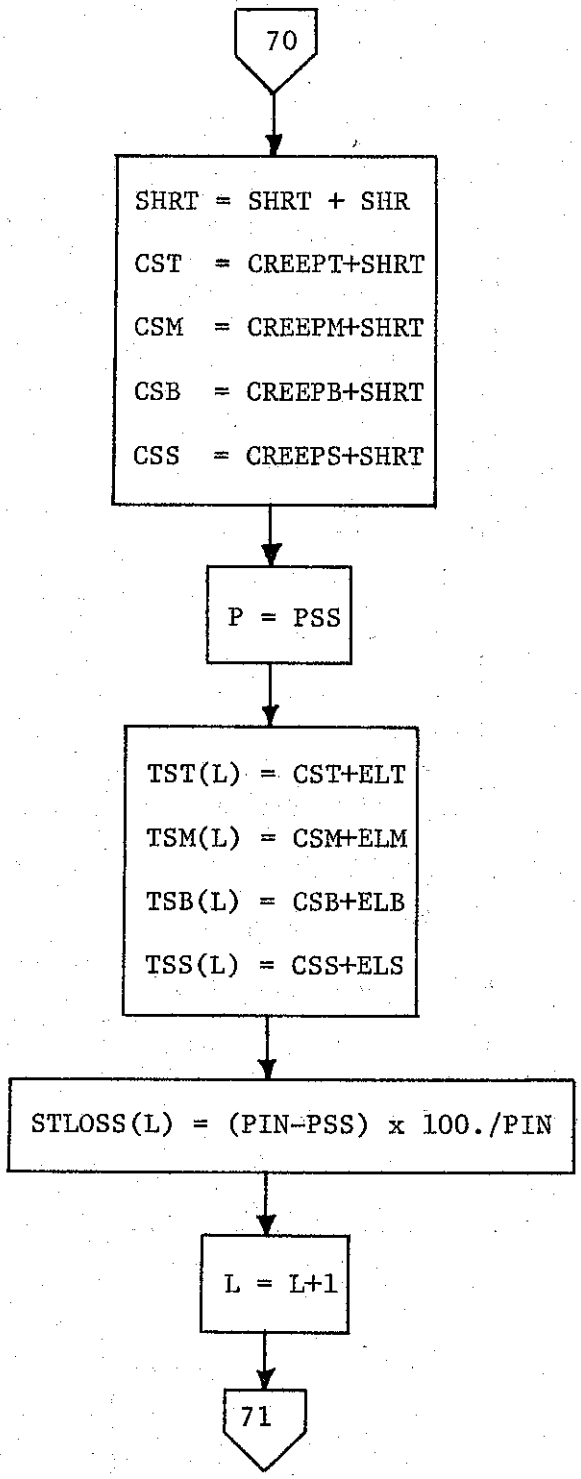
70
SHRT = SHRT + SHR
CST = CREEPT+SHRT
CSM = CREEPM+SHRT
CSB = CREEPB+SHRT
CSS = CREEPS+SHRT
P = PSS
TST(L) = CST+ELT
TSM(L) = CSM+ELM
TSB(L) = CSB+ELB
TSS(L) = CSS+ELS
STLOSS(L) = (PIN-PSS) x 100./PIN
L = L+1
71

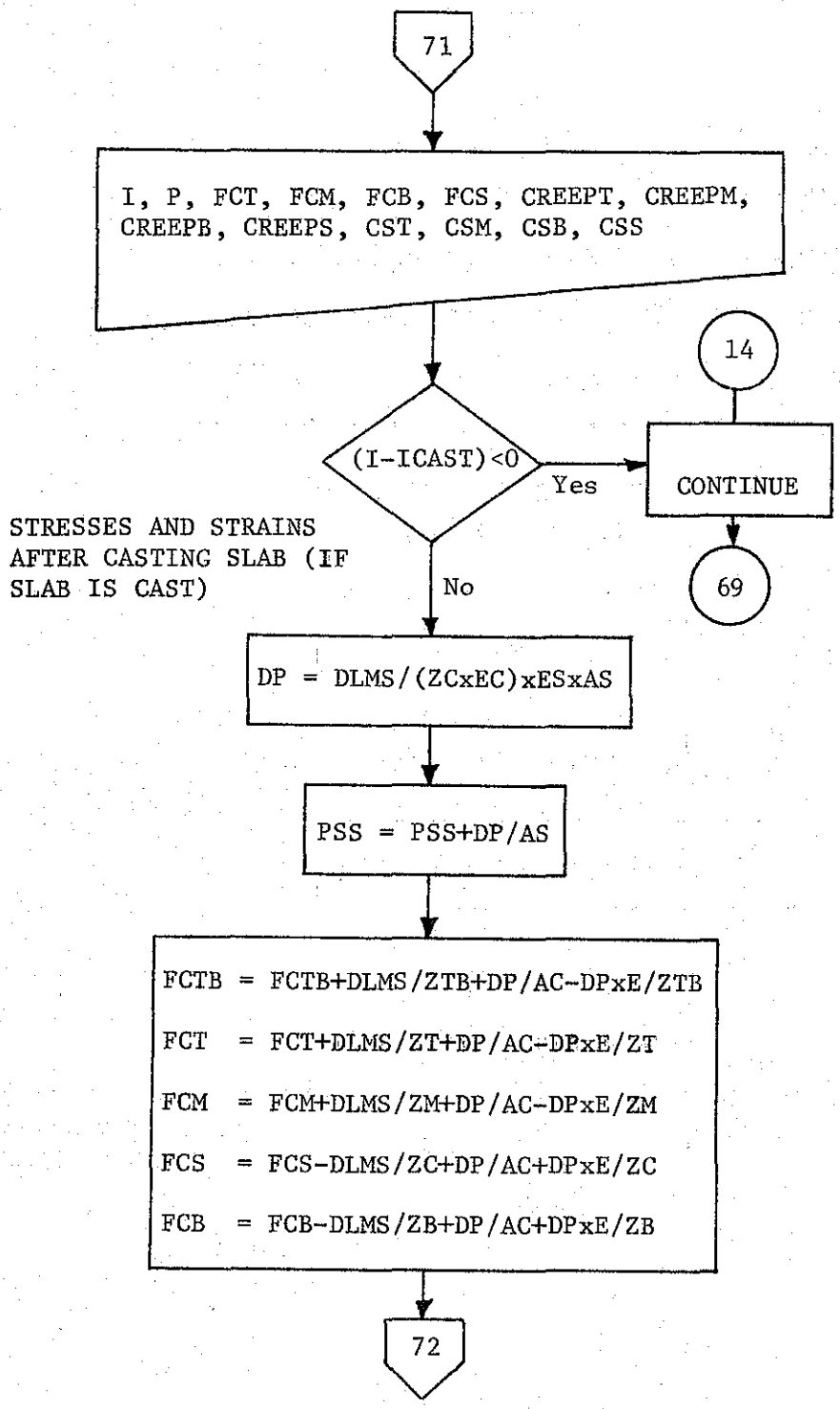
71
I, P, FCT, FCM, FCB, FCS, CREEPT, CREEPM, CREEPB, CREEPS, CST, CSM, CSB, CSS
14
(I-ICAST)<0
Yes
CONTINUE
69
STRESSES AND STRAINS AFTER CASTING SLAB (IF SLAB IS CAST)
No
DP = DLMS/(ZCxEC)xESxAS
PSS = PSS+DP/AS
FCTB = FCTB+DLMS/ZTB+DP/AC-DPxE/ZTB
FCT = FCT+DLMS/ZT+DP/AC-DPxE/ZT
FCM = FCM+DLMS/ZM+DP/AC-DPxE/ZM
FCS = FCS-DLMS/ZC+DP/AC+DPxE/ZC
FCB = FCB-DLMS/ZB+DP/AC+DPxE/ZB
72

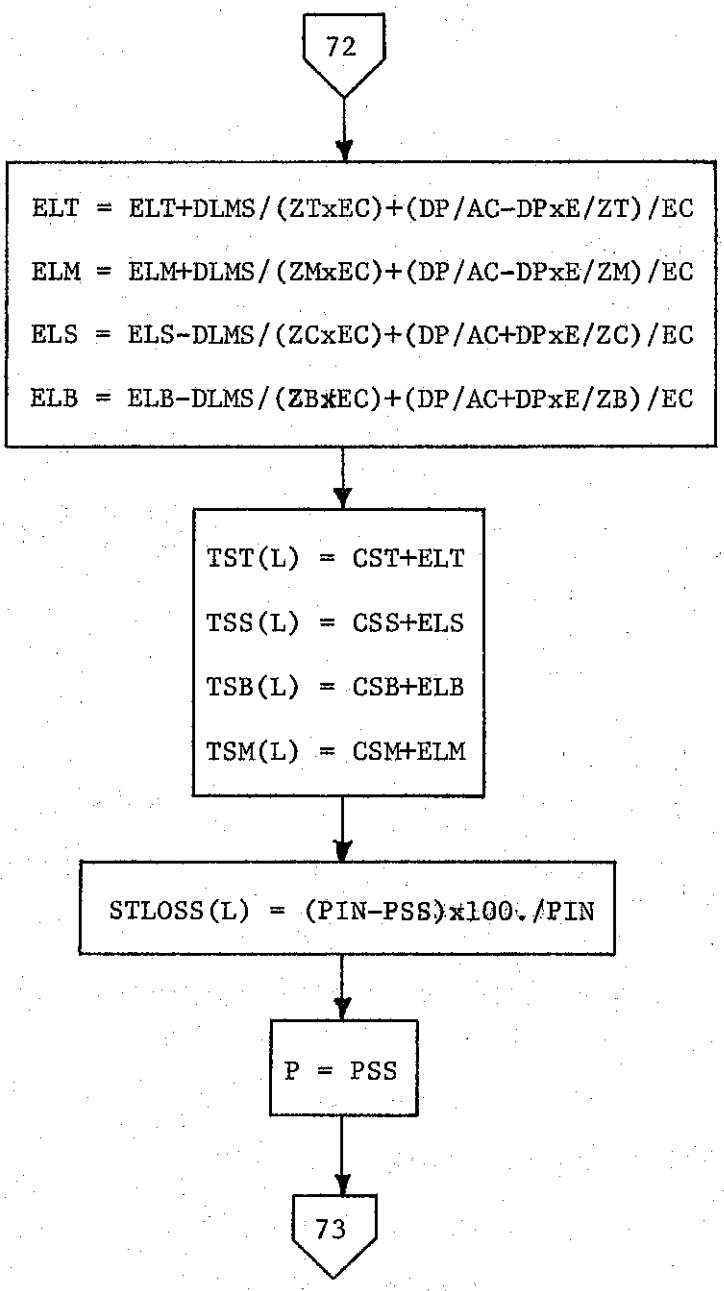
72
ELT = ELT+DLMS/(ZTxEC)+(DP/AC-DPxE/ZT)/EC
ELM = ELM+DLMS/(ZMxEC)+(DP/AC-DPxE/ZM)/EC
ELS = ELS-DLMS/(ZCxEC)+(DP/AC+DPxE/ZC)/EC
ELB = ELB-DLMS/(ZBxEC)+(DP/AC+DPxE/ZB)/EC
TST(L) = CST+ELT
TSS(L) = CSS+ELS
TSB(L) = CSB+ELB
TSM(L) = CSM+ELM
STLOSS(L) = (PIN-PSS)x100./PIN
P = PSS
73

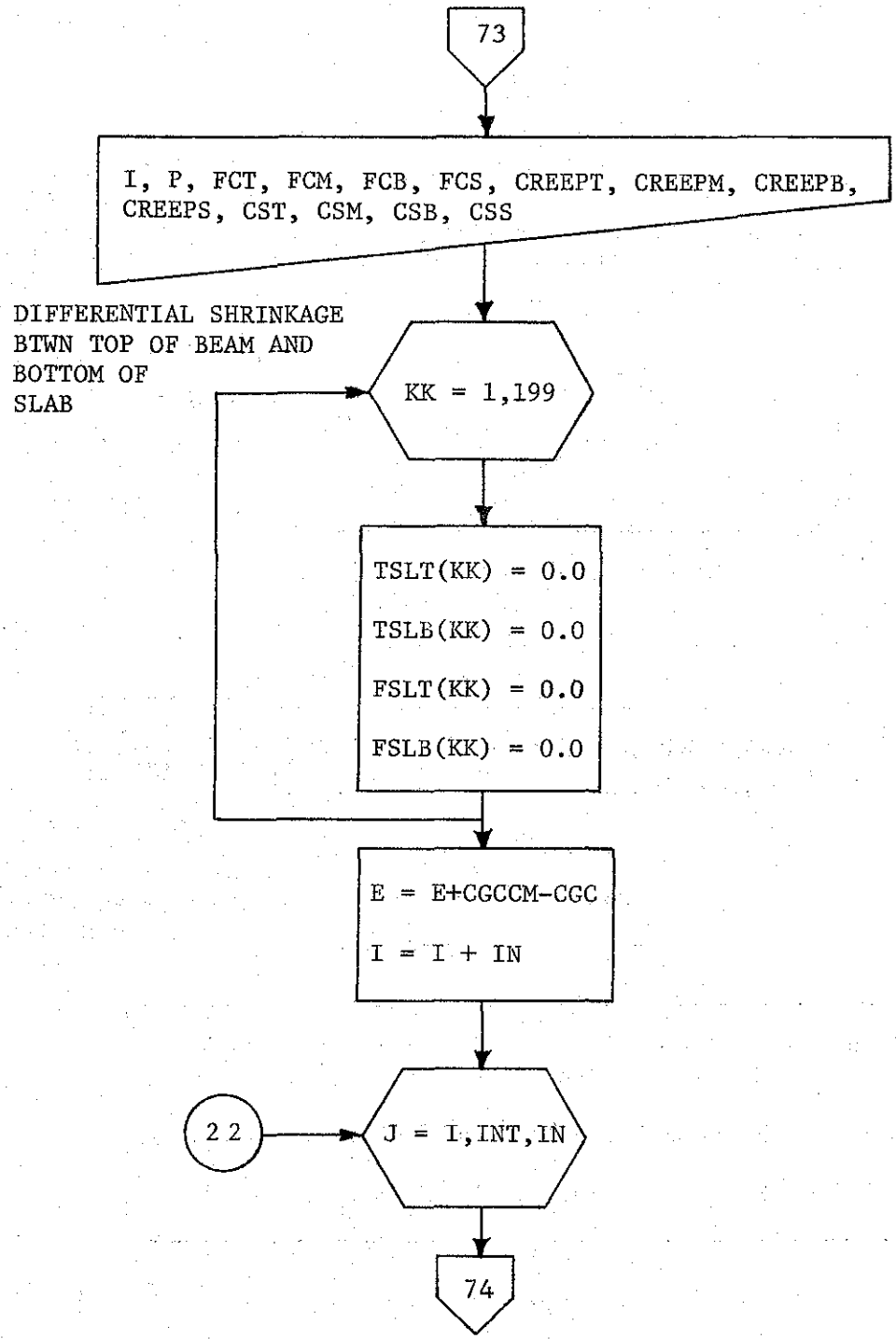
73
I, P, FCT, FCM, FCB, FCS, CREEPT, CREEPM, CREEPB, CREEPS, CST, CSM, CSB, CSS
DIFFERENTIAL SHRINKAGE BTWN TOP OF BEAM AND BOTTOM OF SLAB
KK = 1,199
TSLT(KK) = 0.0
TSLB(KK) = 0.0
FSLT(KK) = 0.0
FSLB(KK) = 0.0
E = E+CGCCM-CGC
I = I + IN
22
J = I,INT,IN
74

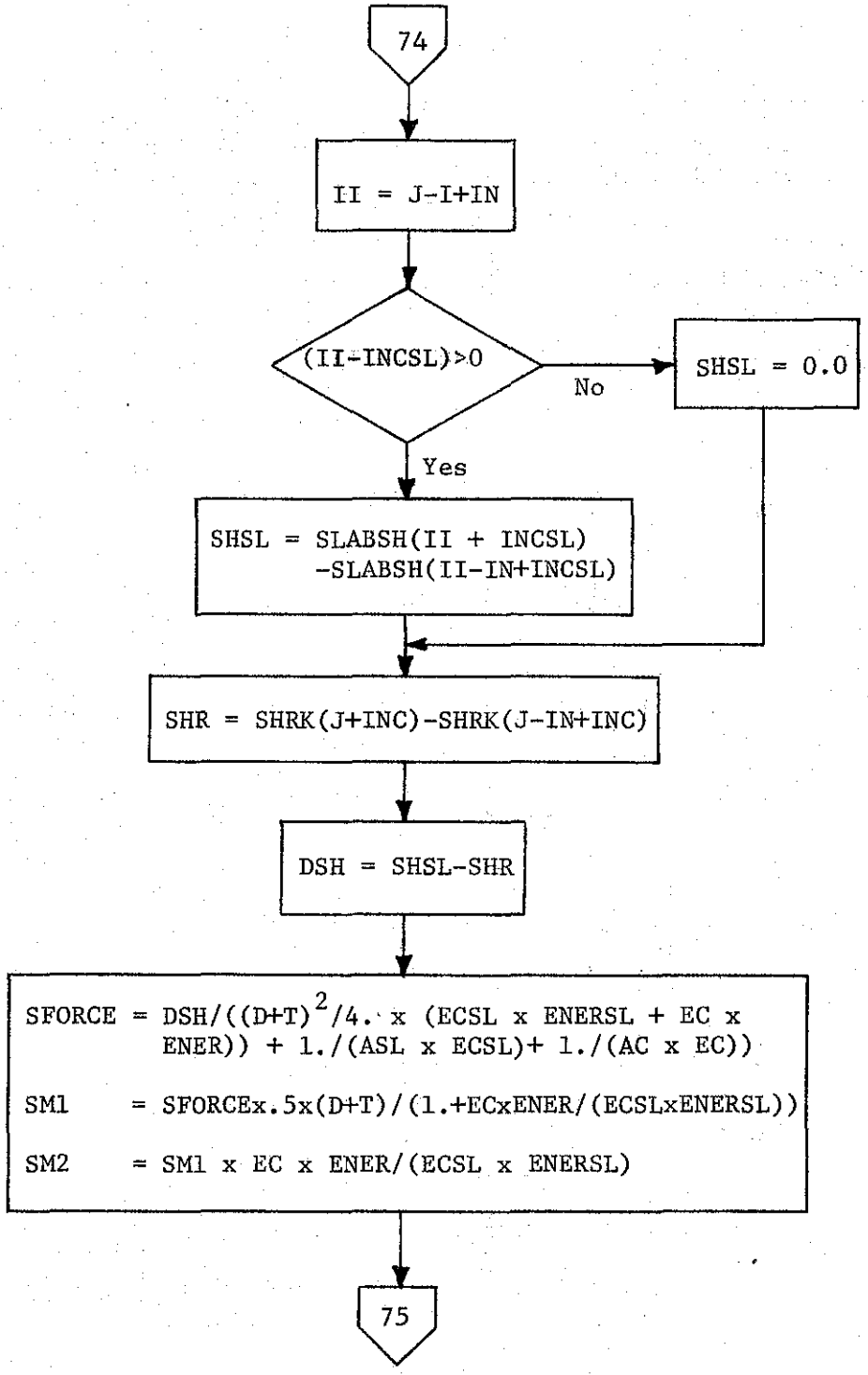
74
II = J-I+IN
(II-INCSL)>0
No
SHSL = 0.0
Yes
SHSL = SLABSH(II + INCSL)
-SLABSH(II-IN+INCSL)
SHR = SHRK(J+INC)-SHRK(J-IN+INC)
DSH = SHSL-SHR
SFORCE = DSH/((D+T)2/4. x (ECSL x ENERSL + EC x ENER)) + 1./(ASL x ECSL)+ 1./(AC x EC))
SM1 = SFORCEx.5x(D+T)/(1.+ECxENER/(ECSLxENERSL))
SM2 = SM1 x EC x ENER/(ECSL x ENERSL)
75

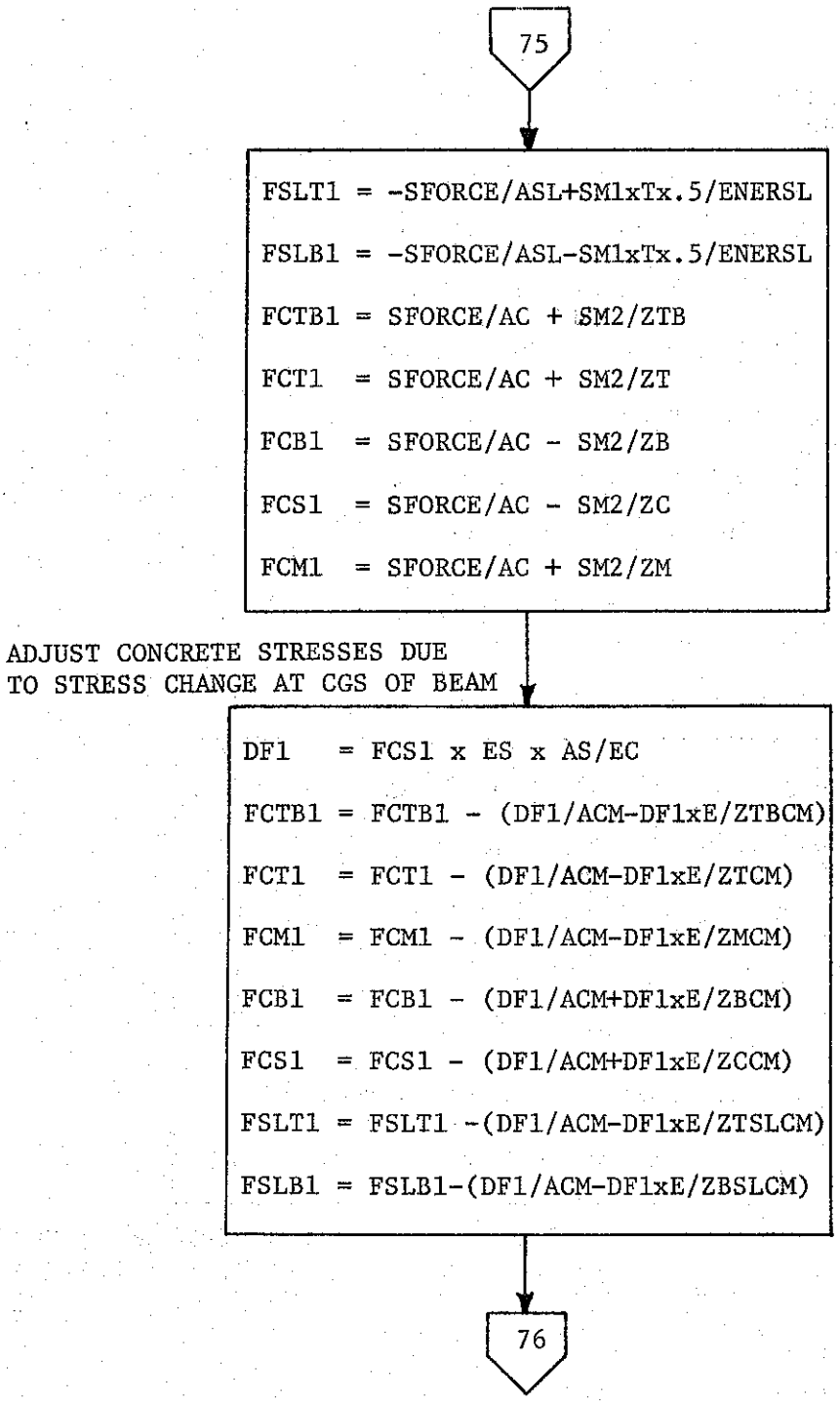
75
FSLT1 = -SFORCE/ASL+SM1xTx.5/ENERSL
FSLB1 = -SFORCE/ASL-SM1xTx.5/ENERSL
FCTB1 = SFORCE/AC + SM2/ZTB
FCT1 = SFORCE/AC + SM2/ZT
FCB1 = SFORCE/AC - SM2/ZB
FCS1 = SFORCE/AC - SM2/ZC
FCM1 = SFORCE/AC + SM2/ZM
ADJUST CONCRETE STRESSES DUE
TO STRESS CHANGE AT CGS OF BEAM
DF1 = FCS1 x ES x AS/EC
FCTB1 = FCTB1 - (DF1/ACM-DF1xE/ZTBCM)
FCT1 = FCT1 - (DF1/ACM-DF1xE/ZTCM)
FCM1 = FCM1 - (DF1/ACM-DF1xE/ZMCM)
FCB1 = FCB1 - (DF1/ACM+DF1xE/ZBCM)
FCS1 = FCS1 - (DF1/ACM+DF1xE/ZCCM)
FSLT1 = FSLT1 -(DF1/ACM-DF1xE/ZTSLCM)
FSLB1 = FSLB1-(DF1/ACM-DF1xE/ZBSLCM)
76

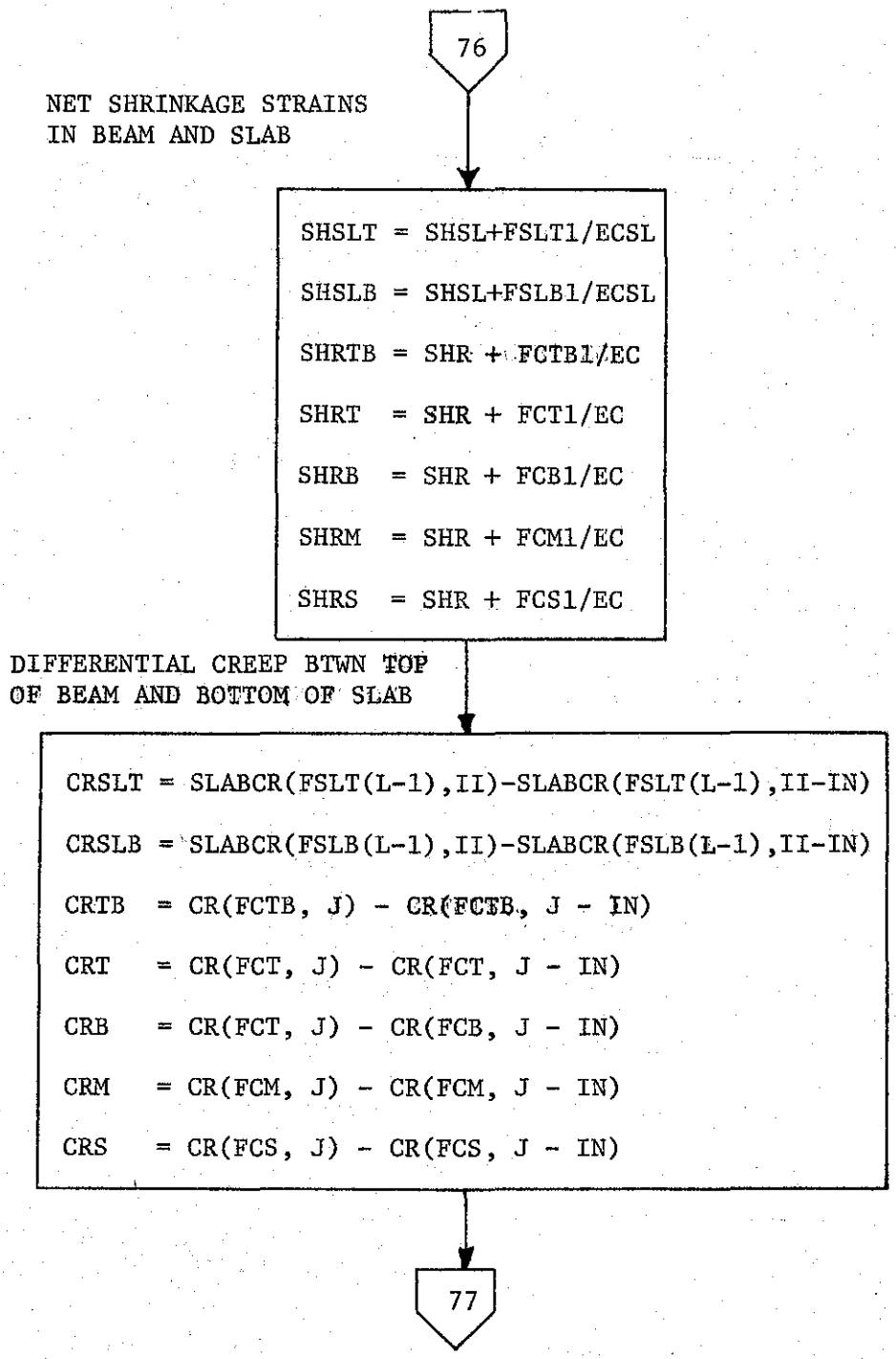
76
NET SHRINKAGE STRAINS
IN BEAM AND SLAB
SHSLT = SHSL+FSLT1/ECSL
SHSLB = SHSL+FSLB1/ECSL
SHRTB = SHR + FCTB1/EC
SHRT = SHR + FCT1/EC
SHRB = SHR + FCB1/EC
SHRM = SHR + FCM1/EC
SHRS = SHR + FCS1/EC
DIFFERENTIAL CREEP BTWN TOP
OF BEAM AND BOTTOM OF SLAB
CRSLT = SLABCR(FSLT(L-1),II)-SLABCR(FSLT(L-1),II-IN)
CRSLB = SLABCR(FSLB(L-1),II)-SLABCR(FSLB(L-1),II-IN)
CRTB = CR(FCTB, J) - CR(FCTB, J - IN)
CRT = CR(FCT, J) - CR(FCT, J - IN)
CRB = CR(FCT, J) - CR(FCB, J - IN)
CRM = CR(FCM, J) - CR(FCM, J - IN)
CRS = CR(FCS, J) - CR(FCS, J - IN)
77

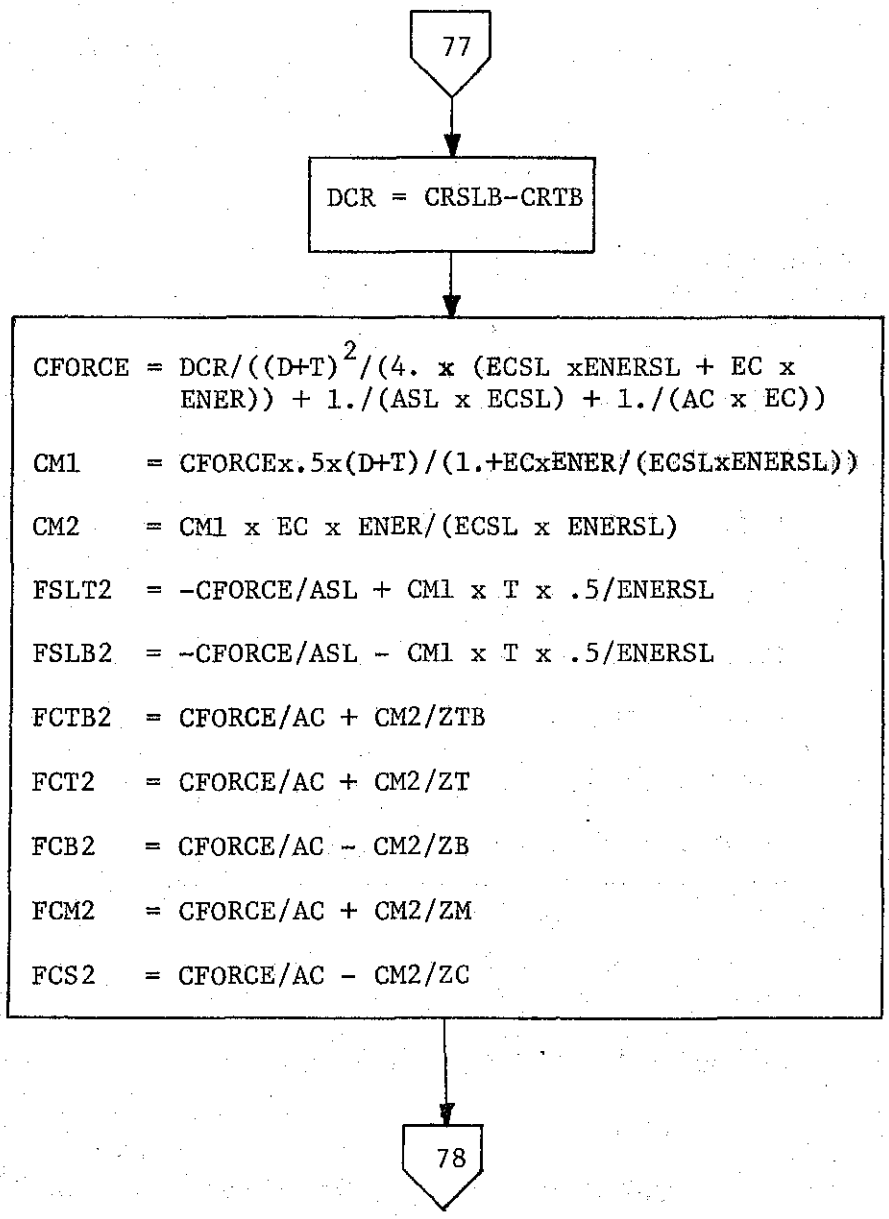
77
DCR = CRSLB-CRTB
CFORCE = DCR/((D+T)**2/(4. x (ECSL xENERSL + EC x ENER)) + 1./(ASL x ECSL) + 1./(AC x EC))
CM1 = CFORCEx.5x(D+T)/(1.+ECxENER/(ECSLxENERSL))
CM2 = CM1 x EC x ENER/(ECSL x ENERSL)
FSLT2 = -CFORCE/ASL + CM1 x T x .5/ENERSL
FSLB2 = -CFORCE/ASL - CM1 x T x .5/ENERSL
FCTB2 = CFORCE/AC + CM2/ZTB
FCT2 = CFORCE/AC + CM2/ZT
FCB2 = CFORCE/AC - CM2/ZB
FCM2 = CFORCE/AC + CM2/ZM
FCS2 = CFORCE/AC - CM2/ZC
78

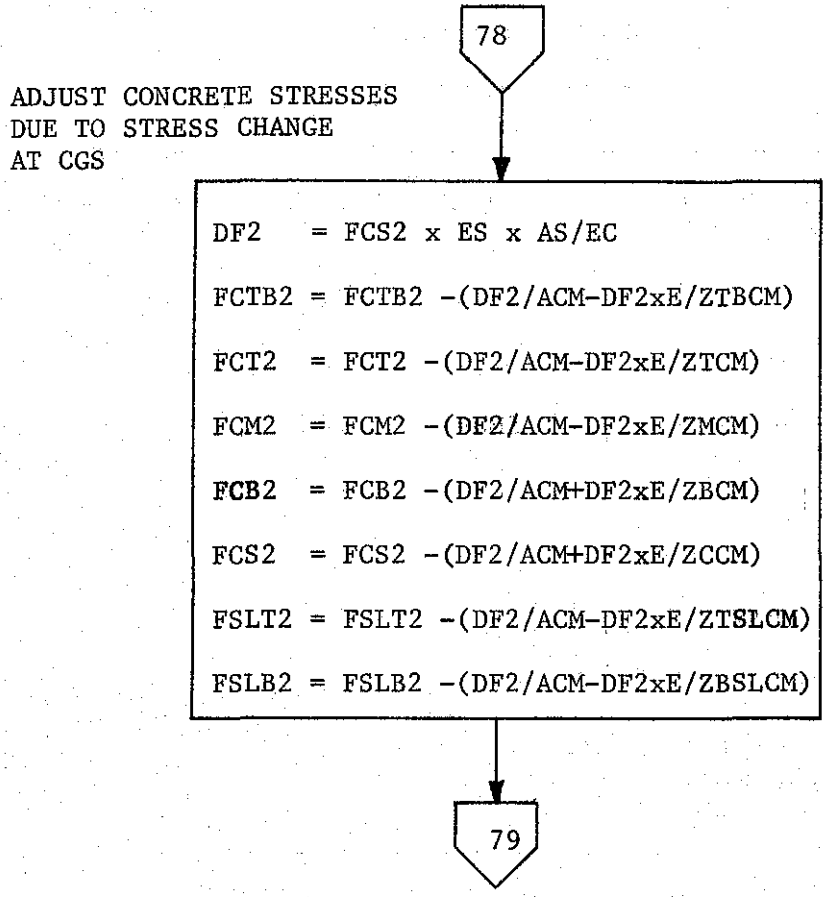
78
ADJUST CONCRETE STRESSES
DUE TO STRESS CHANGE
AT CGS
DF2 = FCS2 x ES x AS/EC
FCTB2 = FCTB2 -(DF2/ACM-DF2xE/ZTBCM)
FCT2 = FCT2 -(DF2/ACM-DF2xE/ZTCM)
FCM2 = FCM2 -(DF2/ACM-DF2xE/ZMCM)
FCB2 = FCB2 -(DF2/ACM+DF2xE/ZBCM)
FCS2 = FCS2 -(DF2/ACM+DF2xE/ZCCM)
FSLT2 = FSLT2 -(DF2/ACM-DF2xE/ZTSLCM)
FSLB2 = FSLB2 -(DF2/ACM-DF2xE/ZBSLCM)
79

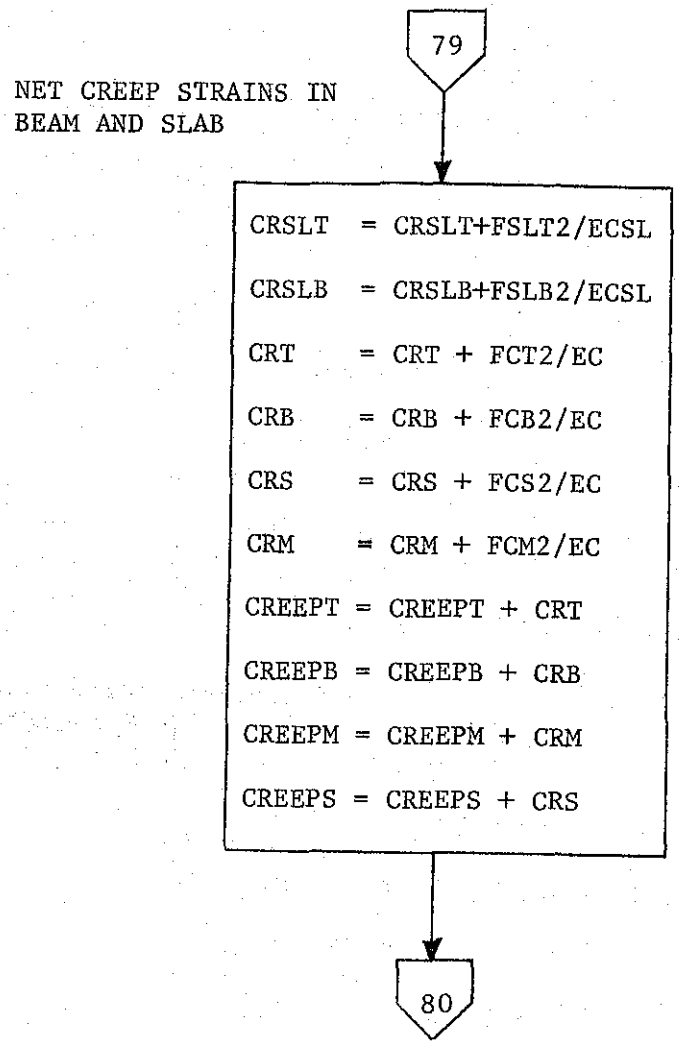
79
NET CREEP STRAINS IN
BEAM AND SLAB
CRSLT = CRSLT+FSLT2/ECSL
CRSLB = CRSLB+FSLB2/ECSL
CRT = CRT + FCT2/EC
CRB = CRB + FCB2/EC
CRS = CRS + FCS2/EC
CRM = CRM + FCM2/EC
CREEPT = CREEPT + CRT
CREEPB = CREEPB + CRB
CREEPM = CREEPM + CRM
CREEPS = CREEPS + CRS
80

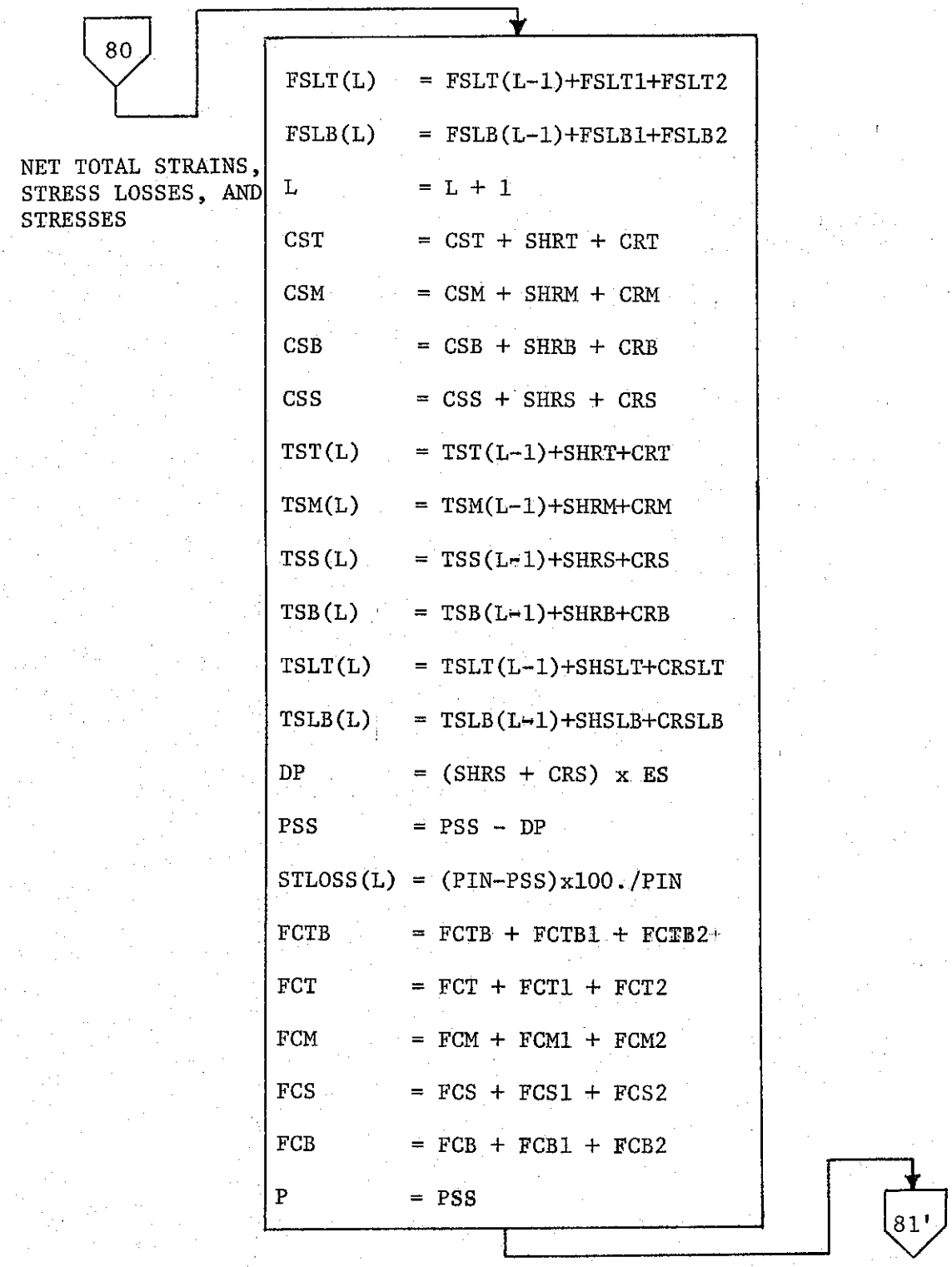
80
NET TOTAL STRAINS, STRESS LOSSES, AND STRESSES
FSLT(L) = FSLT(L-1)+FSLT1+FSLT2
FSLB(L) = FSLB(L-1)+FSLB1+FSLB2
L = L + 1
CST = CST + SHRT + CRT
CSM = CSM + SHRM + CRM
CSB = CSB + SHRB + CRB
CSS = CSS + SHRS + CRS
TST(L) = TST(L-1)+SHRT+CRT
TSM(L) = TSM(L-1)+SHRM+CRM
TSS(L) = TSS(L-1)+SHRS+CRS
TSB(L) = TSB(L-1)+SHRB+CRB
TSLT(L) = TSLT(L-1)+SHSLT+CRSLT
TSLB(L) = TSLB(L-1)+SHSLB+CRSLB
DP = (SHRS + CRS) x ES
PSS = PSS - DP
STLOSS(L) = (PIN-PSS)x100./PIN
FCTB = FCTB + FCTB1 + FCTB2
FCT = FCT + FCT1 + FCT2
FCM = FCM + FCM1 + FCM2
FCS = FCS + FCS1 + FCS2
FCB = FCB + FCB1 + FCB2
P = PSS
81'

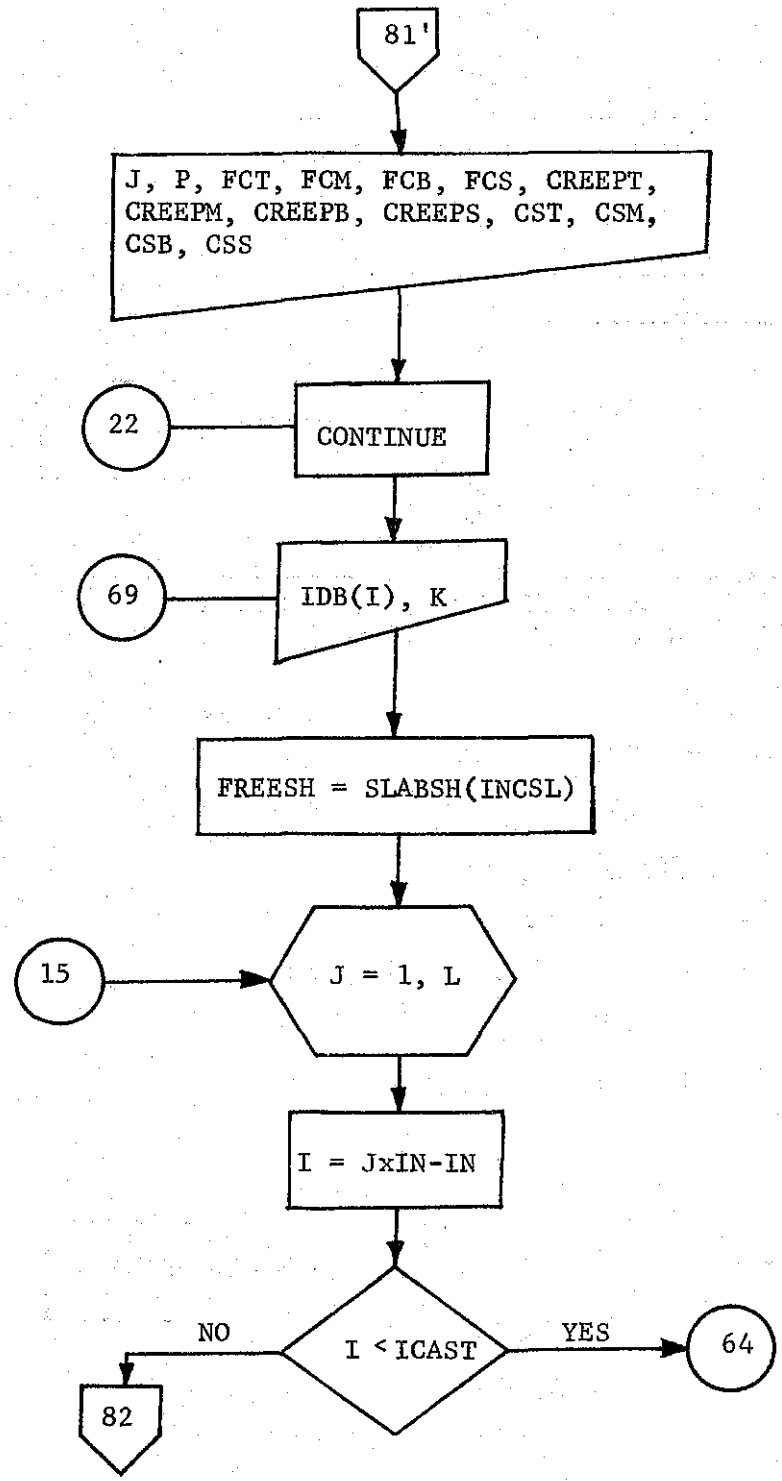
81'
J, P, FCT, FCM, FCB, FCS, CREEPT, CREEPM, CREEPB, CREEPS, CST, CSM, CSB, CSS
22
CONTINUE
69
IDB(I), K
FREESH = SLABSH(INCSL)
15
J = 1, L
I = JxIN-IN
NO
I < ICAST
YES
64
82

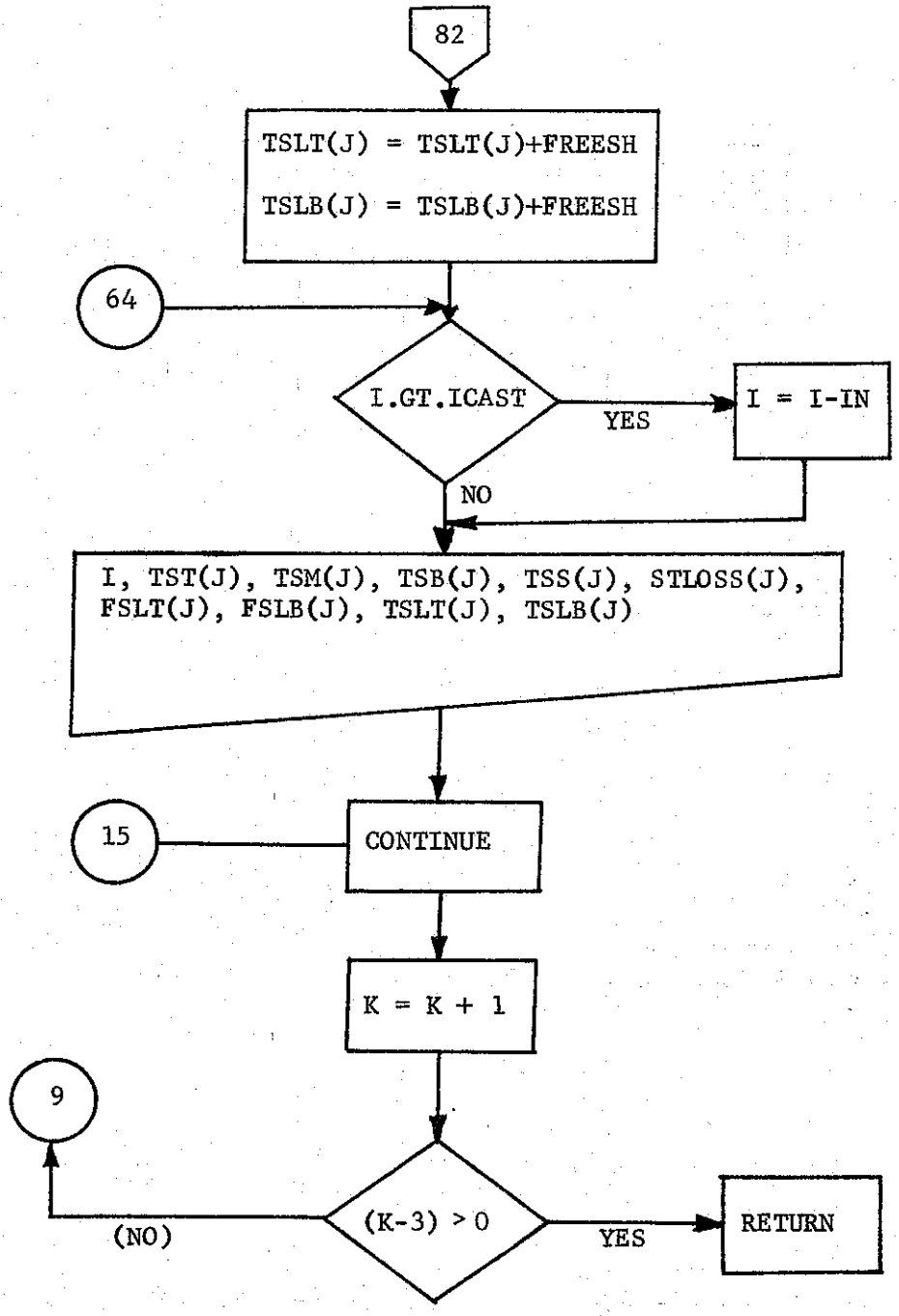
82
TSLT(J) = TSLT(J)+FREESH
TSLB(J) = TSLB(J)+FREESH
64
I.GT.ICAST
YES
I = I-IN
NO
I, TST(J), TSM(J), TSB(J), TSS(J), STLOSS(J),
FSLT(J), FSLB(J), TSLT(J), TSLB(J)
15
CONTINUE
K = K + 1
9
(K-3) > 0
(NO)
YES
RETURN

FUNCTION CR(FC, I) COMMON ASH, BSH, ACR, BCR, ASHSL, BSHSL,ACRSL, BCRSL,
(CREEP AT ANY TIME)

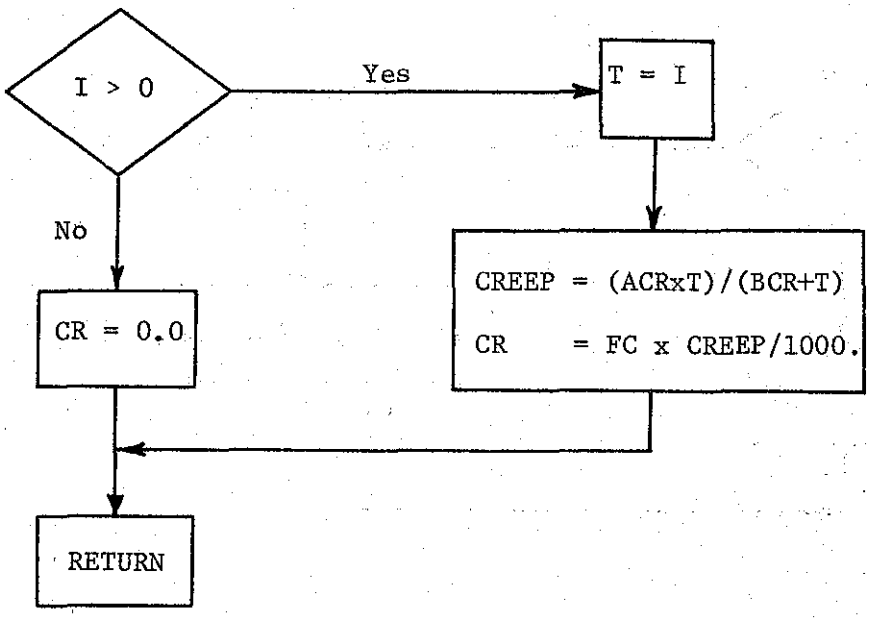

FUNCTION SHR(I) COMMON ASH, BSH, ACR, BCR, ASHSL, BSHSL, ACRSL, BCRSL

SHRINKAGE AT ANY TIME

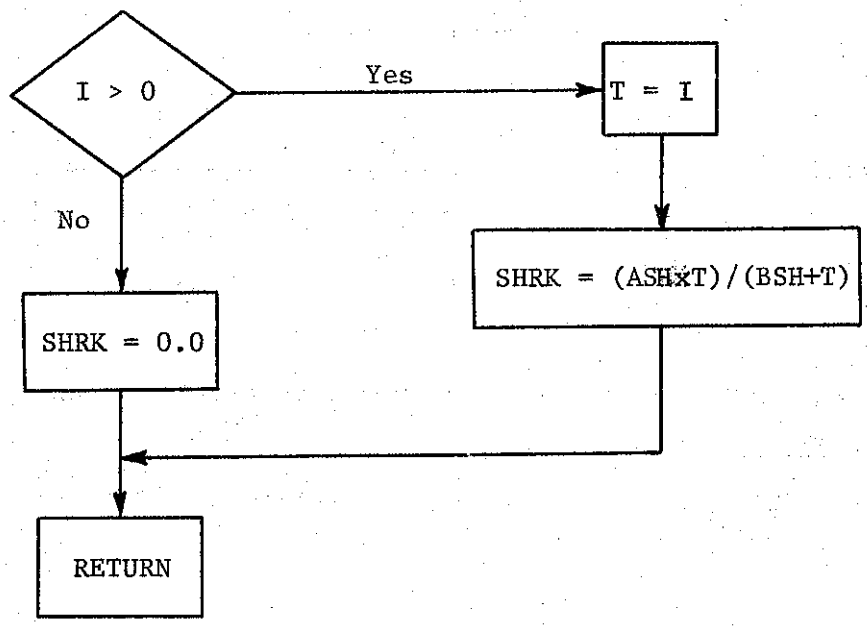

FUNCTION SLABCR (FC, II) COMMON ASH, BSH, ACR, BCR, ASHSL, BSHSL, ACRSL, BCRSL

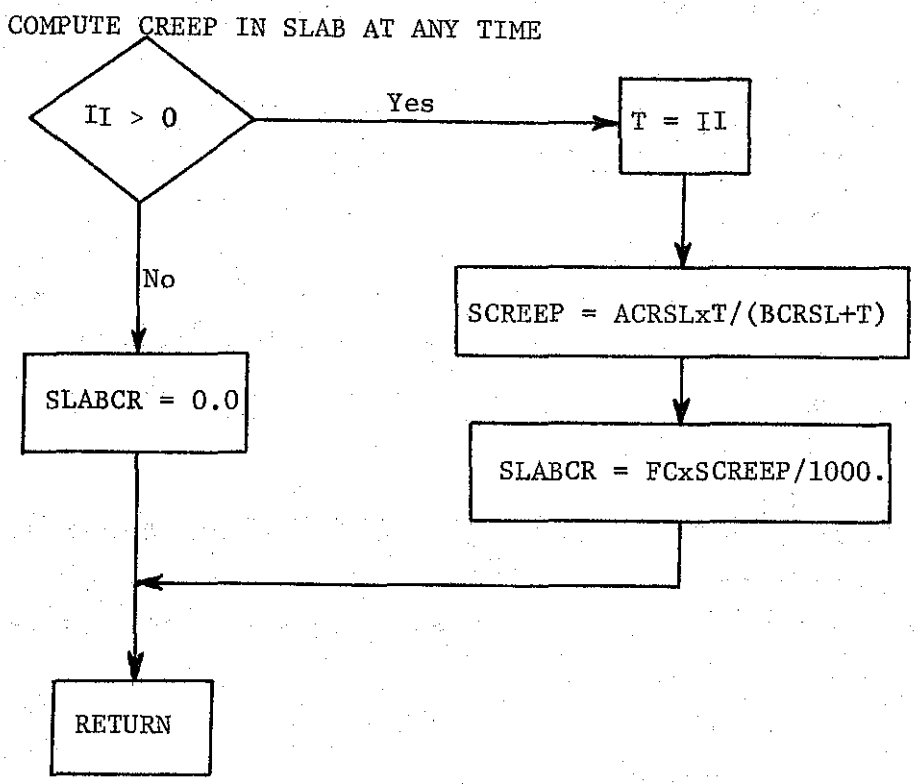

FUNCTION SLABSH (II) COMMON ASH, BSH, ACR, BCR, ASHSL, BSHSL, ACRSL, BCRSL

COMPUTE SHRINKAGE IN SLAB AT ANY TIME

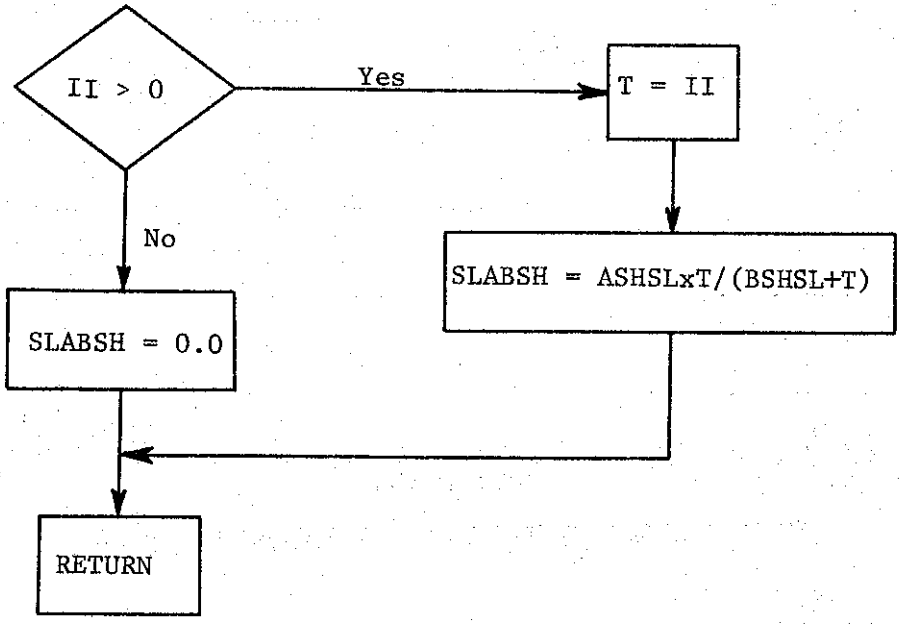

ARRANGEMENT OF DATA CARDS

	1–10	11–20	21–30	31–40	41–50	51–60	61–70	71–80
1	ID HEADER CARD IDENTIFYING THE PROJECT							
2	IDB HEADER CARD IDENTIFYING THE BEAM							
3	ENER	CGC	D	UW	AC	XL	H	
4	STNO	AST	ED	EM	PS	EC	ES	
5	EA	EB	EX					
6	ASH	BSH	ACR	BCR	XN	XNT	XLX	
7	XA	XB	XC	GT	GB	GM	XINC	
8	W	T	UWS	ECSL				
9	ASHSL	BSHSL	ACRSL	BCRSL	XCAST	INCSL	KIF	
10								

See notes on next sheet.

Notes:

1. Cards number 1 and 2 may contain any information, alphabetic or numeric.
2. Each variable in cards 3 through 8 may occupy any position within the ten columns, and all values must be expressed in decimal form.
3. The first 5 variables on card 9 may occupy and position with the ten columns and must be in decimal form.

   INCSL must occupy columns 51 and 52, must be right adjusted, and must not be in decimal form.

   KIF must occupy columns 53 and 54, must be right adjusted, and must not be in decimal form.
4. The last card in the data deck, card number 10, whould carry the number of beams to be run at the same time in columns 1-10 (any position) in decimal form.